General comments to the review:

First we would like to thank the anonymous reviewer for the careful reading of our manuscript and the many insightful comments and suggestions. We think that these inputs have resulted in a much stronger manuscript. Below we respond to each comment in blue, and a revised manuscript has been provided that reflects the suggested updates and changes.

We regret to see that the reviewer does not share our understanding of the importance of the results presented in this paper. The work presented here is the first out of two papers. The second paper (to be submitted) will present a statistical model, in which we use the results from this paper (as also suggested by the reviewer) to derive a satellite based T2m product. This product can be included directly in global surface air temperature analysis such as HadCRUT and GISS (Brohan et al., 2006; Hansen et al., 2010). The potential for the result presented here is thus to improve on the Global surface temperature products in the data sparse polar regions, a topic which in our view is highly important.

From the reviewer comments, we acknowledge, however, that we have not been clear enough on outlining the larger perspectives in our work and on highlighting the high impact this work will have. We have now rewritten the abstract, introduction and conclusions to highlight these key questions

It is our sincere hope that with the new version it is much more clear how important these findings are, for the inclusion of satellite information into global surface temperature products and thus to improve the global climate change assessments, and that the reviewer will take this into account during a potential second review.

MAIN points that have been changed:

- Aim with the paper and the high impact of this study has been highlighted throughout the paper.
- Inclusion of PROMICE data from the lower ablation zone, to a total of 29 stations.
- Addition of one extra year to the PROMICE and ARMS data records.
- Uncertainties and ranges have been added to all estimates.
- Most figures have been reproduced.

Detailed responses are given below.

References

Brohan, P., Kennedy, J. J., Harris, I., Tett, S. F., & Jones, P. D. (2006). Uncertainty estimates in regional and global observed temperature changes: A new data set from 1850. *Journal of Geophysical Research: Atmospheres*, *111*(D12).

Hansen, J., Ruedy, R., Sato, M., & Lo, K. (2010). Global surface temperature change. *Reviews of Geophysics*, *48*(4).

Summary

This paper presents an overview of the relationship between the surface skin temperature and the 2 m air temperature over snow covered surfaces in the Arctic based on in situ observations. The rationale behind this is the satellite retrieval of skin temperature from satellite observations which are interpreted as being air temperature. This paper presents the processes that result in differences in the skin and air temperature over snow covered surfaces. I appreciate the fact that in this paper basically a review is given of these processes, but it is also the reason why I recommend to reject this manuscript, it does not present anything new. It does not present a recommendation on what to do to actually improve the interpretation of satellite products, it only states that these results might be helpfull.

See the general comments above.

Other reasons to reject are that the title suggests that the contents is about the whole of the Arctic, but the contents is limited to snow covered surfaces, and in addition also biased towards Greenland ice sheet stations. The results are thus not general applicable to the Arctic. I also found the writing often not clear, not consize, sometimes incorrect, and at some points I get the impression the author is not completely familiar with the involved processes.

We have changed the title to reflect that these results are only from arctic sea ice and the Greenland ice sheet. We have gone through all the text in order to clarify in cases where we have made unclear formulations.

What this manuscript needs is a clear recommendation that is directly applicable on satellite products, preferably to the whole arctic including snow free surfaces, and an actual application to a satellite product to show the impact of the difference between surface and 2 m air temperature on the satellite derived temperature.

Yes, this is acknowledged and (as stated above) we have now emphasized the potential of improving the global surface temperature products.

To further help the improvement of the manuscript, a list of more specific comments and some technical corrections follows below.

Specific comments

Title: either change the title to reflect the fact that you only look at snow covered surfaces, or extent your analyses to include the regions that are not (seasonally) snow covered. The title has been changed to specify the areas where this paper is applicable: "In situ observed relationships between ice surface skin temperatures and 2 m air temperatures in the Arctic

Present uncertainties. The spread in your results is large, but you do not present any uncertainty estimates.

Uncertainties have been added throughout the paper

Present your results with more confidence. There are numerous sentences that give me the impression that you are not absolutely sure about the result and processes. See for example in the abstract L14-19.

Some formulations might have been too vague, leading to confusion about what we mean. We have gone through the manuscript and clarified what we mean.

Abstract

You do not present any uncertainties in the presented numbers, while the results clearly show a large variability. Numbers are now presented as ranges.

P1 L14-19: Present this differently: first describe the process, then the result. Thus first that there exists a very persisten surface based temperature inversion driven by radiative cooling. Done
P1 L21-22: Formulate more direct, this is not a new insight but already found for Antarctica. Done
P1 L24-28: Formulate more direct: this is basically the new result of your research. Start with the why this is so interesting, then the result. Leave out the last sentence. This should already be clear. Done

Introduction
P2 L10: How does the Arctic contribute to mid latitude weather events.
Text changed to: "Further, the Arctic warming may contribute to mid latitude weather events (Cohen et al., 2014; Overland et al., 2015; Vihma, 2014; Walsh, 2014)"
P2 L28-29: Add what the rationale was of the other studies, and what the rationale is for this study. Being the first to do something is not enough.
As stated above, we have refocused the abstract and introduction to focus upon the large potential in improving the global surface temperature products.
P2 L23, P3 L8: I appreciate that you bring together all these different studies, but in the end you do not provide any new insights.
As stated above, we have made it clearer that this study delivers an unprecedented number of in situ observations and enables the use of satellite products for estimating T2m.
Other studies have not had the focus on deriving a statistical relationship between Tskin from satellite and T2m. We therefore deliver an analysis with a different aim than previously and covering a range of sites, years and Arctic weather conditions never included before. Hence, the conclusions are much more robust and representative compared to previous studies using single records. This is crucial when developing a statistical method covering vast areas. This has been highlighted in the text.
P3 L10: But you limit yourself to snow covered areas and periods only. This limits the applicability of this study in terms of the whole Arctic. The title has been changed to specify the areas where this paper is applicable, which is snow and ice covered surfaces only.
P3 L20: Reformulate, as far as I know Tskin is never observed, it is always derived from a radiative flux, not measured by a radiometer. This has been reformulated.

Data
How do you handle the different lengths of the time series? What do you present when you present averages? Period or Annual averages? Period averages might be biased to a certain season.
Time series of more than a year have now been updated in such a way that they cover an integer number of years to avoid bias towards a certain season.
P3 L29: For the PROMICE stations why did you not include the stations in the ablation area? The processes there are similar to sea ice or melting snow surfaces. The stations we have included do include the ablation area, but in the middle/upper part. However, based on this suggestion we have decided also to include all available PROMICE stations located on the Greenland Ice Sheet including the stations in the lower part of the ablation zone. These have been assigned to a new category: lower ablation zone and all figures and tables have been reproduced.
P4 L1 (and for the other data sets as well): As far as I understood, you do not correct for the changing height of the sensors due to accumulating and melting snow. However, under strong inversion conditions, it is crucial to correct for height changes because it seriously affects your estimated temperature difference between surface and 2 m air temperature. This is a very good point and it has been checked that the overall results do not change if we limit our observations to those obtained in the height 2±0.1 m. These results have now been included in the discussion section and referred to in the Data section.

P4 L9: An albedo of 0.3 is already very low. How much do patches of snow free surface impact the results? And how much data is left when you filter these data out. The albedo is set to the low value of 0.3 to make sure we avoid cases with no snow or ice present as these cases are not included in this analysis (see Good et al., (2017) for a similar analysis over land surfaces).
P4 L18: Are these measurement heights constant? The fact that it works better when taking the 1 m data is not a motivation to take the 1 m data instead of the 2 m data.
We have reformulated this to explain that we do not use the T2m observations here, as we cannot rule out a systematic temperature error in the T2m observations. We now highlight that the use of 1 m observations will lead to a better agreement with Tskin, but that the observations are important for assessing the dependency on other parameters, such as cloud cover and Tskin.
You should correct for height changes any way and recalculate all to 2 m, and when making a choice there must be a scientific rationale behind it.
We have screened the data to include only observations within 1.9 to 2.1 meters and found very small overall differences to using all the data (< 0.2°C for the all-months, all-sky, numbers in Table 2). To have more consistent results, we therefore chose not to screen the data for height. For the observations on Sea ice, we have no further information on the actual height of the data. We have addressed this in the discussions section. We estimate that trying to adjust and compensate for the differences in heights would have larger uncertainties that 0.2, which is why we have not considered this approach.
These points have been added to the discussion section.
P5 L5: Provide reference on which you base these conclusions. Reference added: (Persson, 2002)
P5 L17: How do you retrieve air temperature from these 'profiles'? The profiles are not used in this study, we have therefore deleted the part where we mention the profiles.
P5 L28-32: Here you state that you do not correct for height changes, but this impacts your results. You should correct for it, and at least discuss the impact on your results, and how this affects the uncertainty. See the comment above. We have addressed this in the discussion section
P8 L1-13: Not clearly formulated. What do you mean with 'cold sky'? And what are the 'sky effects'?
We have removed "cold" and reformulated to stress that the sky is typically seen as cold in the infrared during cloud free conditions.
P8 L14: Why not present a scatter plot showing this, and provide more statistics, what is the Root mean square difference?
A scatter plot is now provided for the DMI_Q (the ARM data contains millions of observations, not suitable for scatterplots). However, the overall bias and rms is provided.
P8 L19: Please note that the cloud cover you derive this way is not the same as the cloud cover derived from visual inspection. Better use the term Long wave equivalent cloud cover (Kuipers Munneke et al., Int J. Climatol., 2011) Kuipers Munneke et al also describe the method presented here very clearly. The subsection title has been changed to "2.8 Longwave-equivalent cloud cover fraction" and it should be clear that the cloud cover fraction is actually calculated based on the longwave radiation balance.
P8 L23: This relation varies from station to station. Why not use the observed Long wave radiation and air temperature to derive a relation for each station as done by van As? This is exactly what we do. It is hopefully stated more clearly now after the sentence "from all individual observation sites" has been added.
P8 L26: How do you determine cloudy conditions? Different relation per station or not? See comment above. The calculated cloud cover fraction (CCF) ranges between 0 and 1, and later in the paper we assume that cloudy conditions occur in cases where CCF>0.7 and clear-sky conditions are assumed when CCF<0.3 (stated at p. 17, l. 1 in percent, which has now been changed to fractions throughout the paper)

P9 L6-8: This is not correct. M is either 0 or positive, where positive energy is used for melting. When there is no melt, the ground heat flux G is responsible for heating AND cooling of the snow surface. In general, the snow surface will be below 0 in this case and water can refreeze in the snow pack. Rephrase.
"All fluxes are positive when adding energy to the surface and a positive net surface energy balance results in warming the surface, if the temperature is lower than the freezing point of water, or for melting snow and ice (latent heat) if the temperature is at the freezing point. When the surface energy balance is negative the snow/ice will cool thus driving the conductive heat flux from warmer layers below. If the surface is melting a negative energy balance results in freezing of liquid water."
P9 L14-16: Reformulate: use the term 'individual radiative fluxes' instead of 'large incoming ....'. Also be clear about what surface your are talking about. In this case you refer to papers all about the greenland ice sheet, but write also about 'ice growth'. That is confusing. Changed to: "On average, the non-radiative fluxes are an order of magnitude smaller than the radiation fluxes. However, because the net radiation balance is small compared to the individual radiation fluxes then variations in SH and LH fluxes are anyway important for the total surface energy balance and thus the surface temperature."
P9 L18: Incorrect. The surface indeed cools compared to atmosphere. This is due to the fact that the emissivity of the surface is about 1 while from the atmosphere is 0.6-0.7 depending on moisture content. As a result the surface will even cool when surface and air temperature are the same. In case of clouds the difference is much smaller. Changed to: "During winter and clear-skies when SWd is negligible LWu is higher than the LWd. This drives a positive sensible heat flux and it results in a stable stratification of the lower atmospheric boundary layer (Maykut, 1986)". The impact of clouds is presented in the end of this chapter.
P9 L8: Remove all parts relating to the direction of the wind. It is not of interest in this paper and what you describe is also very specific for glaciers and ice sheets. Furthermore, he 45deg is also incorrect, the angle depends on strength of temperature inversion and surface slope, and with that on wind speed itself. See Ball, 1960. The parts have been removed as suggested.
P9 L25-27: What is the difference between inversion and katabatic winds? As far as I know they are the same. Better use only one term. There is a difference in why a surface based temperature inversion develops that forces these winds, either because of a negative radiative budget or a surface that is limited in temperature to the melting point. In the later case the resulting wind is often referred to as glacier wind.
In the case of PROMICE sites on GrIS we will refer to katabatic winds and in the case of interior Antarctic studies these winds are referred to as inversion winds for consistency with referenced studies.
P9 L29: Effect of clouds is more complicated: clouds change the effective solar zenith angle, and it changes the spectral properties of the radiation, with that it changes the albedo and the amount of short wave absorption can actually increase. You do refer to this later in the manuscript. Changed to: "Clouds play a complex role in the Arctic surface energy budget e.g. they both reflect SWd leading to a cloud shortwave cooling effect, and absorb LWu and emit LWd, which tend to have a warming effect."
P9 L32: Formulation: replace 'More transparant' with 'lower emissivity and with that absorptivity'. Done
P10 L1: Correct but also explain why. We don't think it is necessary to go into much detail here but readers are referred to the following (Curry et al., 1996; Curry and Herman, 1985; Zygmuntowska et al., 2012). The sentence has been rephrased slightly.

Results

In presenting your results you illustrate the results with results from individual stations without motivating why you show a certain station.
Now we show results for each category, whenever we believe it makes sense. In cases where it does not make sense we have addressed why.

Furthermore, you basically have three different types of stations, ice sheet, sea ice and seasonal snow cover sites. I recommend that you present the results in terms of these three characteristics. This way you remove the bias in your presented results towards the Greenland ice sheet sites. This has been done now and we have also included the PROMICE stations located in the lower ablation zone. The observations sites have been divided into 5 different categories: sites in the accumulation zone, upper/middle ablation zone, lower ablation zone, seasonal snow cover, and sea ice.

P10 L10: Please check the accuracy with which you present these results: three digit is too much. Also note that these high correlations are not surprising since the annual temperature cycle is dominated by short wave radiation. It would be strange if the correlation was low. But you need to explain why the correlation is high. Changed to two digits. The correlations reported here are calculated for observations within each month, separately, which means that the annual cycle is not included. This has been clarified in the text and the high correlations are explained with hourly fluctuations in temperature and the diurnal cycles found in both records

P10 L13: Is it correct that the maximum in T coincides with max in Sin? Usually max in T is later than the max in Sin because Sin keeps heating up to close before sunset, usually resulting in a max in T later in the afternoon. This has been rephrased.

P10 L8: Why do you show one station as example? The strength of this paper lies in the large number of sites. Try to utilize that more, by presenting averages per different type of station (ice sheet, sea ice and seasonal snow, melting surface/non melting surface).

The general temperature level depends upon the altitude and latitude of the station and averaging the absolute temperatures do not make sense wrt figure 3. Instead we have now explained that the seasonal behavior is typical for the other stations by adding sentence:

"The seasonal variability in the diurnal temperature at KAN_U is representative of the conditions at the other stations, except for the general temperature level at each station that changes with latitude and altitude."

For the other figures, we have tried to combine more stations into the figures (e.g. Fig. 6 and 14) , or mention that the results are representative for what we show

Furthermore try to explain more and more often link to why this is important for the ultimate goal: satellite retrieval of T2m.

The aim with the paper and the link between our work and the derivation of T2m from satellites has been added here and several other places in the paper

P10 L15: Explain why the largest variability is found in spring and winter. Done

P10 L22: Not surprising that EGP is the coldest, but explain why. The sentence "due to its high elevation" has been added.

P11 L1-2: Not surprising as well, melt in summer limits the surface temp while local circumstances dominate winter. Explain. Sentence has been changed to: "All sites reach a maximum in Tskin in July, regardless of latitude. July is also the month with least variation in temperature among sites, where melt at most stations (exception is ACC sites) limits Tskin, while the winter months show a larger variance in Tskin among sites since local circumstances are dominating Tskin."

P11 L5: I do not agree. In summer sea ice stations have a melting surface, in winter they are cold because they are further north. Not comparable to the coldest sites from Greenland. It is a combination of the melting sites on greenland in summer and the coldest sites in winter when latitude has the same impact as altitude.

This is not what we meant, and the sentence has been rephrased.

P11 L10: Formulate more direct, this is not only probably, but very likely the effect of melt limiting the surface temperature. Range in spring and autumn is largest since it can already cool significantly at night, but still warms during day by the sun. Note also that this spring and autumn signature is not restricted to arctic sites, nor snow covered sites. The sentence has been changed to "This is very likely an effect.."

P11 L11: Formulate more general: this also is true for the lower sites on Greenland, and in Spring for the seasonal snow cover sites. For any snow surface that is melting in summer. Rephrased to: This constraint is seen during spring or summer at almost all data records included in this study (exceptions are the ACC sites).
P12 L6: Why don't you show a figure with the annual cycle in temperature inversion for all sites similar to figure 4 and 5? Then combine 4, 5 and Tinv figure into 1 figure with panels a-c. That provides more information on whether the mean annual cycle is biased to a certain type of stations, for example the Greenland ice sheet sites, and the lack of sites with seasonal cover. Note also that seasonal snow covered areas have in spring the same signature as sea ice and greenland margins, but not in autumn, since it does not have snow yet. That will affect this relation, and cannot be judged in the presented figure. We have now combined the three mentioned figures into one, and left out the original Fig. 6, which indeed mixed the signal from different surface types. However, we do not include data from the seasonal snow covered sites at times without snow cover.

P13 L8: Peak in the diurnal cycle of what parameter? Changed to "During summer the difference decreases and the weakest vertical stratification is found around noon or early afternoon..."

P13 L10: Describe more in processes besides stating what can be seen in the figures. In this case: At night net radiation is negative thus cooling the surface. Sentence changed to "At night the net radiation is negative, thus cooling the surface resulting in a surface-based inversion"

P13 L11: Explain why Tinv is generally higher at KPC_U compared to KAN_U, explain. Figure has been changed to illustrating the surface types ACC and LAB and differences/similarities have been explained.
P13 L11-12: Again, not surprising, since the processes are the same, but explain why it is similar. See comment above.
P13 L14: Rephrase. The term 'due to' does not explain the link between wind speed and the turbulent fluxes. Rephrased to "The surface wind speed is an important component in the near surface thermal stratification since the turbulent mixing increases as a function of wind speed."
P13 L17-18: Rephrase, it is not the elevation that determines the wind speed for Greenland, but the slope. Stronger radiative cooling does not necessarily result in higher wind speeds. Flat terrain there is no link between them. This is exactly what we mean by the sentence "provided a surface slope is present". This sentence has been changed to: "provided a comparable surface slope is present" for clarity.
P13 L19-20: Explain!! These are all sites for which the wind is determined by large scale synoptice conditions combined with local topography, while the Greenland sites the wind is localy generated based on surface slope and inversion strength. Thus totally different origins and signatures. Changed to: "The surface radiative cooling and the terrain play the primary role in the generation of the surface winds (van As et al., 2014). Surface winds at the PROMICE sites in general have a high directional persistence (see Fig. 4 in van As et al., 2014), commonly blowing from inland, which is a strong indication that local winds are often katabatic winds. High elevation sites experience stronger winds due to the larger radiative cooling of the surface (provided a comparable surface slope is present; Fig. 8; van As et al., 2014). The SSC and SICE sites show less variability in wind speed on annual basis. At these sites the wind is determined by large scale synoptic conditions combined with local topography."
P14 L3-4: Reformulate and make sufficient reference to existing literature. The relation between inversion and turbulent mixing is well known. Reference has been added
P14 L5-9: It would be much more interesting to show something like net radiation in colloring instead of counts. You also do not need to binn the data for that but simply show scatter plots. You only need to bin to

calculate the mean. Furthermore, this information is all caption information and not necessary to put in the main txt. The bin information has been moved to the figure caption. We think it is important to keep the information provided in this figure, as the middle panel indicate the number of data and the shape of the distribution (e.g. uni or bimodal) for every wind interval that is used to calculate the mean and standard deviations in the upper panel. Scatter plots with many data tend to be hard to interpret in the same way. We therefore decided to keep these figures.

P14 L9-10: Refering to figure 9, why not make plots of the different type of stations combined. Thus a plot for the greenland station, another for the sea ice stations and the last for the seasonal snow covered stations. And then explain the different signatures.

In the ideal world, we would have one figure for each station. However, considering the length of the paper and the representativeness, we decided to show these two figures as examples. Merging stations with different latitudes and wind regimes would mess up the conclusions reached here, as the strength of the inversion changes with latitude and altitude. The wind dependency effect in the two examples shown here is, however representative of all the stations. This has been clarified in the text.

P14 L13: Rephrase sentence. Stress the local maximum , not the minimum below 2.5 m/s. Thus turn this sentence a bit around. The sentence has been rephrased

P15 L6: When refering to the PROMICE sites explain that it is basically all sites with a surface slope where a katabatic flow develops. This has been explained in the beginning of the section "Surface winds at the PROMICE sites in general have a high directional persistence (see also Fig. 4 in van As et al., 2014), commonly blowing from inland, which is a strong indication that local winds are often katabatic winds."

P15 L6-7: Remove the part about comparing the temperatures and rephrase: and was also found by Adolph et al, 2017 for the summit station. (Not that it would be strange if Adolph had found something else than you, since he/she uses the exact same data!!! However, since this is a feature likely katabatically forced I am surprised you also found it for summit, or has this site still a sloping surface? The first part has been corrected but the latter part is incorrect. We do not use the same data as Adolph. She uses data from the Summit station only, while we use PROMICE data which contains no data from the Summit station (see Figure 1). However, in Adolph's paper you can see the same wind effects (Figure 7) for the Summit station.

P15 L11-17: Rephrase this. Not necessary to explain how they studied this, this is also not unexpected but known phenomena and it is also not surprising but to be expected to see this for Greenland as well. There is basically no difference in the inversion winds for Greenland or Antarctica, processes are the same. Only difference is that Greenland is located a bit closer to the equator and also has sites where the melting surface restricts the surface temperature creating an inversion instead of only a negative radiation budget. This bit gives the impression that you are not familiar with the processes. This part has been rephrased.

P16 L6-14: Remove the part relating to wind direction. For the general discussion, I do not see the point in discussing the wind direction. It is very specific on an ice cap, while here your goal is to be much more general in aid of satellite retrieval. We agree on this, and all parts related to the wind direction have been removed.

P16 L10: I do not agree that 10b supports the hypothesis. Basically all vallues of cloud cover are with this wind direction, which is to be expected since most of the time the wind is katabatic, downslope. Remove the link with cloud cover here. See comment above (figure has been removed)

P16 L12-13: It is correct that less clouds result in more cooling (in winter) but from the figure the same wind direction also has the highest cloud cover, thus what does this tell us? See comment above (figure has been removed)

P16 L13-14: In my opinion these results do not support the Hudson and Brandt result. This part has been removed.

P16 L15-17: This is something you should mention much earlier, since it compromices your general discussion. This part has been deleted.

P16 L21: Please explain why you want to estimate the bias: Something like: in aid of satellite retrieval, the retrieval is done using clear sky conditions only, this is therefore not the average inversion strength, we define the bias here.
We have included a sentence about the cloud free satellite observations and the need to assess this effect in order to facilitate the combinations of in situ and satellite observations.
P17 L4-6: Please explain why. Only stating what we can see in the figure is not sufficient. We think it is outside the scope of this paper to explain the detailed variability in the cloud cover for all stations. The figure should however be used to interpret the clear-sky biases observed in Fig. 12 and the impact of clouds on the inversion strength at different regions.
P17 L9-10: Explain why you look at these individual sites, but better to group them given certain characteristics. (ice sheet vs sea ice vs seasonal snow covered regions. As suggested we now consider the surface categories: ACC, UAB, LAB, SSC, and SICE at made a plot like this for each surface type. However, we decided not to include the figures due to the length of the paper. However, we have put in a few lines on what we see.
P17 L10-11: Again: explain, only stating what we see is not enough. This figure has been removed.
P18 L1: Bin size of what? Explain. Bin size of CCF. The information has been added in the figure text.
P18 L3-6: Also note the large spread! This makes generalizing the results almost impossible. You have to remark on this. Uncertainties have been added to the average slope of each category.
P19 L11: Explain why and is this significant given the spread in different sites? An explaination has been added based on the new categories and ranges have been added to the numbers in Table 2.
We have put in an explanation about the relationship between cloud cover, humidity and differences between Tskin and T2m.
P19/20 L17/L1: What is it that is generally derived from satellites? Tskin or T2m? In case of Tskin, you do not need the whole discussion about inversion strength. In case of T2m, it is important! Please introduce this better.
To reach a representative T2m estimate from temporally averaged satellite derived Tskin, we both need to take into account the inversion strength and the clear sky effects. This has been clarified in the text.
P20 L2-3: What do you mean by 'given time window'? Time window of the gap? Is there a linear interpolation to fill the gap? Or are averages determined over a given window assuming how many satellite retrievals to be necessary to be representative for that period?
No manipulation has happened to the data and we average the available satellite observations within a given time interval. This has been clarified in the text
P20 L3-5: Thus 2 issues: the bias resulting from only using clear sky observations, and the impact of averaging over given time window on the retrieved temperature: Rephrase to make this more clear.
There is only one issue. The clear sky bias only enters when we perform temporal averaging of the data. The paragraph has been rewritten to clarify what we mean with clear-sky bias and temporal averaging.
P20 L7-8: What is the uncertainty? The spread is enormous, so are the values significantly different? The numbers have been removed as we now have 5 categories and it is easier to read directly from the figure.
P20 L8-10: Explain! For example: how does this relate to the way cloud cover is determined? Cloud cover from LWd is not the same as the visual determined cloud cover! How is cloud cover marked in the satellite images?
The satellite cloud screening procedures are not only based upon visible information. The cloud masks use all available information from satellite and NWP, including the thermal Infrared channels. It is outside the scope of this paper to examine the detailed relationship between empirical cloud mask estimates and the satellite cloud screening procedures. We have reformulated the paragraph to include the assumption about the cloud masks.
And why the strange differences between 24, 72 and month?
The larger differences for increased temporal windows are an effect arising from persistent cloud cover for several days. More cloud covered (warm) observations are included in the calculation of e.g. the 72 hours

averages, compared to the 24 hours. This results in a larger clear sky effects. This explanation has been added to the text.
P20 L15: Explain the positive bias over sea ice in spring. The figure has been removed
P20 L18-19: Regarding your statement ’which may.... bias observed’ You have the data to confirm this, to test what the impact is of the omission of certain seasons. Please do so. This has been confirmed and rephrased.
P21 L6-9: I don’ understand what you want to say in this sentence? what does the determination of cloud cover has to do with the T2m determination? That is based on Tskin anyway. Reformulate to make more clear.
The sentence has been reformulated
P21 L13-14:Relating to the FRAM stations: What is the conclusion? Explain. After communication with the data provider we found out that it was more appropriate to use another temperature measurement. This resulted in a more consistent behavior of the station.
P21 L15: Please also present uncertainties! Is the slope presented here significant? Uncertainties have been provided for each of the categories.
P21 L15-16: Can be useful is rather a weak conclusion. Much stronger to come with a clear recomendations, else you only present known phenomena. Reformulated
P22 L3: I have a preference of integrating the discussion in the result sections. That way you do not need to repeat the results here and immediate can answer the questions arising from the presented results. The Discussion section than only contains an additional discussion based on all results. We have chosen to keep them separate as the discussion section has updated and extended.
P22 L5-7:First present an explanation, then state that others found the same thing.
P22 L10: Present uncertainties in the numbers. Ranges have been added for each category.
P22 L19-21: Nothing new, please reformulate: Keep it simple and more professional: The relationship is more complicated over sloping terrain..... Done
P23 L4-7: Reformulate, does not explain anything: what you want to say is that the inversion combined with slope results in a flow which actually destroys its own forcing. As a result there is a optimum in inversion strength and wind speed. Which was also found by Hudson and Brandt. This has been rephrased.
P23 L10-13: Why would Greenland be different? Physics does not change! You even see katabatic winds on much smaller ice caps. Physics is the same, thus the same conclusions. See comment above
P23 L14-18: This is a repeat from the results section. Try to prevent that as much as possible. This has been rephrased.
P23 L25: Why not show a scatter plot showing the relation of Tskin determined by the two different methods. Should be as much as possible on a 1-1 line. Then it is easy to say that the presented results are similar. This has been presented for the DMI_Q in Fig. 3.
P23 L31-32: Rephrase the sentence ’In general... time interval’. The sentence is confusing. The sentence has been rephrased.
P24 L8-10: Rephrase: satellite skin temeratures are often compared to 2 m air temperatures, not the local skin temperatures. Remove reference to ’surface’ air temperature.
The sentence has been rephrased.
P24 L16: I do not agree that you present a wide range of weather conditions: Your presented results are strongly biased towards the Promice Greenland stations, and you present only limited number of seasonal snow cover sites. This has been rephrased.
P24 L18-22: I had hoped for a stronger conclusion. For example what do you need to do to correct a satellite retreived Tskin for T2m?
The conclusion has been rewritten to emphasize the significant findings in this study and to draw the lines to the introduction about the improved climate change assessment through a satellite derived T2m product.

Technical corrections

Introduction
P2 L17: Replace 'important' with 'sensitive'. Done
P2 L23: Formulation is not correct or confusing: there are four radiative flux components, not two. Rephrase. Changed to: The inversion exists because of an imbalance between the radiative fluxes, leading to a cooling of the surface, especially when the absorbed incoming solar radiation is small (during winter and night).
P3 L19: Remove 'to assemble.... study'. Done

Data
P3 L27: Figure 2 is presented before figure 1. Figures should be referenced in order consecutive order. The order of figures has been changed.
P3 L30: Provide sensor information. You do that for other data sets as wel, or remove the sensor information from the main text and provide in a table. The sentence has been updated to: PROMICE Tskin has been calculated from up-welling longwave radiation, measured by Kipp & Zonen CNR1 or CNR4 radiometer, assuming a surface longwave emissivity of 0.97.
P5 L28-32: Move to start of data description section. (P3 L21) Done
P9 L22: Replace 'where' by 'when'. Done

Results
P10 L13: Check your use of colder / warmer versus lower / higher. Tskin is lower than T2m, not colder. Done
P14 L3: Remove sentence: 'This section... to wind.' Rather obvious. Done
P14 L5-6: Remove sentence 'the number ... (red curve).' Not of interest. Deleted as it is already stated in the figure caption.
P14 L11: Replace 'gradients' with 'difference'. Done
P14 L12: Replace 'can sometimes be' with 'is'. Formulate more direct. Done
P14 L12: Replace 'complicated than that' with 'complex'. Done
P15 L6: Replace 'for' with 'to'. Done
P15 L7: Replace 'find' with 'also found'. Done
P15 L8: Replace 'using' by 'at Summit based on', and remove 'at summit' at the end of the sentence. Done
P15 L9-10: Rephrase: Also at .... wind.' With 'Furthermore, Hudson and Brand (2005) show that at south pole the maximum inversion strength occurs at wind speeds of 3-5 m/s. They suggest that it is not the weak wind promoting the strong inversion, but the inversion forcing the air flow resulting in an katabatic wind.
Sentence has been changed to: "Furthermore, Hudson and Brandt (2005) show that at the South Pole the maximum inversion strength occurs at wind speeds of 3-5 m s^{-1}. They suggest that it is not the weak wind of 3-5 m s^{-1} that promotes the strong inversion, but the inversion which forces the air flow resulting in an inversion wind."
P18 L1: Replace 'considering' with 'for'. Done
P18 L2: Remove 'the obvious feature is that'. Done
P18 L3: Replace 'from' with 'due to'. Done
P18 L3-6: Not necessary to mention 'considering all observations/sites' three times in one sentence. Remove. Done
P20 L10: Insert 'monthly' between 'the' and 'mean'. Done
P20 L11-12: Remove 'averaged for each month' Done
P20 L14: Replace 'may be a result of' with 'can partly be explained by' Done
P22 L22: Remove 'a few', replace 'in' with 'for' Done

P22 L22: Add reference to Adolph et al for GrIS. Done
P23 L1: Remove ’The feature...Adolph et al., (2017)’. Done
P23 L1: Reformulate ’It is likely that this feature..’ by ’This feature can be explained by the forcing of a katabatic wind by the surface temperature inversion.’ Changed to: “This feature can be explained by the forcing of a katabatic wind driven by the surface temperature inversion over a sloping terrain.”
P23 L2: Remove ’persistently....terrain’. (remove all reference to wind direction) This has been removed
P23 L3: Remove ’but also other factors such as’. This has been removed
P23 L4: Remove ’coriolis force’. Coriolis only changes the direction of the wind, does not have impact on the strength. This has been removed
P23 L7-9: Remove ’We find that..... at the surface’. (remove all reference to wind direction) Done
P23 L12-13: Remove ’More research... vice versa.’ Done
P23 L18: Replace ’The explanation is that’ with ’The smaller inversion strength under cloudy conditions is explained by the fact that ’ See below.
P23 L18: Remove ’in the Arctic’ Changed to: “The smaller inversion strength under cloudy conditions is explained by the fact that clouds have a predominantly warming effect on the surface in the Arctic.” We believe that “in the Arctic” should be there, as the statement is not true globally.
P23 L20: Remove ’the T2m ...Tskin instead. Done
P23 L22: Replace ’that finds’ with ’who found’ Done
P23 L24: Replace ’are’ with ’is. Done
P24 L5: Replace ’thought to play an important role in’ with ’factors (partly) explaining the’. Done
P24 L15: Replace ’gathered’ with ’used’. Done
P24 L17: Remove ’Historical and present..... T2m observations’. I do not understand this statement. Removed “Historical and present”

Figures and tables
Table 1. You incorrectly classify the arm stations as land ice. They should be classified as seasonal snow covered. This has been changed as suggested.
Table 2. I am missing an indication of variability. The spread as show in figure 13 is enormous!! This should be visible also in these results. Furthermore, I also think you should not put the ARM sites and sea ice sites together. Very different characteristics. 3 categories: sea ice, land ice and land! As suggested the categories have been changed and a range in temperature difference among the sites included in each category has been added to indicate the variability.
Figure 3: Use different y-axis for Temperature and temperature difference. In the present figure, I cannot see the cycle in the temperature difference. Done
Figure 6: present the standard deviation as a band of uncertainty around the mean. And explain what the standard deviation indicates: variability between stations of between different years? Or both? The figure has been deleted and replaced with figure as suggested (P12 L6).
Figure 9: I am not really interested in counts. This figure can be much more instructive when presented as a scatter plot of Tinv as a function of wind speed with coloring of the net radiation. The mean can be plotted in the same figure as a black line and the standard deviation as 2 extra dotted lines around the mean. And the lower plots can be left out. We think it is important to keep the information provided in this figure, as the middle panel indicate the number of data and the shape of the distribution (e.g. uni or bimodal) for every wind interval that is used to calculate the mean and standard deviations in the upper panel. Scatter plots with many data tend to be hard to interpret in the same way. We therefore decided to keep these figures.
Figure 10.: Remove figure. Not interesting in the scope of this manuscript to discuss relation with wind direction. Done

Figure 15: What is the variability in the averages? You can introduce lines that indicate the standard deviation. Explain how you make these averages. Are these averages over all observations? or have you first made annual averages? Could there be a seasonal bias as you explain for DMI_Q. The averages are made by averaging all-sky Tskin temperatures and clear-sky (CCF<0.3) Tskin temperatures separately over a given time window (24 h, 72 h, and 1 month), subtracting the two temperature estimates and finally the average is taken over all temperature differences. If we only have clear-sky observations at a certain season, then the clear-sky bias will be biased towards that season. If we have entire days without clear-sky observations these will be missing values in the 24 h averages. However, if we move to a longer time window the all-sky Tskin of these days will be reflected in the monthly clear-sky bias even though the corresponding clear-sky Tskin is missing.

Figure 16: For me it is more logical to present this in 3 categories instead of 2. (Ice sheet, sea ice and seasonal snow covered.) Present the standard deviation as a band around the mean. What do the standard deviations represent? only variability based on the different stations? Or also an indication of interannual variability? The figure has been changed since the categories are changed and the standard deviation has been included as a band around the mean. Only categories which consist of full year continuously records have been shown. UAB look similar to LAB and is therefore not shown. The standard deviations indicate interannual variability, which has been averaged for all stations.

References

Note that the international custom is to list surnames starting with ’van’ under ’v’ in the alphabetical order. Done

In situ observed relationships between snow and ice surface skin temperatures and 2 m air temperatures in the Arctic

Pia Nielsen-Englyst[1], Jacob L. Høyer[1], Kristine S. Madsen[1], Rasmus Tonboe[1], –Gorm Dybkjær[1], ~~Rasmus Tonboe[1],~~ Emy Alerskans[1]

[1]Danish Meteorological Institute, DK-2100 Copenhagen Ø, Denmark

Correspondence to: Pia Nielsen-Englyst (pne@dmi.dk)

Abstract.

To facilitate the construction of a satellite derived 2 m air temperature (T2m) product for the snow and ice covered regions in the Arctic, observations from weather stations are used to quantify the relationship between the T2m and skin temperature (Tskin). Multiyear data records of simultaneous Tskin and T2m from 29 different in situ sites have been analysed for 5 regions, covering the lower and upper ablation zone and the accumulation zone of the Greenland Ice Sheet (GrIS), sea ice in the Arctic Ocean, and seasonal snow covered land in northern Alaska. The diurnal and seasonal temperature variabilities and the impacts from clouds and wind on the T2m-Tskin differences are quantified. Considering all regions, T2m is on average 0.65-2.65°C higher than Tskin, with the largest differences for the lower ablation area and smallest differences for the sea ice sites. A negative surface radiation balance generally makes the surface colder than the atmosphere, resulting in a surface-driven surface air temperature inversion. Tskin and T2m are often highly correlated, and the two temperatures are almost identical (<0.5°C) at particularly times of the day and year, and during certain conditions. The data analysed here show the best agreement between Tskin and T2m around noon and early afternoon during spring and fall. However, Tskin is often lower than T2m by more than 2°C, with the largest differences occurring, when it is cold or when the surface is melting. In general, the inversion strength increases with decreasing wind speeds, except for the sites on the GrIS where the maximum inversion occurs at wind speeds of about 5 m s^{-1} due to the katabatic winds. Clouds tend to reduce the vertical temperature gradient, by warming the surface, resulting in a mean T2m-Tskin difference ranging from -0.08°C to 1.63°C, with the largest differences for the low ablation zone sites and the smallest differences for the seasonal snow covered sites. To assess the effect of using cloud limited Infrared satellite observations, the influence of clouds on temporally averaged Tskin has been assessed by comparing averaged clear-sky Tskin with averaged all-sky Tskin. The clear-sky effect has been assessed for temporal averaging windows of: 24 h, 72 h and 1 month. The largest clear-sky biases are generally found when 1 month averages are used and smallest for 24 h. In most cases all-sky averages are warmer than clear-sky averages, with the smallest bias during summer.

~~To facilitate the combined use of traditional 2 m air temperature (T2m) observations from weather stations in the Arctic and skin temperature (Tskin) observations from satellites the relationship between high latitude snow and ice Tskin and T2m is quantified. Multiyear data records of simultaneous Tskin and T2m from 20 different in situ sites have been analysed,~~

~~covering the Greenland Ice Sheet (GrIS), sea ice in the Arctic Ocean, and coastal snow covered land in North Alaska. The diurnal and seasonal temperature variabilities and the impacts from clouds and wind on the T2m-Tskin differences are quantified. Considering all stations, T2m is on average 1.37°C warmer than Tskin, with the largest differences at the GrIS stations (mean of diff. of 1.64°C). Tskin and T2m are often highly correlated, and the two temperatures are almost identical (<0.5°C) at particularly times of the day and year, and during certain conditions. The data analysed here indicate the best agreement between Tskin and T2m around noon and early afternoon during spring and fall. However, Tskin is often colder than T2m by 2°C or more, with the largest differences occurring during winter, when it is dark and during night. This is seen for all observation sites, where a negative surface radiation balance makes the surface colder than the atmosphere, resulting in a surface-driven surface air temperature inversion. The observation sites on sea ice and in Alaska show that the surface-based inversion decreases as a function of wind speed, because of turbulent mixing. The sites on the GrIS show an interesting feature, with the maximum inversion occurring not at calm winds, but at wind speeds of about 5 m s~~$^{-1}$~~, likely due to the katabatic winds, which are most prominent at this wind speed. Clouds tend to reduce the vertical temperature gradient, by warming the surface, resulting in a mean T2m-Tskin difference of 0.53°C considering all stations. Following that the influence of clouds on Tskin has been assessed by comparing clear-sky Tskin observations with all-sky observations averaged for the time windows of: 24 h, 72 h and 1 month. The largest clear-sky biases are generally found when 1 month averages are used and smallest for 24 h. The mean clear-sky bias for the 24 h average is -0.28°C, ranging from -0.10°C in summer to -0.95°C in winter. The expected clear-sky biases and the difference between Tskin and T2m are of practical value for researchers and operational users that aim at integrating satellite observations with ocean, sea-ice or atmospheric models.~~

1 Introduction

The Arctic region is warming about twice as much as the global average because of Arctic amplification (Graversen et al., 2008)~~(Graversen et al., 2008)~~. Greenland meteorological data show that the last decade (2000s) is the warmest since meteorological measurements of surface air temperatures started in the 1780s (Cappelen, 2016; Masson-Delmotte et al., 2012)~~(Cappelen, 2016; Masson-Delmotte et al., 2012)~~ and the period 1996-2014 yields an above average warming trend compared to the past six decades (Abermann et al., 2017)~~(Abermann et al., 2017)~~. The reason for the Arctic amplification is a number of positive feedback mechanisms, e.g.~~i.e.~~ the ice-albedo feedback which is driven by the retreat of Arctic sea ice, glaciers, and terrestrial snow cover. The atmospheric warming leads to a declining mass balance of the Greenland Ice Sheet (GrIS), contributing to global sea level rise. The increased mass loss of the GrIS partly comes from increased surface melt (Rignot, 2006), which is driven by changes in the surface energy balance. Several studies have focussed on the assessment of current albedo trends and their possible further enhancement of the impact of atmospheric warming on the GrIS (e.g. Box et al., 2012; Stroeve et al., 2013; Tedesco et al., 2011). However, recent studies have shown that uncorrected sensor degradation in MODIS Collection 5 data was contributing falsely to the albedo decline in the dry snow areas, while the decline in wet and ice areas remain but at lower magnitude than initially thought (Casey et al., 2017).~~, and a darkening of the~~

Formateret: Engelsk (Storbritannien)

~~Greenland Ice Sheet (GrIS). The atmospheric warming and decreasing albedo of the ice sheet have resulted in an accelerated mass loss of the GrIS over the past decade (Box et al., 2012).~~ Future projections of the GrIS mass balance show that the surface melt is exponentially increasing as a function of the surface air temperature (Franco et al., 2013)~~(Franco et al., 2013)~~. Further, the Arctic warming may contribute~~s~~ to mid latitude weather events (Cohen et al., 2014; Overland et al., 2015; Vihma, 2014; Walsh, 2014)~~(Cohen et al., 2014; Screen and Simmonds, 2010; Serreze and Francis, 2006)~~. It is therefore important to monitor the temperature of the Arctic to understand and predict the local as well as global effects of climate change. Current global surface temperature products are fundamental for the assessment of the climate change (Stocker et al., 2014)~~(Stocker, 2014)~~ but in the Arctic ~~traditionally they~~these data traditionally include ~~Arctic~~only ~~-~~near surface air temperatures from buoys and automatic weather stations (AWSs~~;)~~ Hansen et al., 2010; Jones et al., 2012; Rayner, 2003)~~(Hansen et al., 2010; Jones et al., 2012; Rayner, 2003)~~. However, in situ observations are not available everywhere and the time series have gaps and/or limited duration. In particular, the Arctic ice regions are sparsely covered ~~sparsely~~ with in situ measurements, due to the extreme weather conditions and low population density (Reeves Eyre and Zeng, 2017)~~(Reeves Eyre and Zeng, 2017)~~. The global surface temperature products are thus based on a limited number of observations in this very ~~important~~ sensitive region. This means that crucial climatic signals and trends could be missed in the assessment of the Arctic climate changes due to ~~by~~ poor coverage of the observational system.

Satellite observations in the thermal infrared have a large potential for improving upon the surface temperature products in the Arctic due to the good spatial and temporal coverage. However, the variable retrieved from infrared satellite observations is the surface skin temperature (Tskin), whereas current global surface temperature products estimate the 2 m air temperature (T2m; Hansen et al., 2010; Jones et al., 2012). An important step towards integrating the satellite observations in the near surface air products is thus to assess the relationships between Tskin and T2m as we do here.

~~A way to improve the spatial and temporal data coverage of the surface temperature is by the use of satellite remote sensing. However, current global surface temperature products estimate the 2 m air temperature (T2m; Hansen et al., 2010; Jones et al., 2012), whereas the variable retrieved from satellite observations is the surface skin temperature (Tskin).~~ A surface-based air temperature inversion is a common feature of the Arctic winter (Serreze et al., 1992; Zhang et al., 2011)~~(Serreze et al., 1992; Zhang et al., 2011)~~. The inversion exists because of ~~the~~ an imbalance between ~~outgoing longwave radiation and incoming solar radiation~~the radiative fluxes, leading to a cooling of the surface, especially when the absorbed incoming solar radiation is small (during winter and night). An analysis based on observations from the Antarctic Plateau showed that the inversion continues all the way to the surface with the largest gradient between the surface and 20 cm above it (Hudson and Brandt, 2005)~~(Hudson and Brandt, 2005)~~. The surface-driven temperature inversion causes a difference between the T2m and the actual skin temperature at the snow/air interface. Previously, work has been done to characterize the relationship between the T2m and land surface temperatures observed from satellites and identified land cover, vegetation fraction and elevation as the dominating factors (Good et al., 2017)~~(Good et al., 2017)~~. A ~~F~~few studies have investigated the temperature inversion in the ice regions for the lowest 2 m of the atmosphere focusing on limited time periods and single locations e.g. Summit, Greenland (Adolph et al., 2018; Hall et al., 2008)~~-~~, the South Pole (Hudson and Brandt, 2005)~~(Hudson and Brandt,~~

Feltkode ændret

Feltkode ændret

Formateret: Engelsk (Storbritannien)

Formateret: Engelsk (Storbritannien)

~~2005)~~ and the Arctic sea ice (Vihma and Pirazzini, 2005)~~(Vihma and Pirazzini, 2005)~~. Until now, no systematic studies have yet been made for the high latitude ice sheets and over sea ice.

The difference between the T2m and Tskin is very important in validation studies of remotely sensed temperatures. Several studies have used T2m observations for validating satellite Tskin products on the GrIS ~~(~~(Dybkjær et al., 2012; Hall et al., 2008; Koenig and Hall, 2010; Shuman et al., 2014)~~Dybkjær et al., 2012; Hall et al., 2008; Koenig and Hall, 2010; Pérez Díaz et al., 2015; Shuman et al., 2014)~~ and over the Arctic sea ice (Dybkjær et al., 2012)~~(Dybkjær et al., 2012)~~ and found that a significant part of the differences could be attributed to the difference between the Tskin and T2m. Conversely, Rasmussen et al. (2018) used satellite Tskin observations in a simple way to correct the T2m in a coupled ocean and sea ice model and obtained an improved snow cover.

In order to facilitate the integrated use of Tskin and T2m from in situ observations, satellite observations and models, there is ~~thus~~ a need for a better understanding and characterization of the observed relationship. The aim of this paper is to bring further insight into this relationship, using in situ observations. This study extends the previous analyses to include multiyear observational records from 29 ~~0~~ different sites located at the GrIS, Arctic sea ice, and the coastal region of ~~North~~northern Alaska. The aim is to identify the key parameters influencing the temperature difference between the surface and 2 m height and to assess under which conditions Tskin is, or is not, a good proxy for the T2m and to quantify the differences, using Tskin as a proxy for T2m. The findings are intended to aid the users of satellite data and to support ~~estimation~~ the derivation of T2m using satellite Tskin observations. In the response to the latter, an effort has also been made to estimate a clear-sky bias of Tskin based on in situ observations. The paper is structured such that Sect. 2 describes the in situ data. Section 3 gives an introduction to the near surface boundary conditions. The results are presented in Sect. 4 and discussed in Sect. 5. Conclusions are given in Sect. 6.

Formateret: Skrifttype: 10 pkt

Formateret: Skrifttype: 10 pkt

2 Data

In situ observations have been collected from various sources and campaigns covering ice and snow surfaces in the Arctic ~~to assemble the Danish Meteorological Institute (DMI) database used in this study~~. The focus has been on collecting in situ data with simultaneous observations of Tskin, derived from infrared ~~measured with a~~ radiometers~~,~~ and T2m~~,~~ measured with a shielded and ventilated thermometer about 2 m above the surface~~, in the Arctic~~. Table 1 gives an overview of the data and the abbreviations used in this paper. The data has been divided into five different categories based on surface characteristics and location: accumulation area (ACC), upper/middle ablation zone (UAB), lower ablation zone (LAB) of the GrIS, seasonal snow covered (SSC) sites in northern Alaska, and sea ice sites (SICE). All time series which cover multiple full years have been cut to cover an integer number of years (within 5 days), in order to avoid seasonal biases. The geographical distribution and elevations of all sites are shown in Fig. 1, while Fig. 2 shows the temporal data coverage. Observations from the sites in Table 1 include T2m, Tskin, wind speed, shortwave- and longwave radiation. Measurement heights vary depending on the site and snow depth, but for this paper near-surface air temperatures are referred to as 2 m air temperature despite these variations. The impact of these height variations are discussed in Sect. 5. Further details are provided for each data source in Sect. 2.1-2.6.

2.1 PROMICE

Data have been obtained from the Programme for Monitoring of the Greenland Ice Sheet (PROMICE) provided by the Geological Survey of Denmark and Greenland (GEUS). PROMICE was initiated in 2007 by the Danish Ministry of Climate and Energy, and operated by GEUS in collaboration with the National Space Institute at the Technical University of Denmark and Asiaq (Greenland Survey; e.g. Ahlstrøm et al., 2008). PROMICE collects in situ observations from a number of AWSs mostly located along the margin of the GrIS (Fig. 1~~2~~). Each observational site has one or more stations; typically one located in the lower ablation zone close to the ice sheet margin, and one or two located in the middle/upper ablation zone ~~and another located~~ near the equilibrium line altitude. Exceptions are KAN_U and KPC_U located in the lower accumulation area and EGP, which is located in the upper accumulation area. ~~Only the high altitude sites (elevation>500 m) have been used in this study in order to ensure year-round snow cover.~~ All 22 PROMICE AWSs located on the GrIS have been used in this study. PROMICE Tskin has been calculated from up-welling longwave radiation, measured by Kipp & Zonen CNR1 or CNR4 radiometer, ~~-~~assuming ~~blackbody radiation properties for snow and ice~~a surface longwave emissivity of 0.97 (van As, 2011). The air temperature is measured by a thermometer at a height of 2.7 m, while the wind speed is measured at about 3.1 m height, if no snow is present. Snow accumulation during winter reduces the measurement height. In this study, we use hourly averages of the data, provided by PROMICE.

2.2 ARM

The Atmospheric Radiation Measurement (ARM) Program (Ackerman and Stokes, 2003; Stamnes et al., 1999)~~(Ackerman and Stokes, 2003; Stamnes et al., 1999)~~ was established in 1989 and it provides data on the cloud and radiative processes at high latitudes. Three ARM sites from the North Slope of Alaska (NSA) are used in this study: Atqasuk (ATQ), Barrows (BAR), and Oliktok Point (OLI). The stations provide surface snow infrared (IR) temperature measured using a Heitronics KT19.85 IR Radiation Pyrometer (Moris, 2006)~~(Moris, 2006)~~ and air temperature measured at 2 m height. Wind speed is measured at 10 m height. The ARM stations have seasonal snow coverage, i.e. the snow melts away in summer. Data where the surface albedo is less than 0.30 indicate that the snow has disappeared and these have been excluded to ensure that we only consider snow/ice covered surfaces.

2.3 ICEARC

We use the ICEARC sea ice temperature and radiation data set from the Danish Meteorological Institute (DMI) field campaign in Qaanaaq. The DMI AWS is deployed on first-year sea ice in Qaanaaq and is funded by the European climate research project, ICE-ARC. The AWS was deployed for the first time in late January 2015 at the north side of the fjord Inglefield Bredning and recovered in early June before break-up of the fjord ice. The campaign has been repeated every year

Feltkode ændret

Feltkode ændret

since then and the data used in this study is procured by fieldwork done in the periods Jan.-Jun., 2015-2017. The AWS is equipped to measure snow surface IR temperature and air temperature at 1 and 2 m heights. In this study, the 1 m air temperature is used instead of the ~~1~~ 2 m air temperature, as careful analysis of the 2 m air observations revealed anomalies that could arise from a systematic temperature dependent error. Using the 1 m instead of 2 m air temperatures observations will have an impact on the strength of the relationship with the Tskin observations, but the observations are included here as the dependency with other parameters, such as cloud cover and wind, is still important to assess. ~~as the differences Tskin vs. 1 m temperature resembled the other stations significantly better than the Tskin vs. 2 temperature at this site, during winter and spring.~~ The data used here are 10 minute snapshots (Høyer et al., 2017) and are referenced as: DMI_Q in this paper.

2.4 SHEBA

The Surface Heat Budget of the Arctic (SHEBA) experiment was~~is~~ a multiagency program led by the National Science Foundation and the Office of Naval Research. The data used in this study originates from deployment of a Canadian icebreaker, DesGroseilliers, in the Arctic ice pack 570 km northeast of Prudhoe Bay, Alaska in 1997 (Uttal et al., 2002)~~(Uttal et al., 2002)~~. During its year-long deployment, SHEBA provided atmospheric and sea ice measurements from the icebreaker and the surrounding frozen ice floe. The data used here contain hourly averaged data collected by the SHEBA Atmospheric Surface Flux Group (ASFG) and Dr. J. Liljegren from the ARM project. The SHEBA ASFG installed a 20 m tall tower, which was used to obtain measurements of the surface energy budget, focusing on the turbulent heat fluxes and the near surface boundary layer structure (Bretherton et al., 2000; Persson, 2002)~~(Bretherton et al., 2000; Persson, 2002)~~. Five different levels, varying in height from 2.2-18.2 m, had mounted a temperature/humidity probe and a sonic anemometer. We use air temperature and wind data from the lowest mounted instruments (2.2 m), which vary in height from 1.9 to 3 m depending on snow accumulation and snow melt.

Three surface temperature measurements were measured from a General Eastern thermometer, an Eppley radiometer and a Barnes radiometer, available from April to September 2007. The Eppley is the most reliable, though there are periods when the other two are also reasonable, and one period (May), when the Eppley data may be slightly off (Persson, 2002). We use the best estimate of Tskin, which is based on slight corrections to the Eppley temperatures and the Barnes temperatures when Eppley was known to be wrong (Persson, 2002)~~(Persson, 2002)~~.

Feltkode ændret

2.5 FRAM2014/15

The scientific program of the FRAM2014/15 expedition is carried out by the Nansen Center (NERSC) in co-operation with Alfred Wegener Institute, Helmholtz Centre for Polar and Marine Research, Germany, University of Bergen, Bjerknes Center for Climate Research and Norwegian Meteorological Institute. FRAM2014/15 is a Norwegian ice drift station deployed near the North Pole in August 2014 using a medium-sized hovercraft as logistic and scientific platform (Kristoffersen and Hall, 2014)~~(Kristoffersen and Hall, 2014)~~. This type of mission allows exploration of the Arctic Ocean not accessible to icebreakers, and enables scientific field experiments, which require physical presence. The hovercraft was operated by two people and by the end of March 2015 they had drifted 1.450 km. During the drift with sea ice they obtained Tskin measurements by Campbell Scientific IR120 (later corrected for sky temperature and surface emissivity) and near surface ~~T2m~~air temperature from a temperature sensor.~~and 100 profiles of air temperature.~~

2.6 TARA

TARA is a French polar schooner that was built to withstand the forces from the Arctic sea ice. In late August 2006 TARA sailed to the Arctic Ocean, where she drifted for fifteen months frozen into the sea ice. The TARA~~ara~~ multidisciplinary experiment was a part of the international polar year DAMOCLES (Developing Arctic Modelling and Observing Capabilities for Long-term Environmental Studies) program (Gascard et al., 2008; Vihma et al., 2008)~~(Gascard et al., 2008; Vihma et al., 2008)~~.~~ The experiment took place from late August 2006 and the ship drifted for fifteen months frozen into the sea ice in the transpolar drift through the Arctic Ocean.~~ Air temperature and wind speed were measured from a 10 m tall Aanderaa weather mast at the heights of 1, 2, 5, and 10 m and wind direction was measured at 10 m height. We use the air temperatures and wind speed measured at 2 m height. They also had an Eppley broadband radiation mast with two sensors for longwave fluxes and two sensors for shortwave fluxes (upward and downward looking). The downward looking IR sensor also provide~~s~~d Tskin from April to September 2007. The data used in this study are 10 minute averages.

~~Table 1 gives an overview of the data and the abbreviations used in this paper. nFigure 1 shows the temporal data coverage, while the geographical distribution and elevations are shown in Fig. 2. Observations from the sites in Table 1 include T2m, Tskin, wind speed, shortwave- and longwave radiations. Measurement heights vary depending on the site and snow depth, but for this paper near-surface air temperatures are referred to as 2 m air temperature despite these variations. All data has been screened for spikes and other data artefacts using both automated and visual quality checks.~~

2.7 Radiometric observations of Tskin

The Tskin observations used in this study are all derived from radiometric observations, but with spectral characteristics that range from the Heitronics KT19.85 with a spectral response function from 9.5-11.5 μm over Campbell Scientific IR~~-~~120 with a 8-14 μm spectral window to broadband longwave observations from ~4-40 μm. The emissivity of the ice surface varies for the different spectral windows and this leads to a difference in actual observed Tskin as the ~~reflected~~ sky temperature, which is reflected, tends to be much colder than the ice surface in the infrared, in particular during cloud free conditions. The contribution from the reflected ~~cold~~ sky is thus included in the radiometric observations but the ice and snow surfaces have generally very high emissivities, which reduce the effects from the reflected sky radiation.~~ effects (e.g. Dozier and Warren, 1982).~~ In Høyer et al. (2017), the difference in emissivity between the KT15.85 and the IR120 was modelled using an IR snow ~~and ice~~ emissivity model with the spectral response functions for the two types of instruments (e.g. Dozier and Warren, 1982). This resulted in averaged emissivities of 0.998 for the KT15.85 and 0.996 for the IR120 spectral windows for a typical snow surface and an incidence angle of 25 degrees. Using the same type of model for a broadband 4-40 µm spectrum resulted in an emissivity of 0.997. The high emissivities for all three instruments mean that the contributions from the sky are small. For realistic conditions in the Arctic, this e.g. introduces an average difference of 0.06°C between the IR120 and the KT15.85 radiometer (which has a similar spectral response function as the KT19.85), with the IR120 being colder than the KT15.85 (Høyer et al., 2017)~~(Høyer et al., 2017)~~.

Several of the stations (ATQ, BAR, OLI, DMI_Q, SHEBA and FRAM) used here observed both narrow band and wide band IR observations of the ice surface. The two types of Tskin have been calculated and compared for each of the stations. Figure 3 shows an example with a comparison of the two Tskin estimates from DMI_Q. There is close to a 1:1 relation between the two observations, meaning that there are no systematic temperature dependencies in the comparison. Considering all sites, ~~A~~a good agreement ~~was observed~~if found with a mean difference between the two Tskin types of 0.06~~34~~°C and a mean root mean squared value of 0.96°C.~~.~~ ~~In addition there is close to a 1:1 relation between the two observations, meaning that there is no systematic temperature dependencies in the comparison.~~ In the following we use the narrow band Tskin observations when available and the broadband at the other stations and assume that all the Tskin derived observations have the same characteristics.

2.8 Longwave-equivalent c~~C~~loud cover fraction

For each~~all~~ site~~s~~, the cloud cover fraction (CCF) has been estimated based on the relationship between T2m and down-welling longwave radiation (LW_d), following the cloud cover estimation already included in the PROMICE data sets (van As, 2011; van As et al., 2005)~~(van As, 2011; van As et al., 2005)~~. It is based on Swinbank (1963), who presented a very simple approach for estimation of clear-sky (CCF=0) atmospheric longwave radiation as a function of T2m:

$$\cancel{LW}\,LW\cancel{d}_{d\_clear} = 9.365 \cdot 10^{-6} \cdot \mathrm{T2m}^2 \cdot \sigma \cdot \mathrm{T2m}^4, \qquad (1)$$

where σ is Stefan-Boltzmann's constant. Overcast conditions (CCF=1) are assumed to occur when the observed LW_d exceeds the blackbody radiation emitted from the surface, which is calculated using T2m. The CCF for any observed T2m and LW_d pair from all individual observation sites is then calculated by linear interpolation of the observed LW_d, between the~~se~~ theoretical clear-sky (from Equation 1) and the overcast estimates. See van As (2011)~~(van As, 2011)~~ for more details on the CCF calculation.

Formateret: Skrifttype: 10 pkt

Feltkode ændret

3. Introduction to the near surface boundary conditions

To perform an analysis of the Tskin and T2m relationship and interpret the results it is important to consider the surface energy balance and the specific characteristics that apply in the Arctic. The surface temperature and surface melt are driven by the surface energy balance. The net surface energy balance is defined by the fluxes of energy between the atmosphere, the snow/ice surface and the underlying land, snow/ice, or ocean. The surface energy balance can be written

$$SW_d - SW_u + LW_d - LW_u + SH + LH + G = M,$$

where M is the net energy flux at the surface and SW_d, SW_u, LW_d, LW_u, *SH*, *LH*, and *G* represent the down- and upwelling shortwave radiation, down- and upwelling longwave radiation, sensible and latent heat flux, and subsurface conductive ~~energy~~heat flux, respectively. The energy fluxes have the unit W m^{-2}. All fluxes are positive when energy is added to the surface. A positive net surface energy balance results in warming of the surface, if the temperature is lower than the freezing point of water, or in melting of snow and ice (latent heat) if the temperature is at the freezing point. When the surface energy balance is negative the snow/ice will cool thus driving the conductive heat flux from warmer layers below. If the surface is melting, a negative energy balance results in freezing of liquid water. ~~All fluxes are defined as positive when adding energy to the surface. The net energy flux can be positive or negative. When it is negative the snow/ice will cool or liquid water will refreeze. Positive net energy flux is used for warming the surface or melting snow and ice at the surface, when the fluxes on the left cannot be balanced i.e. when the surface temperature is limited to the melting point.~~

The radiative budget of the polar regions is dominated by longwave radiation during much of the year and even during summer the shortwave radiation input is in the same order of magnitude as the incoming longwave radiation flux because of extensive cloud cover especially during late summer, and the high surface albedo of the snow (Maykut, 1986)~~(Maykut, 1986)~~. SW_d is the dominating source for ice melt in Greenland (van den Broeke et al., 2008; Box et al., 2012; van As et al., 2012), even though non-radiative energy fluxes can dominate during shorter periods (Fausto et al., 2016). On average, the non-radiative fluxes are an order of magnitude smaller than the radiation fluxes. However, because the net radiation balance is small compared to the individual radiation fluxes the variations in SH and LH fluxes are important for the total surface energy balance and thus the surface temperature~~On average, the non-radiative fluxes are an order of magnitude smaller than the radiation fluxes. However, because the net radiation balance is small compared to the large incoming and outgoing radiation fluxes then variations in *SH* and *LH* fluxes are anyway important for the total surface energy balance, the surface temperature, sea ice growth and melt processes~~. Surface winds interact strongly with the surface energy fluxes as the turbulent mixing increases as a function of wind speed (van As et al., 2005)~~(van As et al., 2005)~~.

During winter and clear-skies when *SWd* is negligible, *LWu* is higher than the *LWd*. This drives a positive sensible heat flux and it results in a stable stratification of the lower atmospheric boundary layer ~~During winter and clear skies when SW_d is negligible LW_u is higher than the LW_d at the surface because the atmosphere above the atmospheric boundary layer is colder than the surface and because the atmosphere is very dry~~ (Maykut, 1986)~~(Maykut, 1986)~~. When the heat conduction flux from below is limited on thick sea ice and on continental ice sheets the negative radiation budget at the surface makes the surface

Formateret: Skrifttype: Kursiv

Formateret: Skrifttype: Kursiv

Formateret: Skrifttype: Kursiv

temperature colder than the surface air temperature, resulting in a surface-based temperature inversion. At low to moderate wind-speeds, ~~where~~ when turbulent mixing is limited, this creates a very stable stratification of the lower atmosphere. On a sloping surface, the surface air starts to flow downslope, driven by the existence of a horizontal temperature gradient and gravity~~, crossing the contour lines at an angle of about 45° to the right (in the northern hemisphere) by the Coriolis force~~. The generated winds are called inversion or ~~/~~katabatic winds, and are characterised by stronger winds at more negative surface net radiation and a strong correlation between slope and wind direction ~~-depending on the slope~~ (Lettau and Schwerdtfeger, 1967)~~(Lettau and W. Schwerdtfeger, 1967)~~. In the case of PROMICE sites on GrIS, we will refer to these winds as katabatic winds and in the case of interior Antarctic studies these winds are referred to as inversion winds for consistency with referenced studies. ~~Both inversion winds and katabatic winds are characterised by stronger winds at more negative surface net radiation and a strong correlation between slope and wind direction.~~

Clouds play a complex role in the Arctic surface energy budget e.g. they~~,~~ both reflect~~ing~~ SW_d, leading to a cloud shortwave cooling effect, and absorb~~ing~~ LW_u and emit~~ting~~ LW_d, which tend to have a warming effect. In the Arctic clouds have a predominantly warming effect on the surface (Intrieri, 2002; Walsh and Chapman, 1998)~~(Intrieri, 2002; Walsh and Chapman, 1998)~~ as the dry ~~background~~ atmosphere, with lower emissivity and with that absorptivity ~~more transparent~~ to *LW* radiation, enhances the cloud longwave warming effect, while the high surface albedo and the high solar zenith angles ~~act to reduce~~ thus the impact of the cloud shortwave cooling effect (Curry et al., 1996; Curry and Herman, 1985; Zygmuntowska et al., 2012)~~(Curry et al., 1996; Curry and Herman, 1985; Zygmuntowska et al., 2012)~~.

4 Results

4.1 Diurnal and seasonal temperature variability

The local air and surface temperature conditions in the Arctic are to a large extent influenced by the length of the day or night in the Arctic, with extreme variations depending on latitude and time of the year. The temperature variability has several important temporal scales. In this study we will focus on the diurnal and seasonal temperature variations, which are key temporal scales of variability, considering the aim of deriving T2m from satellite observations. As an example of the large seasonal variations, Fig. 4~~3~~ shows the 2014 monthly mean diurnal temperature variation of Tskin and T2m at the upper PROMICE site in Kangerlussuaq, KAN_U, during January, April, July and October. The seasonal variability in the diurnal temperature at KAN_U is representative of the conditions at the other stations, except for the general temperature level at each station, ~~that~~which changes with latitude and altitude. Considering all months individually, there is high correlation between Tskin and T2m ranging from an average value of 0.92 in January to an average of 0.99 in July considering the entire time series of ~~0.957 in April to 0.995 in October at~~ KAN_U. The high correlations arise from hourly variability and daily cycles in temperatures that are seen in both temperature records.~~.~~ The correlation decreases for stations which have occasional surface melt, where Tskin is constrained to the freezing point of water. Both Tskin and T2m reach a maximum in July, while the coldest month is December (not shown). During winter and polar night, there is no clear diurnal cycle in

~~n~~either T2m or Tskin, and T2m is higher than Tskin. However, during spring there is a strong diurnal cycle~~, with maximum temperatures coinciding with maximum daily insolation.~~, with ~~At night,~~ Tskin~~ is~~ ~~colder~~ lower than T2m at night and small T2m-Tskin differences ~~, while the T2m-Tskin difference is small~~ during daytime. The shadings indicate the standard deviations in T2m and Tskin, respectively. The largest variability is found in spring and winter as a result of more frequent and rapid passages of cold and warm air masses in contrast to the summer months (Steffen, 1995). The summer temperature variability is moreover limited by the upper limit of 0°C on ~~constrain of~~ Tskin ~~variability once~~ when the surface melting begins.~~,~~

The large seasonal variations in Fig. 4~~3~~ and the relationship between T2m and Tskin are typical for all sites. Figure 5a~~4~~ shows the monthly mean Tskin for all sites and all years. EGP is by far the coldest site ~~included in this analysis~~due to its high elevation, with a monthly mean Tskin of -42°C in January and a maximum of -11°C in July. All sites reach a maximum in Tskin in July, regardless of latitude. July is also the month with least variation in temperature among sites, where melt at most stations (exception is ACC sites) constrains Tskin, while the winter months show a larger variance in Tskin among sites since local conditions are dominating Tskin. The AWS data from the GrIS show the effect of altitude and latitude on Tskin, with the high altitude sites being the coldest (EGP, KAN_U and KAN_M) together with the most northern sites (THU_U and KPC_U). The southern (e.g. QAS_A and QAS_U) and low altitude sites (most LAB sites, TAS_U, TAS_A) occur to be the warmest~~ (e.g. TAS_U, TAS_A and SCO_U)~~. The SICE sites~~ on sea ice~~ are comparable in temperature with the coldest sites on the GrIS (except from EGP), but are slightly warmer in summer and fall.

Figure 5b shows the mean daily range (daily max – daily min difference) of Tskin as a function of month for all sites and all years. Again, the observations show a similar pattern across the diverse geographical locations. ~~The mean daily range of all sites is 7.1°C during winter (Dec. Feb.), 8.4°C in spring (Mar. May), 3.3°C in summer (Jun. Aug.), and 6.7°C in autumn (Sep. Nov.).~~ During summer, the high elevation sites tend to have the largest daily range in Tskin, while the observations from LAB and SICE sites ~~sea ice~~ show the smallest daily range. This is ~~probably~~ very likely an effect of the warmer temperatures and the Tskin upper temperature limit at 0°C, the melting point for ice. This constraint is ~~often seen for the sea ice data records~~seen during summer at almost all data records included in this study (exceptions are the ACC sites). Figure 5c

~~Focusing on the relationship between T2m and Tskin, it is clear that even though Fig. 3 showed that the two temperatures have high correlation, it also showed that the T2m-Tskin difference is not constant throughout the day and year (at KAN_U). The~~shows the mean difference between T2m and Tskin for all observation sites~~, weighted equal,~~ as a function of time of year~~, is shown in Fig. 6~~. In general, the SICE sites show the weakest inversion, while the LAB sites show the strongest inversion. For the ACC sites the weakest inversion is found during summer, while the LAB sites tend to have the strongest inversion during summer. This is explained by differences in surface conditions during summer, where the LAB sites have surface melt in contrast to the high elevation ACC sites, where the surface warms but not reaches the ceiling of variability (the melting point).~~On average the monthly mean T2m is 1.44°C warmer than monthly mean Tskin with the largest differences in July and August. The figure also shows the monthly mean standard deviation of the T2m-Tskin difference.~~

Formateret: Fremhævning

Formateret: Fremhævning

~~The largest variability of the difference is found in Mar. May, while the summer months have least variability in the T2m-Tskin difference.~~

Figure~~s~~ 5~~3-6~~ indicates~~d~~ both yearly and daily variations in the observed Tskin and T2m relationship. A detailed analysis of these variations can be seen in Figures 6~~7~~a-b, which illustrate the mean diurnal and seasonal T2m-Tskin differences for the ACC and LAB sites, respectively. The SSC and SICE sites have not been included as none of the individual sites have a continuous data record throughout the year without gaps~~cover an entire season (SSC data during summer is removed since the snow is melted).~~ ~~at two GrIS stations at different latitudes and altitudes (KAN_U and KPC_U).~~ As also noticed in Fig. 4~~3~~, the winter months have very little diurnal variability in the T2m-Tskin difference, with an approximately constant difference of about 1.5-2.5°C for the LAB sites and 0.5-1.5 °C for the ACC sites. During spring and summer the differences decrease~~s~~ at the ACC sites and the weakest vertical stratification is found ~~close to the peak of the diurnal cycle~~around noon or early afternoon, where Tskin may even exceed T2m slightly resulting in an unstable stratification of the surface air column. For the LAB sites, the weakest stratification is found in spring and fall, around noon and early afternoon. The summer months show large differences due to the constrain of Tskin for melting surfaces, which is common to all LAB sites. At night the net radiation is negative, thus ~~During night,~~ cooling the surface resulting in ~~the surface is often colder than the atmosphere and~~ a surface-based inversion for both surface types ~~is established~~. The T2m-Tskin differences are ~~generally~~ higher (especially in summer) at the LAB sites~~KPC_U~~ compared to ~~KAN_U~~the ACC sites, and the UAB sites have temperature differences in between. The reason for the higher temperature difference at the lower altitude sites is the longer time periods with surface melt.~~, but they have similar variability throughout the year and day. This pattern is also recognized for the other stations.~~

4.2 Impact from wind

The surface wind speed is an important component in the near surface thermal stratification since the turbulent mixing increases as a function of wind speed (Monin and Obukhov, 1954)~~due to the turbulent heat fluxes~~. Figure 7 shows how t~~T~~he wind regimes differ among the observation sites used in this study. In general, winds on the GrIS are strongest in winter and reach a minimum around July (see also~~Fig. 8;~~ Steffen and Box, 2001). The surface radiative cooling and the terrain play the primary role in the generation of the surface winds ~~(van As et al., 2014)~~. The direction and strength of the prevailing surface winds are closely related to the direction and steepness of the slope and the strength of the inversion. ~~We find that the s~~Surface winds at the PROMICE sites ~~in~~ generally have a high directional persistence (see ~~also~~ Fig. 4 in van As et al., 2014), commonly blowing from inland, which is an ~~strong~~ indication that local winds are often katabatic winds. ~~The wind regimes differ among the observation sites used in this study.~~ High elevation sites experience stronger winds due to the larger radiative cooling of the surface (provided a comparable surface slope is present; Fig. 8; van As et al., 2014). The SSC and SICE sites show less variability in wind speed on annual basis. At these sites the wind is determined by large scale synoptic conditions combined with local topography. ~~The THU_U site experiences wind speeds of about the same monthly mean~~

Feltkode ændret

~~magnitude all year around. Similar, the ARM and sea ice sites show less variability in wind speed on an annual basis. In general, the sea ice sites experience weaker winds.~~

~~This section relates the surface-based temperature inversion to wind.~~ The expectation is that stronger inversions can develop in low wind speed conditions because of reduced turbulent mixing. Figure 8~~9~~a-b shows the T2m-Tskin difference as a function of binned wind speed. ~~with a bin size of 0.5 m s^{-1}. Only bins with more than 50 members are included. The number of members in each bin is shown in the bottom plots (blue curve) together with the cumulative percentage (red curve).~~ The middle plots show the binned distribution of the T2m-Tskin difference (with bin size of 1 K) as a function of binned wind speed, where the colour bar is the number of ~~matchups~~ members in each bin. The top plots show the mean (solid lines) and standard deviation (dashed lines) of the T2m-Tskin difference as a function of the binned wind speeds. Figure 8~~9~~a shows data from the DMI_Q AWS on sea ice. As expected, the strongest temperature inversion occurs at low wind speeds and larger wind speeds have larger turbulent mixing and thus smaller vertical temperature ~~gradients~~ differences between Tskin and T2m. However, THU_U (Fig. 8~~9~~b) shows that this relationship ~~can sometimes be~~is more complex~~icated than that~~. The maximum inversion is reached at wind speeds from 3-5 m s^{-1}, whereas the mean and standard deviation~~s and~~ decrease for calm winds (<2.5 m s^{-1})

~~At calm winds (<2.5 m s^{-1}) the mean and standard deviation reach a local minimum, and the inversion tends to be strongest around 3-5 m s^{-1}.~~ The wind dependencies shown in Fig. 8~~9~~ are representative for all the stations in this paper~~s~~, where the SICE and the SSC ~~stations~~sites resemble Fig 8~~9~~a and all the PROMICE stations have a wind dependency similar to Fig. 8~~9~~b. The pattern is explained by the inversion combined with a surface slope that results in a flow, which actually destroys its own forcing and as a result there is an optimum in inversion strength and wind speed. The

~~This behaviour is common for to all~~ PROMICE behaviour ~~sites and~~ is also found by Adolph et al. (2018) at the Summit station on the GrIS~~, where 2 m air temperature has been compared to IR skin temperature (Adolph et al., 2017)~~. Miller et al. (2013) also fou~~i~~nd that the surface based inversion intensity peaks at wind speeds ranging from 3 to 10 m s^{-1} at Summit based on~~using~~ microwave radiometer retrieved profiles~~ at Summit~~. Furthermore, Hudson and Brandt (2005) show that at the South Pole the maximum inversion strength occurs at wind speeds of 3-5 m s^{-1}. They suggest that it is not the weak wind of 3-5 m s^{-1} that promotes the strong inversion, but the inversion which forces the air flow resulting in an inversion wind.~~Also at the South Pole the maximum inversion tend to occur at wind of 3-5 m s^{-1} and not calm winds considering the 22 m and 2 m air temperature difference (Hudson and Brandt, 2005). Hudson and Brandt suggest that it is not the weak wind of 3-5 m s^{-1} that promotes strong inversion, but the inversion, which causes an inversion wind.~~ They investigated this using the model by Mahrt and Schwerdtfeger (1970), which relates the slope of the terrain and the strength of the inversion to the inversion wind. Their results supported the idea that the inversion wind can explain the “unexpected” location of the maximum in inversion strength. ~~These independent studies suggest that this might also be a real feature of the GrIS. It is likely that the GrIS represents a different case for inversion winds than for the interior of Antarctica due to Greenland’s smaller dimensions. However, i~~It seems that the nature of the surface winds and the directional constancy are highly comparable between the sloping surfaces of Antarctica and Greenland (van den Broeke et al., 1994; King and Turner, 1997)~~(van den Broeke et al., 1994; King and Turner, 1997)~~ and in both cases the maximum inversion occurs at non-zero wind speeds.

~~Figure 10a shows the T2m-Tskin difference plotted as a function of the wind direction at THU_U. Nearly all measurements correspond to winds blowing from the upslope direction (55° north east) but deflected to the right (100° south east) due to the Coriolis force. The strongest inversion occurs at wind directions from 25-125°. We find that the surface winds at the PROMICE sites in general have a high directional persistence (see also Fig. 4 in van As et al., 2014), commonly blowing from inland, which is a strong indication that local winds are often katabatic winds. This hypothesis is supported by Fig. 10b, which shows the wind direction as a function of the cloud cover fraction. Winds from the upslope direction are coincident with a minimum in the cloud cover fraction. The result is a negative surface net radiation (Fig. 10c), which allows a larger radiative cooling of Tskin and therefore a stronger inversion generating/driving the katabatic winds. These results support the idea by Hudson and Brandt (2005) that the inversion wind explains the maximum in inversion strength at about 5 m s^{-1}.~~

~~It is outside the scope of this paper to fully explain all the features observed at the GrIS, but it is interesting to note that the unique environmental conditions and regional topography makes the GrIS different than the sites located on sea ice and land ice, with limited topography such as DMI_Q, SHEBA, FRAM and the ARM sites.~~

4.3 Impact from clouds

The difference in LW_d radiation between clear-sky and overcast conditions can result in large differences in both T2m and Tskin due to the cloud effects on the surface radiation budget. As satellite ~~retrieved~~ Tskin can only be ~~done~~retrieved ~~for~~during clear-sky conditions, the assessment of the cloud effects on the average conditions is essential to facilitate the combination of satellite and in situ observations. In this section, we therefore assess the inversion strength as a function of the cloud cover and in Sect. 4.3.1 the~~a~~ clear-sky bias is estimated for all sites.

Clear-sky conditions are defined to be cases ~~with~~ where CCF<0.3~~30 %~~, while overcast conditions are defined to have CCF>0.7~~0 %~~. The frequency of clear-sky (overcast) observations is defined as the number of clear-sky (overcast) observations compared to the total number of observations. Figure 9~~11~~ shows the frequency of clear-sky and overcast observations for each of the observation sites used in this study. ~~The frequency of clear-sky observations ranges from 4 % at ATQ to 52 % at SCO_U, while the frequency of overcast observations ranges from 25 % at SCO_U to 63 % at DMI_Q.~~ The SSC, SICE sites, and EGP all show a much larger frequency of overcast conditions compared to the frequency of clear-sky conditions. The ACC sites show a strong seasonal dependence with more clear-sky observations during summer and more overcast conditions during winter. A similar but much weaker seasonal cycle is seen for UAB. The LAB and SSC sites show limited seasonal variability, while the SICE sites have almost only clear-sky observations from April to July.~~Except for KAN_M, SCO_U and UPE_U the frequency of overcast conditions is larger than the frequency of clear-sky observations at all sites.~~

Formateret: Engelsk (Storbritannien)

Formateret: Fremhævning

Formateret: Fremhævning

~~Similar to most PROMICE sites KAN_U (Fig. 12a) shows the greatest frequency of clear sky observations during the summer months and greatest frequency of overcast conditions during the winter months. The ARM site BAR (Fig. 12b) shows a year-round predominance of overcast conditions compared to clear-sky conditions.~~

The relation between the inversion strength and CCF is shown in Fig 10~~3~~ for~~, considering~~ all sites. ~~The bin size is 5 % and only bins with more than 50 members are considered.~~ As expected, ~~the obvious feature is that~~ the inversion strength decreases with increasing LW_d radiation ~~from~~ due to a more extensive cloud cover. ~~The observation sites show the strongest inversion during clear-sky conditions, reaching a mean value of 2.31°C for CCFs in the range 0-30%, considering all sites. Overcast conditions lead to a weaker inversion of 0.53°C considering all observations with a CCF of 70-100%.~~ The average slope is~~–~~ calculated for each category: ACC=-0.011±0.0037 °C/%, UAB = -0.019±0.0012 °C/%, LAB = -0.021±0.0016 °C/%, SSC = -0.016±0.0026 °C/%, SICE = -0.017±0.0048 °C/% ~~-0.023K/% considering all sites.~~ where the uncertainties are given as 95% confidence intervals.

Figure 11~~4~~a-b show how the temperature differences at ~~KAN_U~~the ACC sites vary as a function of season and local time for clear-sky and overcast conditions, respectively. Clear-sky conditions show the largest stratification with temperature differences up to 2-3°C during winter and night time. Overcast conditions reduce the temperature gradient at all times, with the ~~largest~~ maximum temperature differences of about 1~~.5~~°C. During summer around noon, overcast conditions usually lead to an unstable stratification of the order of -1°C. An unstable stratification may also occur during clear-sky conditions and large solar insolation. This behaviour is common for all ~~stations~~ sites included in this study, but the strength of the inversion varies among the different sites~~.~~

~~Figure 14 demonstrates the factors that influence the T2m-Tskin differences, such as day of year, time of day and cloud cover.~~ The impact of season and sky conditions on the T2m-Tskin differences is ~~of this variability differences for all stations is~~ quantified in Table 2~~,~~. The table ~~which~~ summarizes the findings of the dependencies of cloud/clear and summer/winter on the T2m-Tskin difference for all 5 categories ~~for all sites (ALL) and for the subregions defined in Table 1~~. Note that DMI_~~-~~Q is withheld from the averaging for the ~~Sea-ice~~SICE sites to avoid systematic impacts from the 1 m height observations.~~,~~ The categories which experience summer surface melt (UAB + ACC) tend to have larger T2m-Tskin differences during summer than winter. The SSC sites also experience melt, but the snow melts away in summer, which limits the time where Tskin is constrained to the melting point. It is difficult to interpret the results for the SICE sites, as none of the individual sites cover an entire year. For all surface types ~~a division into SEAICE+, which includes the Arctic sea ice sites and the ARM sites, and PROMICE sites, all sites weighted equal. In general, the SEAICE+ sites show a weaker inversion than the PROMICE sites, which is most likely related to differences in the atmospheric conditions, such as cloud cover and humidity.~~. ~~In all cases~~ and for all times of the year, cloud cover tends to decrease the inversion strength.~~ and~~. ~~Both groups of stations experience the strongest inversion during winter clear-sky conditions.~~

Formateret: Fremhævning

4.3.1 Clear-sky bias

The most accurate surface temperature satellite observations are thermal IR observations that can only be observed during clear-sky conditions. As the satellite IR observations thus have gaps in cloudy conditions, the satellite Tskin products are often averages of the available satellite observations within 1-3 days (see e.g. Rasmussen et al., 2018). However, these satellite averages can be colder than the all-sky average temperature due to ~~This fact will potentially introduce~~ a clear-sky bias arising from the fact that Tskin is typically colder in clear-sky conditions compared to the cloudy conditions where the satellite cannot observe. ~~when satellites are used to estimate the average Tskin. To facilitate the use of satellite observations it is therefore important to get a measure of the influence of clouds on Tskin. As the satellite IR observations have gaps in cloudy conditions, the satellite Tskin products are often averages over a given time window (see e.g. Rasmussen et al., 2018).~~ When using the averaged Tskin observations for monitoring or in combination with ocean, ~~-~~sea ice or atmospheric models, it is therefore important to assess the impact on the clear-sky bias, by~~of~~ using different ~~-~~temporal averaging windows ~~on the clear-sky bias~~. Hall et al. (2012) show monthly temperature maps from MODIS and discuss the fact that the monthly average temperatures (from satellites) are likely lower that the ~~true~~all-sky monthly average temperatures. Here, we use the in situ observations to estimate the clear-sky effects that satellite observations would introduce. We use the cloud mask derived from the longwave-equivalent cloud cover fraction and assum~~ee~~ that it is equivalent to the cloud masks used for IR satellite processing. Th~~T~~~~th~~e clear-sky bias has been assessed by comparing clear-sky Tskin observations with all-sky Tskin (where clear-sky has been defined as a CCF < 0.3~~ ??~~) observations, averaged for different time windows: 24 h, 72 h and 1 month, for all sites. The results are shown in Fig. 12~~5~~. ~~The average clear-sky biases are -0.28°C, -0.36°C and -1.40°C using the time windows 24 h, 72 h and 1 month, respectively.~~ For most stations all-sky observations are warmer than clear-sky observations for all time windows. However, there is large variability among the stations and at a few stations e.g. EGP, KPC_U, ATQ, OLI and DMI_Q the all-sky observations are colder than clear-sky observations using one or more of the ~~the 24 h and/or 1 month~~ time windows.

~~The average clear-sky biases are -0.28°C, -0.36°C and -1.40°C using the time windows 24 h, 72 h and 1 month, respectively.~~

The larger clear sky biases for ~~larger~~longer temporal averaging windows arise from persistent cloud cover ~~that can~~ lasting for days. For e.g. the 72 hours temporal averaging intervals, observations from periods with >1 day persistent cloud cover (and higher Tskin) are included, which are otherwise missing in the 24 hour clear-sky averages, resulting in a warmer all-sky averaged Tskin, compared to the average clear-sky Tskin.

Figure 13 shows ~~The top panels of Fig. 16 show~~ the monthly mean difference in 24 h averaged clear-sky and all-sky Tskin for the ~~PROMICE~~ ACC stations (a) and the ~~SEAICE+ sites~~LAB stations (b)~~, averaged for each month~~. For both groups of stations it is found that the 24 h averaged clear-sky bias is ~~smaller~~ closest to zero during summer ~~(ALL: -0.10°C; SEAICE+: -0.19°C; PROMICE: -0.05°C) than winter (ALL: -0.95°C; SEAICE+: -0.42°C; PROMICE: -1.26°C)~~, which can partly be explained by~~may be a result of~~ the smaller daily Tskin range in summer (Fig. 5b). The UAB sites look very similar to the LAB sites, but with a slightly more pronounced seasonal cycle in the clear-sky bias. The figures have not been produced for the SSC and SICE sites as none of the individual sites included in these categories cover an entire season. ~~The SEAICE+ stations have an overall positive clear-sky bias of 0.79°C in spring.~~ The orange graphs show the mean number of hours with clear-sky per day, which illustrate more hours with clear-skies for LAB stations compared to ACC stations except for May-July. The positive clears-sky biases observed in Fig. 12 are very likely an effect of seasonal differences in cloud cover e.g. it is found that ~~The bottom panels of Fig. 16 show the amount of hours with clouds (CCF>70%) per day, averaged for each month. Both groups of stations have a minimum in the hours with cloud cover during summer. On average the SEAICE+ sites have about 4 h more with clouds per day compared to the PROMICE stations.~~ EGP has no clear-sky observations in Dec.-Feb. and at DMI_Q there is no clear-sky observations ~~are only~~ available Jan-Mar~~Feb.-Jun~~., which means that the results in Fig. 12 is biased towards the months where a zero or positive clear-sky bias is observed. ~~which may explain the overall positive 24 h clear-sky bias observed in Fig. 15.~~ The 72 h and 1 month averaged clear-sky biases show the same seasonal variation as in Fig. 13~~6~~, with the smallest biases in summer and largest biases in winter.

4.4 Relationship with skin surface temperature

Section 4.3 showed how clouds impact the T2m and Tskin relationship, and Sect. 4.3.1 revealed a close relationship between Tskin and the CCF. With ~~In reality it is, however, difficult to obtain reliable observations of cloud cover from the entire Arctic using, e.g. satellite observations.~~ the aim of deriving T2m based upon satellite Tskin observations, it is important to examine ~~This section therefore investigates~~ how the T2m-Tskin difference is related to the skin temperature itself. The relationship with Tskin is corroborated in Fig. 14~~7~~ where the strength of the surface-based inversion is shown as a function of Tskin. ~~The Tskin bin size is 1°C and only bins with more than 50 members are considered.~~ All PROMICE sites show an almost linear trend towards weaker inversion strength for ~~warmer~~ higher skin temperatures with the steepest slope of the curve for low elevation sites. ~~Strong trends are also seen for BAR, SHEBA, TARA and DMI_Q. ATQ and OLI show a similar but weaker trend, while FRAM shows an opposite trend with larger T2m-Tskin differences for higher skin temperatures. However, the standard deviation (not shown) decreases for higher temperatures for FRAM.~~ The average slopes for all categories are found to: ACC=-0.030±0.003, UAB =-0.066±0.004, LAB=-0.101±0.004, SSC = -0.044±0.005, SICE = -0.043±0.007, where the uncertainty estimates are given as 95 % confidence intervals. ~~of the curve for all stations except FRAM is -0.055 K/K.~~ The results of this section are very encouraging in a situation where we would like to ~~can be useful to~~ relate Tskin to T2m~~ in situations~~, but ~~where~~ the cloud cover and longwave radiation are not available, such as the case with satellite observations.

5 Discussion

T~~The initial study on t~~he T2m and Tskin variability shows that the coldest month ranges from December to March, whereas the warmest month is July for all sites considering both Tskin and T2m. This is in agreement with mean air temperatures found in Steffen and Box (2001) for Greenland GC-Net AWSs, Persson (2002) for Arctic sea ice and Rigor et al. (2000) for

North Pole stations and land stations in Alaska. The monthly mean daily temperature range is largest in April-May and reaches a minimum in July, related to the upper temperature limit when the ice or snow is melting. Surface temperature inversions are very common for the Arctic region. Considering ~~the sites included in this analysis,~~all categories the mean temperature difference between T2m and Tskin is on average 0.65-2.65°C~~1.37°C~~ with the strongest inversion for the sites located in the lower part of the ablation zone and the weakest inversion for the sea ice sites. ~~over the GrIS (1.64°C) compared to the sites in Alaska and on the Arctic sea ice (0.88°C).~~ Inversions are predominantly found during winter (low-sun and polar night periods), which allows for a strong radiative cooling at the surface. Smaller temperature differences are dominating in spring and summer, around noon and early afternoon, where the sun is warming the surface. This is in agreement with Adolph et al. (2018) ~~Adolph et al. (2017) that~~who found large T2m-Tskin differences during night time and small differences during the peak solar irradiance (see Fig. 5 in Adolph et al., 2018) ~~Adolph et al., 2017)~~. During summer and local noon Tskin ~~exhibits~~ has the closest coupling to T2m and the satellite observed Tskin observations will therefore have the best agreement with the T2m at these times.

Increasing wind speeds are expected to decrease the inversion strength through increased turbulence, and mixing warmer air downwards. This is also seen at the ARM sites and Arctic sea ice sites, where the strongest inversion occurs at calm winds and weaker inversions occur with increasing wind speed. ~~Although the effect from wind speed seems easy to understand, the relationship has turned out to be more complicated than that at sites with a sloping terrain.~~ The relationship is more complicated over a sloping terrain~~All sites on the GrIS showed a unique feature~~ with the maximum inversion strength at winds of about 5 m s^{-1} and not at calm winds. This feature has previously been identified by ~~a few~~ others for~~in~~ Antarctica (Hudson and Brandt, 2005) and at Summit, GrIS (Adolph et al., 2018; Miller et al., 2013)~~(Miller et al., 2013)~~ and~~. The feature is also noticed at Summit in Figure 7 in Adolph et al., (2017). This feature~~ can be explained by the presence ~~forcing~~ of a katabatic wind driven by the surface temperature inversion over a sloping terrain. The katabatic wind destroys part of its own forcing and as a result there exist an optimum in inversion strength and wind speed. This is in agreement with what Hudson and Brandt (2005) found for the Antarctic ice sheet. ~~It is likely that this feature is driven by the inversion/katabatic winds. The inversion/katabatic winds blow persistently perpendicular to the fall line of the terrain, with a speed related to the magnitude of the slope but also other factors such as the strength of the inversion, the velocity of the wind above the inversion layer, surface friction, Coriolis force, and gravity. Hudson and Brandt (2005) performed an analysis on the surface wind resulting from the inversion over sloped terrain and found that the inversion can induce winds of this magnitude at the South Pole, suggesting that this may be why the maximum inversions occur at non-zero wind speeds. We find that all PROMICE sites show persistent winds blowing from the upslope direction and deflected to the right (see also Fig. 4 in van As et al., 2014). We also find that the downslope winds typically occur during cloud-free conditions, which result in a strong radiative cooling of the surface and therefore a more negative net radiation at the surface. It is likely that the GrIS represents a different case for inversion winds than for the interior of Antarctica due to Greenland's smaller dimensions, but it does seem like the nature of the surface winds and the directional persistence found in Antarctica are comparable to the results~~

Formateret: Engelsk (USA)

Feltkode ændret

Formateret: Engelsk (USA)

Feltkode ændret

Formateret: Engelsk (USA)

Formateret: Engelsk (USA)

~~found here for the GrIS. More research is needed to completely understand and explain the impact of wind on the inversion, and vice versa.~~

The analysis of the impact of clouds showed an almost linear relationship between cloud cover and the T2m-Tskin difference, with a trend towards zero with increasing CCF (Fig. 10~~3~~). ~~Also the variability of the inversion strength tends to decrease with increasing CCF (not shown).~~ Considering all ~~sites~~ categories the T2m-Tskin difference decreases from an all-sky mean value ranging from 0.65-2.65°C to a difference ranging from -0.08-1.63~~of 1.37~~°C ~~to 0.53°C~~ considering observations with a CCF above ~~70 %~~0.7. On the other hand, the difference increases to the range of 1.05-3.44~~2.31~~°C by only considering observations with CCFs below ~~30 %~~0.3. The smaller inversion strength under cloudy conditions is explained by the fact that ~~The explanation is that~~ clouds ~~in the Arctic~~ have a predominantly warming effect on the surface in the Arctic (Intrieri, 2002; Walsh and Chapman, 1998)~~(Intrieri, 2002; Walsh and Chapman, 1998)~~. In cases where the cloud cover and longwave radiation are not available, the ~~T2m and Tskin~~ relationship can be quantified by using the Tskin~~instead~~. We have found an almost linear relationship between the inversion strength and the skin temperatures, with weaker inversions for higher Tskin. This is in agreement with Adolph et al. (2018) ~~Adolph et al. (2017) that~~ who ~~finds~~found larger T2m-Tskin differences at lower temperatures at the Summit station, during summer.

As mentioned earlier, the measurement height changes with snowfall and snow melt at with that the strength of the inversion measured. The PROMICE ~~observations~~data ~~included~~includes a height of the sensor boom~~ height above the surface~~, which can be used to determine the impact of using different measurement height on our results. ~~-and differences in measurement heights could impact the results obtained here, such as the strength of the inversion. The overall impact from varying observation heights is, however small.~~ We reproduced the numbers in Table 2, based upon observations measured at a height of ~~from~~ 1.9-2.1 m~~eters~~ only and found~~–~~ overall all-sky, all-months differences less than 0.22°C for all the different PROMICE regions. In addition, the screening did not change the conclusions regarding ~~a cold clear-sky~~the impact of clouds and the seasonal behaviour of the T2m-Tskin differences. Data from the other sites do not all include such information on the measurement height. -For consistency, we therefore chose not to screen the PROMICE data. In addition, we chose not to perform an adjustment of the observations, as we estimate~~d~~ the uncertainty of such an adjustment to be equal to or larger than the actual uncertainty on the results obtained here and again, it would not be possible to make such a correction for all sites.~~.~~

To assess if there ~~are~~is any impact of clear-sky observations on the radiometer observations due to the different spectral characteristics (broad band versus narrow band, as discussed in Sect. 2.7), the T2m~~.~~-Tskin differences as a function of CCF were calculated for narrow band Tskin and broad band Tskin for the stations containing both instruments (ATQ, BAR, OLI, DMI_Q, SHEBA, and FRAM). This resulted in a ~~very~~ small change in the slope from -0.017 to 0.020~~-0.025 to -0.022~~°C/% for narrow band and broad band Tskin estimates, respectively. Similarly, the T2m-Tskin differences were calculated for both types of radiometers as a function of Tskin. Again, the change in trend was small from -0.046 to -0.055~~-0.045 to -0.052, excluding the FRAM site as in Sect. 4.4.~~.

The influence of clouds on Tskin has been assessed by comparing clear-sky Tskin observations with all-sky Tskin observations averaged for different time intervals: 24 h, 72 h and 1 month, for all sites. In general, the ~~cloud-free only~~clear-sky ~~monthly~~ average is colder than the ~~true~~ all-sky ~~monthly~~ average with increasing bias with ~~a mean clear-sky bias of -0.28°C using the 24 h time interval. The clear-sky bias tends to increase with~~ the length of the averaging time interval ~~used for averaging, but the clear-sky biases vary among the stations~~.~~. However, the frequency of clear-sky observations also varies a lot among the stations, with SEAICE+ stations having a clear-sky frequency of 10 % compared to the PROMICE stations with a clear-sky frequency of 34 % (Fig. 11). In general,~~ and the clear-sky bias is smaller during summer than winter for all averaging windows. This is also reported by Comiso (2000), who finds a monthly mean clear-sky bias of about -0.3°C during summer (Jan.) and -0.5°C during winter (Jul.) at Antarctic stations. The range in temperature over the averaging window as well as the frequency and timing of clear-sky observations are factors partly explaining the~~are thought to play an important role in the~~ clear-sky bias variations observed among the stations.

The observed clear-sky bias explains part of the cold ~~-~~bias observed in IR satellite retrievals of skin surface temperature compared to in situ surface temperatures (Høyer et al., 2017; Rasmussen et al., 2018; Shuman et al., 2014)~~(Høyer et al., 2017; Rasmussen et al., 2018; Shuman et al., 2014)~~. Another part of the explanation is related to the fact that the satellite skin observations are compared to in situ ~~"surface" air temperature~~ measured at typically ~~the surface, typically is measured at about~~ 2 m height, where ~~t.~~t ~~T~~he ~~significant~~ temperature gradients in the lowest 2 m of the atmosphere will result in the ~~mean that~~ satellite retrievals of surface temperature ~~will be~~ being colder than the in situ measurements at 2 m height.

6 Conclusions

Coincident in situ skin temperature (Tskin) and 2 m air temperatures (T2m) from 2~~0~~9 deployments in the Arctic region have been analysed to assess the variability and the factors controlling the Tskin and T2m variations in order to facilitate the combined use of satellite observed Tskin and traditional observations of T2m. The extensive data set~~s~~ ~~gathered~~used in this study represents a wide range of ~~weather~~ conditions including all-year observations from Arctic sea ice, land ice in northern Alaska as well as low and high altitude land ice covering the lower, middle and upper ablation zones and the accumulation ~~different~~ region~~s~~ of the Greenland Ice Sheet. It has been found that ~~, from melting sea ice in the summer, over land based Arctic stations to high altitude sites on the GrIS. t~~~~T~~here is a good correspondence between the Tskin and T2m and that the main factors ~~that~~ influencinge the ~~Tskin and T2m~~ relationship~~,~~ ~~include~~ are ~~found to be~~ seasonal variations, wind speed, ~~, and~~ cloud cover and the Tskin of the surface. The assessment of the tight relationship and the identification of the main variables that controls the variability are important findings when developing a statistical model that can convert satellite Tskin observations to T2m. All the identified parameters can be derived from either the satellite retrievals themselves or from NWP analysis and the generation of a daily satellite derived T2m product for the Polar Regions is thus made possible with these results. Such a satellite derived product will be independent of other existing surface temperature products and NWP reanalysis and can therefore contribute significantly to improvements in the Arctic climate change assessment since the

Formateret: Fremhævning

Formateret: Skrifttype: 10 pkt

satellite era started in the early 1980'ies. ~~The extensive data sets gathered in this study represent a wide range of weather conditions, from melting sea ice in the summer, over land based Arctic stations to high altitude sites on the GrIS.~~ ~~Historical and present in situ records consist to a large degree of a limited set of T2m observations. Conversely, satellite observations can provide global coverage on a daily basis of clear-sky Tskin.~~

~~There is thus a large potential in combining these types of observations either for satellite validation purposes or for extension of the time series in space and time, but this requires a detailed knowledge and quantification of the relationship between Tskin and T2m and of the factors determining the relationships. It is our hope that this study has contributed to a better understanding of the relationships.~~

7 Author contribution

Pia Nielsen-Englyst, ~~and~~ Kristine S. Madsen, Rasmus Tonboe, Gorm Dybkjær and Emy Alerskans ~~-~~compiled ~~and quality checked~~ the in situ data. Pia Nielsen-Englyst, Jacob L. Høyer and Kristine S. Madsen designed the experiments and Pia Nielsen-Englyst carried them out. Pia Nielsen-Englyst prepared the manuscript with contributions from all authors.

8 Competing interests

The authors declare that they have no conflict of interest.

9 Acknowledgements

This study was carried out as a part of the European Union Surface Temperatures for All Corners of Earth (EUSTACE), which is financed by the European Union's Horizon 2020 Programme for Research and Innovation, under Grant Agreement no 640171. The aim of EUSTACE is to provide a spatially complete daily field of air temperatures since 1850 by combining satellite and in situ observations. The author would like to thank the data providers. Data was provided by PROMICE, which is funded by the Danish Ministry of Climate, Energy and Building, operated by the Geological Survey of Denmark and Greenland and conducted in collaboration with the National Space Institute (DTU Space) and Asiaq (Greenland Survey)~~.~~, at http://www.promice.dk. Data were also obtained from the Atmospheric Radiation Measurement (ARM) Climate Research Facility, a U.S. Department of Energy Office of Science user facility sponsored by the Office of Biological and Environmental Research. We thank our colleagues in the SHEBA Atmospheric Surface Flux Group, Ed Andreas, Chris Fairall, Peter Guest, and Ola Persson for help collecting and processing the data. The National Science Foundation supported this research with grants to the U.S. Army Cold Regions Research and Engineering Laboratory, NOAA's Environmental Technology Laboratory, and the Naval Postgraduate School. Data was also provided by Timo Palo from the Tara expedition, supported by the European Commission 6th Framework Integrated Project DAMOCLES and in part by the Academy of Finland through the CACSI project. ~~Finally, w~~We thank Steinar Eastwood from the Norwegian Meteorological Institute for providing us with data from the FRAM2014/15 expedition. Finally, we would like to thank the anonymous reviewers for their carefully reading and their insightful suggestions and comments, which substantially improved this manuscript.

Formateret: Skrifttype: (Standard) Times New Roman, 10 pkt, Ikke Kursiv, Skriftfarve: Automatisk, Engelsk (Storbritannien)

References

Abermann, J., Hansen, B., Lund, M., Wacker, S., Karami, M. and Cappelen, J.: Hotspots and key periods of Greenland climate change during the past six decades, Ambio, 46(S1), 3–11, doi:10.1007/s13280-016-0861-y, 2017.

Ackerman, T. P. and Stokes, G. M.: The Atmospheric Radiation Measurement Program, Phys. Today, 56(1), 38–44, doi:10.1063/1.1554135, 2003.

Adolph, A. C., Albert, M. R. and Hall, D. K.: Near-surface temperature inversion during summer at Summit, Greenland, and its relation to MODIS-derived surface temperatures, The Cryosphere, 12(3), 907–920, doi:10.5194/tc-12-907-2018, 2018.

Ahlstrøm, A., van As, D., Citterio, M., Andersen, S., Fausto, R., Andersen, M., Forsberg, R., Stenseng, L., Lintz Christensen, E. and Kristensen, S. S.: A new Programme for Monitoring the Mass Loss of the Greenland Ice Sheet, Geol. Surv. Den. Greenl. Bull., 15, 61–64, 2008.

Box, J. E., Fettweis, X., Stroeve, J. C., Tedesco, M., Hall, D. K. and Steffen, K.: Greenland ice sheet albedo feedback: thermodynamics and atmospheric drivers, The Cryosphere, 6(4), 821–839, doi:10.5194/tc-6-821-2012, 2012.

Bretherton, C. S., Roode, S. R. de, Jakob, C., Andreas, E. L., Intrieri, J., Moritz, R. E. and Persson, O. G.: A comparison of the ECMWF forecast model with observations over the annual cycle at SHEBA. Unpublished manuscript, 2000.

Cappelen, J.: Greenland—DMI Historical Climate Data Collection 1784–2015. Danish Meteorological Institute., 2016.

Casey, K. A., Polashenski, C. M., Chen, J. and Tedesco, M.: Impact of MODIS sensor calibration updates on Greenland Ice Sheet surface reflectance and albedo trends, The Cryosphere, 11(4), 1781–1795, doi:10.5194/tc-11-1781-2017, 2017.

Cohen, J., Screen, J. A., Furtado, J. C., Barlow, M., Whittleston, D., Coumou, D., Francis, J., Dethloff, K., Entekhabi, D., Overland, J. and Jones, J.: Recent Arctic amplification and extreme mid-latitude weather, Nat. Geosci., 7(9), 627–637, doi:10.1038/ngeo2234, 2014.

Comiso, J. C.: Variability and Trends in Antarctic Surface Temperatures from In Situ and Satellite Infrared Measurements, J. Clim., 13(10), 1674–1696, doi:10.1175/1520-0442(2000)013<1674:VATIAS>2.0.CO;2, 2000.

Curry, J. A. and Herman, G. F.: Infrared Radiative Properties of Summertime Arctic Stratus Clouds, J. Clim. Appl. Meteorol., 24(6), 525–538, doi:10.1175/1520-0450(1985)024<0525:IRPOSA>2.0.CO;2, 1985.

Curry, J. A., Schramm, J. L., Rossow, W. B. and Randall, D.: Overview of Arctic Cloud and Radiation Characteristics, J. Clim., 9(8), 1731–1764, doi:10.1175/1520-0442(1996)009<1731:OOACAR>2.0.CO;2, 1996.

Dozier, J. and Warren, S. G.: Effect of viewing angle on the infrared brightness temperature of snow, Water Resour. Res., 18(5), 1424–1434, doi:10.1029/WR018i005p01424, 1982.

Dybkjær, G., Tonboe, R. and Høyer, J. L.: Arctic surface temperatures from MetOp AVHRR compared to in situ ocean and land data, Ocean Sci., 8(6), 959–970, doi:10.5194/os-8-959-2012, 2012.

Franco, B., Fettweis, X. and Erpicum, M.: Future projections of the Greenland ice sheet energy balance driving the surface melt, The Cryosphere, 7(1), 1–18, doi:10.5194/tc-7-1-2013, 2013.

Gascard, J.-C., Festy, J., le Goff, H., Weber, M., Bruemmer, B., Offermann, M., Doble, M., Wadhams, P., Forsberg, R., Hanson, S., Skourup, H., Gerland, S., Nicolaus, M., Metaxian, J.-P., Grangeon, J., Haapala, J., Rinne, E., Haas, C., Wegener,

Formateret: Bibliografi, Beskyt mod horeunger, Juster mellemrum mellem latinsk og asiatisk tekst, Juster mellemrum mellem asiatisk tekst og tal

Feltkode ændret

Formateret: Skrifttype: 10 pkt

A., Heygster, G., Jakobson, E., Palo, T., Wilkinson, J., Kaleschke, L., Claffey, K., Elder, B. and Bottenheim, J.: Exploring Arctic Transpolar Drift During Dramatic Sea Ice Retreat, Eos Trans. Am. Geophys. Union, 89(3), 21, doi:10.1029/2008EO030001, 2008.

Good, E. J., Ghent, D. J., Bulgin, C. E. and Remedios, J. J.: A spatiotemporal analysis of the relationship between near-surface air temperature and satellite land surface temperatures using 17 years of data from the ATSR series, J. Geophys. Res. Atmospheres, 122(17), 9185–9210, doi:10.1002/2017JD026880, 2017.

Graversen, R. G., Mauritsen, T., Tjernström, M., Källén, E. and Svensson, G.: Vertical structure of recent Arctic warming, Nature, 451(7174), 53–56, doi:10.1038/nature06502, 2008.

Hall, D., Box, J., Casey, K., Hook, S., Shuman, C. and Steffen, K.: Comparison of satellite-derived and in-situ observations of ice and snow surface temperatures over Greenland, Remote Sens. Environ., 112(10), 3739–3749, doi:10.1016/j.rse.2008.05.007, 2008.

Hall, D. K., Comiso, J. C., DiGirolamo, N. E., Shuman, C. A., Key, J. R. and Koenig, L. S.: A Satellite-Derived Climate-Quality Data Record of the Clear-Sky Surface Temperature of the Greenland Ice Sheet, J. Clim., 25(14), 4785–4798, doi:10.1175/JCLI-D-11-00365.1, 2012.

Hansen, J., Ruedy, R., Sato, M. and Lo, K.: Global surface temperature change, Rev. Geophys., 48(4), doi:10.1029/2010RG000345, 2010.

Høyer, J. L., Lang, A. M., Tonboe, R., Eastwood, S., Wimmer, W. and Dybkjær, G.: Towards field inter-comparison experiment (FICE) for ice surface temperature (ESA Tech. Rep. FRM4STS OP-40)., [online] Available from: http://www.frm4sts.org/wp-content/uploads/sites/3/2017/12/OFE-OP-40-TR-5-V1-Iss-1-Ver-1-Signed.pdf, 2017.

Hudson, S. R. and Brandt, R. E.: A Look at the Surface-Based Temperature Inversion on the Antarctic Plateau, J. Clim., 18(11), 1673–1696, doi:10.1175/JCLI3360.1, 2005.

Intrieri, J. M.: An annual cycle of Arctic surface cloud forcing at SHEBA, J. Geophys. Res., 107(C10), doi:10.1029/2000JC000439, 2002.

Jones, P. D., Lister, D. H., Osborn, T. J., Harpham, C., Salmon, M. and Morice, C. P.: Hemispheric and large-scale land-surface air temperature variations: An extensive revision and an update to 2010:, J. Geophys. Res. Atmospheres, 117(D5), n/a-n/a, doi:10.1029/2011JD017139, 2012.

King, J. C. and Turner, J.: Antarctic Meteorology and Climatology, Cambridge University Press, Cambridge., 1997.

Koenig, L. S. and Hall, D. K.: Comparison of satellite, thermochron and air temperatures at Summit, Greenland, during the winter of 2008/09, J. Glaciol., 56(198), 735–741, doi:10.3189/002214310793146269, 2010.

Kristoffersen, Y. and Hall, J.: Hovercraft as a Mobile Science Platform Over Sea Ice in the Arctic Ocean, Oceanography, 27(2), doi:10.5670/oceanog.2014.33, 2014.

Lettau, H. H. and Schwerdtfeger, W.: Dynamics of the surface-wind regime over the interior of Antarctica, Antarct. J. U. S., 2(5), 155–158, 1967.

Mahrt, L. J. and Schwerdtfeger, W.: Ekman spirals for exponential thermal wind, Bound.-Layer Meteorol., 1(2), 137–145, doi:10.1007/BF00185735, 1970.

Masson-Delmotte, V., Swingedouw, D., Landais, A., Seidenkrantz, M.-S., Gauthier, E., Bichet, V., Massa, C., Perren, B., Jomelli, V., Adalgeirsdottir, G., Hesselbjerg Christensen, J., Arneborg, J., Bhatt, U., Walker, D. A., Elberling, B., Gillet-Chaulet, F., Ritz, C., Gallée, H., van den Broeke, M., Fettweis, X., de Vernal, A. and Vinther, B.: Greenland climate change: from the past to the future: Greenland climate change, Wiley Interdiscip. Rev. Clim. Change, 3(5), 427–449, doi:10.1002/wcc.186, 2012.

Maykut, G. A.: The Surface Heat and Mass Balance, in The Geophysics of Sea Ice, edited by N. Untersteiner, pp. 395–463, Springer US, Boston, MA., 1986.

Miller, N. B., Turner, D. D., Bennartz, R., Shupe, M. D., Kulie, M. S., Cadeddu, M. P. and Walden, V. P.: Surface-based inversions above central Greenland, J. Geophys. Res. Atmospheres, 118(2), 495–506, doi:10.1029/2012JD018867, 2013.

Monin, A. S. and Obukhov, A. M.: Basic Laws of Turbulent Mixing in the Surface Layer of the Atmosphere, Contrib. Geophys. Inst. Slovak Acad. Sci., USSR 151.163, 1954.

Moris, V. R.: Infrared Thermometer (IRT) Handbook Atmospheric Radiation Measurement publication ARM TR-015 available from https://www.arm.gov/instruments/irt, 2006.

Overland, J., Francis, J. A., Hall, R., Hanna, E., Kim, S.-J. and Vihma, T.: The Melting Arctic and Midlatitude Weather Patterns: Are They Connected?*, J. Clim., 28(20), 7917–7932, doi:10.1175/JCLI-D-14-00822.1, 2015.

Persson, P. O. G.: Measurements near the Atmospheric Surface Flux Group tower at SHEBA: Near-surface conditions and surface energy budget, J. Geophys. Res., 107(C10), doi:10.1029/2000JC000705, 2002.

Rasmussen, T. A. S., Høyer, J. L., Ghent, D., Bulgin, C. E., Dybkjaer, G., Ribergaard, M. H., Nielsen-Englyst, P. and Madsen, K. S.: Impact of Assimilation of Sea-Ice Surface Temperatures on a Coupled Ocean and Sea-Ice Model, J. Geophys. Res. Oceans, 123(4), 2440–2460, doi:10.1002/2017JC013481, 2018.

Rayner, N. A.: Global analyses of sea surface temperature, sea ice, and night marine air temperature since the late nineteenth century, J. Geophys. Res., 108(D14), doi:10.1029/2002JD002670, 2003.

Reeves Eyre, J. E. J. and Zeng, X.: Evaluation of Greenland near surface air temperature datasets, The Cryosphere, 11(4), 1591–1605, doi:10.5194/tc-11-1591-2017, 2017.

Rignot, E.: Changes in the Velocity Structure of the Greenland Ice Sheet, Science, 311(5763), 986–990, doi:10.1126/science.1121381, 2006.

Rigor, I. G., Colony, R. L. and Martin, S.: Variations in Surface Air Temperature Observations in the Arctic, 1979–97, J. Clim., 13(5), 896–914, doi:10.1175/1520-0442(2000)013<0896:VISATO>2.0.CO;2, 2000.

Serreze, M. C., Schnell, R. C. and Kahl, J. D.: Low-Level Temperature Inversions of the Eurasian Arctic and Comparisons with Soviet Drifting Station Data, J. Clim., 5(6), 615–629, doi:10.1175/1520-0442(1992)005<0615:LLTIOT>2.0.CO;2, 1992.

Shuman, C. A., Hall, D. K., DiGirolamo, N. E., Mefford, T. K. and Schnaubelt, M. J.: Comparison of Near-Surface Air Temperatures and MODIS Ice-Surface Temperatures at Summit, Greenland (2008–13), J. Appl. Meteorol. Climatol., 53(9), 2171–2180, doi:10.1175/JAMC-D-14-0023.1, 2014.

Stamnes, K., Ellingson, R. G., Curry, J. A., Walsh, J. E. and Zak, B. D.: Review of Science Issues, Deployment Strategy, and Status for the ARM North Slope of Alaska–Adjacent Arctic Ocean Climate Research Site, J. Clim., 12(1), 46–63, doi:10.1175/1520-0442-12.1.46, 1999.

Steffen, K.: Surface energy exchange at the equilibrium line on the Greenland ice sheet during onset of melt, Ann. Glaciol., 21, 13–18, doi:10.3189/S0260305500015536, 1995.

Steffen, K. and Box, J.: Surface climatology of the Greenland Ice Sheet: Greenland Climate Network 1995-1999, J. Geophys. Res. Atmospheres, 106(D24), 33951–33964, doi:10.1029/2001JD900161, 2001.

Stocker, T. F., Qin, D., Plattner, G.-K., Tignor, M., Allen, S. K., Boschung, J., Nauels, A., Xia, Y., Bex, V., Midgley, P. M. and (eds.): Climate Change 2013 - The Physical Science Basis: Working Group I Contribution to the Fifth Assessment Report of the Intergovernmental Panel on Climate Change, Cambridge University Press, Cambridge., 2014.

Stroeve, J., Box, J. E., Wang, Z., Schaaf, C. and Barrett, A.: Re-evaluation of MODIS MCD43 Greenland albedo accuracy and trends, Remote Sens. Environ., 138, 199–214, doi:10.1016/j.rse.2013.07.023, 2013.

Swinbank, W. C.: Long-wave radiation from clear skies, Q. J. R. Meteorol. Soc., 89(381), 339–348, doi:10.1002/qj.49708938105, 1963.

Tedesco, M., Fettweis, X., van den Broeke, M. R., van de Wal, R. S. W., Smeets, C. J. P. P., van de Berg, W. J., Serreze, M. C. and Box, J. E.: The role of albedo and accumulation in the 2010 melting record in Greenland, Environ. Res. Lett., 6(1), 014005, doi:10.1088/1748-9326/6/1/014005, 2011.

Uttal, T., Curry, J. A., Mcphee, M. G., Perovich, D. K., Moritz, R. E., Maslanik, J. A., Guest, P. S., Stern, H. L., Moore, J. A., Turenne, R., Heiberg, A., Serreze, M. C., Wylie, D. P., Persson, O. G., Paulson, C. A., Halle, C., Morison, J. H., Wheeler, P. A., Makshtas, A., Welch, H., Shupe, M. D., Intrieri, J. M., Stamnes, K., Lindsey, R. W., Pinkel, R., Pegau, W. S., Stanton, T. P. and Grenfeld, T. C.: Surface Heat Budget of the Arctic Ocean, Bull. Am. Meteorol. Soc., 83(2), 255–275, doi:10.1175/1520-0477(2002)083<0255:SHBOTA>2.3.CO;2, 2002.

van As, D.: Warming, glacier melt and surface energy budget from weather station observations in the Melville Bay region of northwest Greenland, J. Glaciol., 57(202), 208–220, doi:10.3189/002214311796405898, 2011.

van As, D., Broeke, M. van den, Reijmer, C. and Wal, R. van de: The Summer Surface Energy Balance of the High Antarctic Plateau, Bound.-Layer Meteorol., 115(2), 289–317, doi:10.1007/s10546-004-4631-1, 2005.

van As, D., Fausto, R., Steffen, K., Ahlstrøm, A., Andersen, S. B., Andersen, M. L., Box, J., Charalampidis, C., Citterio, M., Colgan, W. T., Edelvang, K., Larsen, S. H., Nielsen, S., Martin, V. and Weidick, A.: Katabatic winds and piteraq storms: Observations from the Greenland ice sheet, Geol. Surv. Den. Greenl. Bull., (31), 83–86, 2014.

van den Broeke, M., Duynkerke, P. and Oerlemans, J.: The observed katabatic flow at the edge of the Greenland ice sheet during GIMEX-91, Glob. Planet. Change, 9(1–2), 3–15, doi:10.1016/0921-8181(94)90003-5, 1994.

Vihma, T.: Effects of Arctic Sea Ice Decline on Weather and Climate: A Review, Surv. Geophys., 35(5), 1175–1214, doi:10.1007/s10712-014-9284-0, 2014.

Vihma, T. and Pirazzini, R.: On the Factors Controlling the Snow Surface and 2-m Air Temperatures Over the Arctic Sea Ice in Winter, Bound.-Layer Meteorol., 117(1), 73–90, doi:10.1007/s10546-004-5938-7, 2005.

Formateret: Bibliografi, Beskyt mod horeunger, Juster mellemrum mellem latinsk og asiatisk tekst, Juster mellemrum mellem asiatisk tekst og tal

Formateret: Skrifttype: 10 pkt

Vihma, T., Jaagus, J., Jakobson, E. and Palo, T.: Meteorological conditions in the Arctic Ocean in spring and summer 2007 as recorded on the drifting ice station Tara, Geophys. Res. Lett., 35(18), doi:10.1029/2008GL034681, 2008.

Walsh, J. E.: Intensified warming of the Arctic: Causes and impacts on middle latitudes, Glob. Planet. Change, 117, 52–63, doi:10.1016/j.gloplacha.2014.03.003, 2014.

Walsh, J. E. and Chapman, W. L.: Arctic Cloud–Radiation–Temperature Associations in Observational Data and Atmospheric Reanalyses, J. Clim., 11(11), 3030–3045, doi:10.1175/1520-0442(1998)011<3030:ACRTAI>2.0.CO;2, 1998.

Zhang, Y., Seidel, D. J., Golaz, J.-C., Deser, C. and Tomas, R. A.: Climatological Characteristics of Arctic and Antarctic Surface-Based Inversions, J. Clim., 24(19), 5167–5186, doi:10.1175/2011JCLI4004.1, 2011.

Zygmuntowska, M., Mauritsen, T., Quaas, J. and Kaleschke, L.: Arctic Clouds and Surface Radiation – a critical comparison of satellite retrievals and the ERA-Interim reanalysis, Atmospheric Chem. Phys., 12(14), 6667–6677, doi:10.5194/acp-12-6667-2012, 2012.

~~Abermann, J., Hansen, B., Lund, M., Wacker, S., Karami, M. and Cappelen, J.: Hotspots and key periods of Greenland climate change during the past six decades, Ambio, 46(S1), 3–11, doi:10.1007/s13280-016-0861-y, 2017.~~

~~Ackerman, T. P. and Stokes, G. M.: The Atmospheric Radiation Measurement Program, Phys. Today, 56(1), 38–44, doi:10.1063/1.1554135, 2003.~~

~~Adolph, A. C., Albert, M. R. and Hall, D. K.: Near-surface temperature inversion during summer at Summit, Greenland, and its relation to MODIS-derived surface temperatures, The Cryosphere, 12(3), 907–920, doi:10.5194/tc-12-907-2018, 2018.~~

~~Ahlstrøm, A., van As, D., Citterio, M., Andersen, S., Fausto, R., Andersen, M., Forsberg, R., Stenseng, L., Lintz Christensen, E. and Kristensen, S. S.: A new Programme for Monitoring the Mass Loss of the Greenland Ice Sheet, Geol. Surv. Den. Greenl. Bull., 15, 61–64, 2008.~~

~~van As, D.: Warming, glacier melt and surface energy budget from weather station observations in the Melville Bay region of northwest Greenland, J. Glaciol., 57(202), 208–220, doi:10.3189/002214311796405898, 2011.~~

~~van As, D., Broeke, M. van den, Reijmer, C. and Wal, R. van de: The Summer Surface Energy Balance of the High Antarctic Plateau, Bound.-Layer Meteorol., 115(2), 289–317, doi:10.1007/s10546-004-4631-1, 2005.~~

~~van As, D., Fausto, R., Steffen, K., Ahlstrøm, A., Andersen, S. B., Andersen, M. L., Box, J., Charalampidis, C., Citterio, M., Colgan, W. T., Edelvang, K., Larsen, S. H., Nielsen, S., Martin, V. and Weidick, A.: Katabatic winds and piteraq storms: Observations from the Greenland ice sheet, Geol. Surv. Den. Greenl. Bull., (31), 83–86, 2014.~~

~~Box, J. E., Fettweis, X., Stroeve, J. C., Tedesco, M., Hall, D. K. and Steffen, K.: Greenland ice sheet albedo feedback: thermodynamics and atmospheric drivers, The Cryosphere, 6(4), 821–839, doi:10.5194/tc-6-821-2012, 2012.~~

~~Bretherton, C. S., Roode, S. R. de, Jakob, C., Andreas, E. L., Intrieri, J., Moritz, R. E. and Persson, O. G.: A comparison of the ECMWF forecast model with observations over the annual cycle at SHEBA. Unpublished manuscript, 2000.~~

~~van den Broeke, M., Duynkerke, P. and Oerlemans, J.: The observed katabatic flow at the edge of the Greenland ice sheet during GIMEX-91, Glob. Planet. Change, 9(1–2), 3–15, doi:10.1016/0921-8181(94)90003-5, 1994.~~

~~Cappelen, J.: Greenland – DMI Historical Climate Data Collection 1784–2015. Danish Meteorological Institute., 2016.~~

~~Casey, K. A., Polashenski, C. M., Chen, J. and Tedesco, M.: Impact of MODIS sensor calibration updates on Greenland Ice Sheet surface reflectance and albedo trends, The Cryosphere, 11(4), 1781–1795, doi:10.5194/tc-11-1781-2017, 2017.~~

~~Cohen, J., Screen, J. A., Furtado, J. C., Barlow, M., Whittleston, D., Coumou, D., Francis, J., Dethloff, K., Entekhabi, D., Overland, J. and Jones, J.: Recent Arctic amplification and extreme mid-latitude weather, Nat. Geosci., 7(9), 627–637, doi:10.1038/ngeo2234, 2014.~~

~~Comiso, J. C.: Variability and Trends in Antarctic Surface Temperatures from In Situ and Satellite Infrared Measurements, J. Clim., 13(10), 1674–1696, doi:10.1175/1520-0442(2000)013<1674:VATIAS>2.0.CO;2, 2000.~~

~~Curry, J. A. and Herman, G. F.: Infrared Radiative Properties of Summertime Arctic Stratus Clouds, J. Clim. Appl. Meteorol., 24(6), 525–538, doi:10.1175/1520-0450(1985)024<0525:IRPOSA>2.0.CO;2, 1985.~~

~~Curry, J. A., Schramm, J. L., Rossow, W. B. and Randall, D.: Overview of Arctic Cloud and Radiation Characteristics, J. Clim., 9(8), 1731–1764, doi:10.1175/1520-0442(1996)009<1731:OOACAR>2.0.CO;2, 1996.~~

~~Dozier, J. and Warren, S. G.: Effect of viewing angle on the infrared brightness temperature of snow, Water Resour. Res., 18(5), 1424–1434, doi:10.1029/WR018i005p01424, 1982.~~

~~Dybkjær, G., Tonboe, R. and Høyer, J. L.: Arctic surface temperatures from MetOp AVHRR compared to in situ ocean and land data, Ocean Sci., 8(6), 959–970, doi:10.5194/os-8-959-2012, 2012.~~

~~Franco, B., Fettweis, X. and Erpicum, M.: Future projections of the Greenland ice sheet energy balance driving the surface melt, The Cryosphere, 7(1), 1–18, doi:10.5194/tc-7-1-2013, 2013.~~

~~Gascard, J. C., Festy, J., le Goff, H., Weber, M., Bruemmer, B., Offermann, M., Doble, M., Wadhams, P., Forsberg, R., Hanson, S., Skourup, H., Gerland, S., Nicolaus, M., Metaxian, J. P., Grangeon, J., Haapala, J., Rinne, E., Haas, C., Wegener, A., Heygster, G., Jakobson, E., Palo, T., Wilkinson, J., Kaleschke, L., Claffey, K., Elder, B. and Bottenheim, J.: Exploring Arctic Transpolar Drift During Dramatic Sea Ice Retreat, Eos Trans. Am. Geophys. Union, 89(3), 21, doi:10.1029/2008EO030001, 2008.~~

~~Good, E. J., Ghent, D. J., Bulgin, C. E. and Remedios, J. J.: A spatiotemporal analysis of the relationship between near-surface air temperature and satellite land surface temperatures using 17 years of data from the ATSR series, J. Geophys. Res. Atmospheres, 122(17), 9185–9210, doi:10.1002/2017JD026880, 2017.~~

~~Graversen, R. G., Mauritsen, T., Tjernström, M., Källén, E. and Svensson, G.: Vertical structure of recent Arctic warming, Nature, 451(7174), 53–56, doi:10.1038/nature06502, 2008.~~

~~Hall, D., Box, J., Casey, K., Hook, S., Shuman, C. and Steffen, K.: Comparison of satellite-derived and in-situ observations of ice and snow surface temperatures over Greenland, Remote Sens. Environ., 112(10), 3739–3749, doi:10.1016/j.rse.2008.05.007, 2008.~~

~~Hall, D. K., Comiso, J. C., DiGirolamo, N. E., Shuman, C. A., Key, J. R. and Koenig, L. S.: A Satellite-Derived Climate-Quality Data Record of the Clear-Sky Surface Temperature of the Greenland Ice Sheet, J. Clim., 25(14), 4785–4798, doi:10.1175/JCLI-D-11-00365.1, 2012.~~

~~Hansen, J., Ruedy, R., Sato, M. and Lo, K.: Global surface temperature change, Rev. Geophys., 48(4), doi:10.1029/2010RG000345, 2010.~~

~~Høyer, J. L., Lang, A. M., Tonboe, R., Eastwood, S., Wimmer, W. and Dybkjær, G.: Towards field inter-comparison experiment (FICE) for ice surface temperature (ESA Tech. Rep. FRM4STS OP-40)., [online] Available from: http://www.frm4sts.org/wp-content/uploads/sites/3/2017/12/OFE-OP-40-TR-5-V1-Iss-1-Ver-1-Signed.pdf, 2017.~~

~~Hudson, S. R. and Brandt, R. E.: A Look at the Surface-Based Temperature Inversion on the Antarctic Plateau, J. Clim., 18(11), 1673–1696, doi:10.1175/JCLI3360.1, 2005.~~

~~Intrieri, J. M.: An annual cycle of Arctic surface cloud forcing at SHEBA, J. Geophys. Res., 107(C10), doi:10.1029/2000JC000439, 2002.~~

~~Jones, P. D., Lister, D. H., Osborn, T. J., Harpham, C., Salmon, M. and Morice, C. P.: Hemispheric and large-scale land-surface air temperature variations: An extensive revision and an update to 2010:, J. Geophys. Res. Atmospheres, 117(D5), n/a-n/a, doi:10.1029/2011JD017139, 2012.~~

~~King, J. C. and Turner, J.: Antarctic Meteorology and Climatology, Cambridge University Press, Cambridge., 1997.~~

~~Koenig, L. S. and Hall, D. K.: Comparison of satellite, thermochron and air temperatures at Summit, Greenland, during the winter of 2008/09, J. Glaciol., 56(198), 735–741, doi:10.3189/002214310793146269, 2010.~~

~~Kristoffersen, Y. and Hall, J.: Hovercraft as a Mobile Science Platform Over Sea Ice in the Arctic Ocean, Oceanography, 27(2), doi:10.5670/oceanog.2014.33, 2014.~~

~~Lettau, H. H. and Schwerdtfeger, W.: Dynamics of the surface-wind regime over the interior of Antarctica, Antarct. J. U. S., 2(5), 155–158, 1967.~~

~~Mahrt, L. J. and Schwerdtfeger, W.: Ekman spirals for exponential thermal wind, Bound. Layer Meteorol., 1(2), 137–145, doi:10.1007/BF00185735, 1970.~~

~~Masson-Delmotte, V., Swingedouw, D., Landais, A., Seidenkrantz, M. S., Gauthier, E., Bichet, V., Massa, C., Perren, B., Jomelli, V., Adalgeirsdottir, G., Hesselbjerg Christensen, J., Arneborg, J., Bhatt, U., Walker, D. A., Elberling, B., Gillet-Chaulet, F., Ritz, C., Gallée, H., van den Broeke, M., Fettweis, X., de Vernal, A. and Vinther, B.: Greenland climate change: from the past to the future: Greenland climate change, Wiley Interdiscip. Rev. Clim. Change, 3(5), 427–449, doi:10.1002/wcc.186, 2012.~~

~~Maykut, G. A.: The Surface Heat and Mass Balance, in The Geophysics of Sea Ice, edited by N. Untersteiner, pp. 395–463, Springer US, Boston, MA., 1986.~~

~~Miller, N. B., Turner, D. D., Bennartz, R., Shupe, M. D., Kulie, M. S., Cadeddu, M. P. and Walden, V. P.: Surface-based inversions above central Greenland, J. Geophys. Res. Atmospheres, 118(2), 495–506, doi:10.1029/2012JD018867, 2013.~~

~~Moris, V. R.: Infrared Thermometer (IRT) Handbook Atmospheric Radiation Measurement publication ARM TR-015 available from https://www.arm.gov/instruments/irt, 2006.~~

~~Persson, P. O. G.: Measurements near the Atmospheric Surface Flux Group tower at SHEBA: Near-surface conditions and surface energy budget, J. Geophys. Res., 107(C10), doi:10.1029/2000JC000705, 2002.~~

~~Rasmussen, T. A. S., Høyer, J. L., Ghent, D., Bulgin, C. E., Dybkjaer, G., Ribergaard, M. H., Nielsen-Englyst, P. and Madsen, K. S.: Impact of Assimilation of Sea-Ice Surface Temperatures on a Coupled Ocean and Sea-Ice Model, J. Geophys. Res. Oceans, 123(4), 2440–2460, doi:10.1002/2017JC013481, 2018.~~

~~Rayner, N. A.: Global analyses of sea surface temperature, sea ice, and night marine air temperature since the late nineteenth century, J. Geophys. Res., 108(D14), doi:10.1029/2002JD002670, 2003.~~

~~Reeves Eyre, J. E. J. and Zeng, X.: Evaluation of Greenland near surface air temperature datasets, The Cryosphere, 11(4), 1591–1605, doi:10.5194/tc-11-1591-2017, 2017.~~

~~Rignot, E.: Changes in the Velocity Structure of the Greenland Ice Sheet, Science, 311(5763), 986–990, doi:10.1126/science.1121381, 2006.~~

~~Rigor, I. G., Colony, R. L. and Martin, S.: Variations in Surface Air Temperature Observations in the Arctic, 1979–97, J. Clim., 13(5), 896–914, doi:10.1175/1520-0442(2000)013<0896:VISATO>2.0.CO;2, 2000.~~

~~Screen, J. A. and Simmonds, I.: The central role of diminishing sea ice in recent Arctic temperature amplification, Nature, 464(7293), 1334–1337, doi:10.1038/nature09051, 2010.~~

~~Serreze, M. C. and Francis, J. A.: The Arctic Amplification Debate, Clim. Change, 76(3–4), 241–264, doi:10.1007/s10584-005-9017-y, 2006.~~

~~Serreze, M. C., Schnell, R. C. and Kahl, J. D.: Low-Level Temperature Inversions of the Eurasian Arctic and Comparisons with Soviet Drifting Station Data, J. Clim., 5(6), 615–629, doi:10.1175/1520-0442(1992)005<0615:LLTIOT>2.0.CO;2, 1992.~~

~~Shuman, C. A., Hall, D. K., DiGirolamo, N. E., Mefford, T. K. and Schnaubelt, M. J.: Comparison of Near-Surface Air Temperatures and MODIS Ice-Surface Temperatures at Summit, Greenland (2008–13), J. Appl. Meteorol. Climatol., 53(9), 2171–2180, doi:10.1175/JAMC-D-14-0023.1, 2014.~~

~~Stamnes, K., Ellingson, R. G., Curry, J. A., Walsh, J. E. and Zak, B. D.: Review of Science Issues, Deployment Strategy, and Status for the ARM North Slope of Alaska-Adjacent Arctic Ocean Climate Research Site, J. Clim., 12(1), 46–63, doi:10.1175/1520-0442-12.1.46, 1999.~~

~~Steffen, K. and Box, J.: Surface climatology of the Greenland Ice Sheet: Greenland Climate Network 1995-1999, J. Geophys. Res. Atmospheres, 106(D24), 33951–33964, doi:10.1029/2001JD900161, 2001.~~

~~Stocker, T. (Ed.). (2014). Climate change 2013: the physical science basis: Working Group I contribution to the Fifth assessment report of the Intergovernmental Panel on Climate Change. Cambridge University Press.~~

~~Stroeve, J., Box, J. E., Wang, Z., Schaaf, C. and Barrett, A.: Re-evaluation of MODIS MCD43 Greenland albedo accuracy and trends, Remote Sens. Environ., 138, 199–214, doi:10.1016/j.rse.2013.07.023, 2013.~~

~~Swinbank, W. C.: Long-wave radiation from clear skies, Q. J. R. Meteorol. Soc., 89(381), 339–348, doi:10.1002/qj.49708938105, 1963.~~

~~Tedesco, M., Fettweis, X., van den Broeke, M. R., van de Wal, R. S. W., Smeets, C. J. P. P., van de Berg, W. J., Serreze, M. C. and Box, J. E.: The role of albedo and accumulation in the 2010 melting record in Greenland, Environ. Res. Lett., 6(1), 014005, doi:10.1088/1748-9326/6/1/014005, 2011.~~

~~Uttal, T., Curry, J. A., Mcphee, M. G., Perovich, D. K., Moritz, R. E., Maslanik, J. A., Guest, P. S., Stern, H. L., Moore, J. A., Turenne, R., Heiberg, A., Serreze, M. C., Wylie, D. P., Persson, O. G., Paulson, C. A., Halle, C., Morison, J. H., Wheeler, P. A., Makshtas, A., Welch, H., Shupe, M. D., Intrieri, J. M., Stamnes, K., Lindsey, R. W., Pinkel, R., Pegau, W.~~

~~S., Stanton, T. P. and Grenfeld, T. C.: Surface Heat Budget of the Arctic Ocean, Bull. Am. Meteorol. Soc., 83(2), 255–275, doi:10.1175/1520-0477(2002)083<0255:SHBOTA>2.3.CO;2, 2002.~~

~~Vihma, T. and Pirazzini, R.: On the Factors Controlling the Snow Surface and 2-m Air Temperatures Over the Arctic Sea Ice in Winter, Bound.-Layer Meteorol., 117(1), 73–90, doi:10.1007/s10546-004-5938-7, 2005.~~

~~Vihma, T., Jaagus, J., Jakobson, E. and Palo, T.: Meteorological conditions in the Arctic Ocean in spring and summer 2007 as recorded on the drifting ice station Tara, Geophys. Res. Lett., 35(18), doi:10.1029/2008GL034681, 2008.~~

~~Walsh, J. E. and Chapman, W. L.: Arctic Cloud Radiation Temperature Associations in Observational Data and Atmospheric Reanalyses, J. Clim., 11(11), 3030–3045, doi:10.1175/1520-0442(1998)011<3030:ACRTAI>2.0.CO;2, 1998.~~

~~Zhang, Y., Seidel, D. J., Golaz, J. C., Deser, C. and Tomas, R. A.: Climatological Characteristics of Arctic and Antarctic Surface-Based Inversions, J. Clim., 24(19), 5167–5186, doi:10.1175/2011JCLI4004.1, 2011.~~

~~Zygmuntowska, M., Mauritsen, T., Quaas, J. and Kaleschke, L.: Arctic Clouds and Surface Radiation – a critical comparison of satellite retrievals and the ERA-Interim reanalysis, Atmospheric Chem. Phys., 12(14), 6667–6677, doi:10.5194/acp-12-6667-2012, 2012.~~

Table 1 Observation sites used in this study covering the following surface types: Accumulation zone (ACC), upper/middle ablation zone (UAB), lower ablation zone (LAB), seasonal snow cover (SSC), sea ice (SICE).

Formateret: Engelsk (Storbritannien)

Project	Site	Station	Surface Type	Latitude (°N)	Longitude (°W)	Elevation (m)	Start date	End date
PROMICE	East Grip	EGP	ACC	75.62	35.97	2660	01/05/2016	30/04/2018
PROMICE	Kangerlussuaq	KAN_U	ACC	67.00	47.03	1840	04/04/2009	03/04/2018
PROMICE	Crown Prince Christian Land	KPC_U	ACC	79.83	25.17	870	17/07/2008	16/07/2018
PROMICE	Kangerlussuaq	KAN_M	UAB	67.07	48.84	1270	02/09/2008	01/09/2018
PROMICE	Nuuk	NUK_N	UAB	64.95	49.89	920	25/07/2010	24/07/2014
PROMICE	Nuuk	NUK_U	UAB	64.51	49.27	1120	20/08/2007	19/08/2018
PROMICE	Qassimiut	QAS_A	UAB	61.24	46.73	1000	20/08/2012	19/08/2015
PROMICE	Qassimiut	QAS_M	UAB	61.10	46.83	630	11/08/2016	10/08/2018
PROMICE	Qassimiut	QAS_U	UAB	61.18	46.82	900	07/08/2008	06/08/2018
PROMICE	Scoresbysund	SCO_U	UAB	72.39	27.23	970	21/07/2008	20/07/2018
PROMICE	Tasiilaq	TAS_A	UAB	65.78	38.90	890	28/08/2013	27/08/2018
PROMICE	Tasiilaq	TAS_U	UAB	65.67	38.87	570	11/03/2008	10/03/2015
PROMICE	Thule	THU_U	UAB	76.42	68.15	760	09/08/2010	08/08/2018
PROMICE	Upernavik	UPE_U	UAB	72.89	53.58	940	18/08/2009	17/08/2018
PROMICE	Kangerlussuaq	KAN_L	LAB	67.10	49.95	670	01/09/2008	31/08/2018
PROMICE	Crown Prince Christian Land	KPC_L	LAB	79.91	24.08	370	17/07/2008	16/07/2018
PROMICE	Nuuk	NUK_L	LAB	64.48	49.54	530	20/08/2007	19/08/2018
PROMICE	Qassimiut	QAS_L	LAB	61.03	46.85	280	24/08/2007	23/08/2018
PROMICE	Scoresbysund	SCO_L	LAB	72.22	26.82	460	22/07/2008	21/07/2018
PROMICE	Tasiilaq	TAS_L	LAB	65.64	38.90	250	23/08/2007	22/08/2018
PROMICE	Thule	THU_L	LAB	76.40	68.27	570	09/08/2010	08/08/2018
PROMICE	Upernavik	UPE_L	LAB	72.90	54.30	220	17/08/2009	16/08/2018
ARM	Atqasuk	ATQ	SSC	70.47	149.89	2	07/11/2003	06/11/2010

ARM	Barrow	BAR	SSC	71.32	156.62	8	31/10/2003	28/10/2018
ARM	Oliktok Point	OLI	SSC	70.50	157.41	20	18/10/2013	13/10/2018
ICEARC	Qaanaaq	DMI_Q	SICE	77.43	69.14	Sea level	31/01/2015	08/06/2017
FRAM2014/15	Arctic Ocean	FRAM	SICE	82.22-89.35	-180.00-180.00	Sea level	05/09/2014	3/07/2015
SHEBA	Arctic Ocean	SHEBA	SICE	74.62-80.37	143.92-168.15	Sea level	01/11/1997	26/09/1998
TARA	Arctic Ocean	TARA	SICE	71.41-88.54	0.01-148.28	Sea level	01/04/2007	20/09/2007

Formateret: Normal, Hold ikke sammen med næste

~~Project~~	~~Site~~	~~Station~~	~~Surface~~	~~Latitude (°N)~~	~~Longitude (°W)~~	~~Elevation (m)~~	~~Start date~~	~~End date~~
~~PROMICE~~	~~East Grip~~	~~EGP~~	~~Land ice~~	~~75.62~~	~~35.97~~	~~2660~~	~~01/05/2016~~	~~15/09/2017~~
~~PROMICE~~	~~Kangerlussuaq~~	~~KAN_M~~	~~Land ice~~	~~67.07~~	~~48.84~~	~~1270~~	~~02/09/2008~~	~~16/09/2017~~
~~PROMICE~~	~~Kangerlussuaq~~	~~KAN_U~~	~~Land ice~~	~~67.00~~	~~47.03~~	~~1840~~	~~04/04/2009~~	~~16/09/2017~~
~~PROMICE~~	~~Crown Prince Christian Land~~	~~KPC_U~~	~~Land ice~~	~~79.83~~	~~25.17~~	~~870~~	~~17/07/2008~~	~~16/09/2017~~
~~PROMICE~~	~~Nuuk~~	~~NUK_N~~	~~Land ice~~	~~64.95~~	~~49.89~~	~~920~~	~~25/07/2010~~	~~25/07/2014~~
~~PROMICE~~	~~Nuuk~~	~~NUK_U~~	~~Land ice~~	~~64.51~~	~~49.27~~	~~1120~~	~~20/08/2007~~	~~16/09/2017~~
~~PROMICE~~	~~Qassimiut~~	~~QAS_A~~	~~Land ice~~	~~61.24~~	~~46.73~~	~~1000~~	~~20/08/2012~~	~~24/08/2015~~
~~PROMICE~~	~~Qassimiut~~	~~QAS_U~~	~~Land ice~~	~~61.18~~	~~46.82~~	~~900~~	~~07/08/2008~~	~~16/09/2017~~
~~PROMICE~~	~~Scoresbysund~~	~~SCO_U~~	~~Land ice~~	~~72.39~~	~~27.23~~	~~970~~	~~21/07/2008~~	~~16/09/2017~~
~~PROMICE~~	~~Tasiilaq~~	~~TAS_A~~	~~Land ice~~	~~65.78~~	~~38.90~~	~~890~~	~~28/08/2013~~	~~16/09/2017~~
~~PROMICE~~	~~Tasiilaq~~	~~TAS_U~~	~~Land ice~~	~~65.67~~	~~38.87~~	~~570~~	~~15/08/2007~~	~~13/08/2015~~
~~PROMICE~~	~~Thule~~	~~THU_U~~	~~Land ice~~	~~76.42~~	~~68.15~~	~~760~~	~~09/08/2010~~	~~16/09/2017~~
~~PROMICE~~	~~Upernavik~~	~~UPE_U~~	~~Land ice~~	~~72.89~~	~~53.58~~	~~940~~	~~17/08/2009~~	~~16/09/2017~~
~~ARM~~	~~Atqasuk~~	~~ATQ~~	~~Land ice~~	~~70.47~~	~~149.89~~	~~2~~	~~07/11/2003~~	~~17/01/2011~~
~~ARM~~	~~Barrows~~	~~BAR~~	~~Land ice~~	~~71.32~~	~~156.62~~	~~8~~	~~31/10/2003~~	~~26/10/2017~~
~~ARM~~	~~Oliktok Point~~	~~OLI~~	~~Land ice~~	~~70.50~~	~~157.41~~	~~20~~	~~18/10/2013~~	~~26/10/2017~~
~~ICEARC~~	~~Qaanaaq~~	~~DMI_Q~~	~~Sea ice~~	~~77.43~~	~~69.14~~	~~Sea level~~	~~31/01/2015~~	~~08/06/2017~~
~~FRAM2014/15~~	~~Arctic Ocean~~	~~FRAM~~	~~Sea ice~~	~~82.22-89.35~~	~~-180.00-180.00~~	~~Sea level~~	~~05/09/2014~~	~~3/07/2015~~

~~SHEBA~~	~~Arctic Ocean~~	~~SHEBA~~	~~Sea ice~~	~~74.62-80.37~~	~~143.92-168.15~~	~~Sea level~~	~~01/11/1997~~	~~26/09/1998~~
~~TARA~~	~~Arctic Ocean~~	~~TARA~~	~~Sea ice~~	~~71.41-88.54~~	~~0.01-148.28~~	~~Sea level~~	~~01/04/2007~~	~~20/09/2007~~

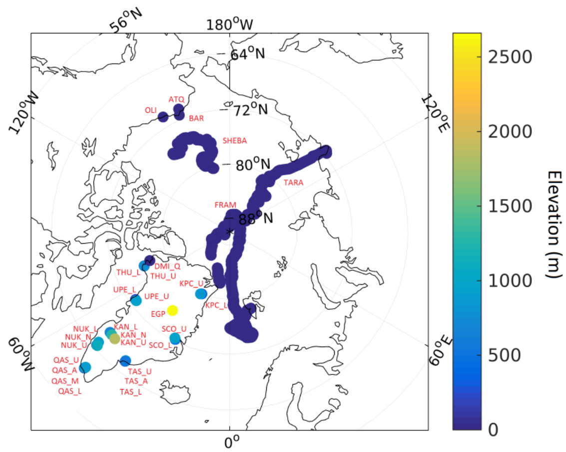

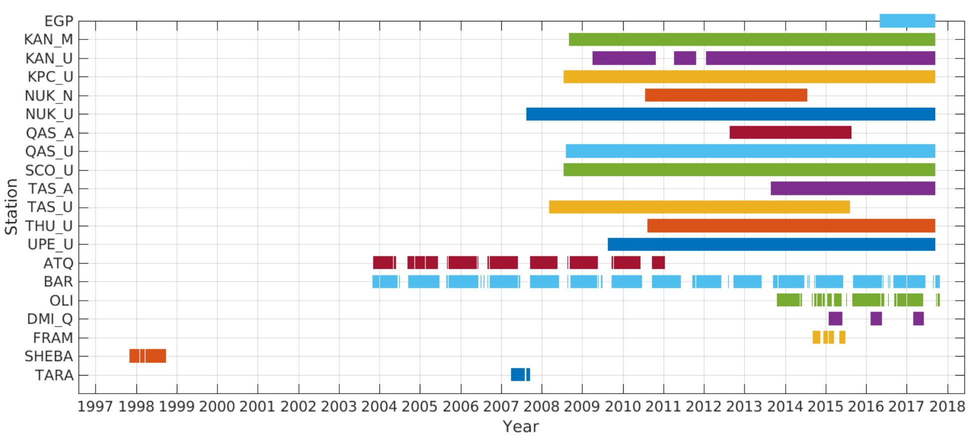

~~**Figure 1: Temporal coverage for each data site included in this study.**~~

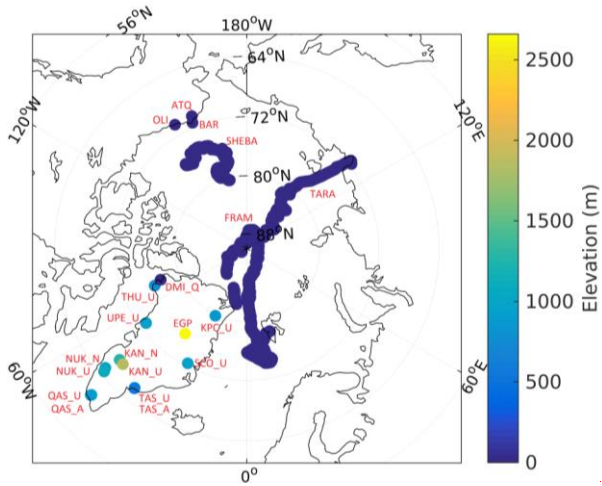

Figure ~~2~~1: Spatial coverage and elevation for each site included in this study. The colour bar is elevation in meters.

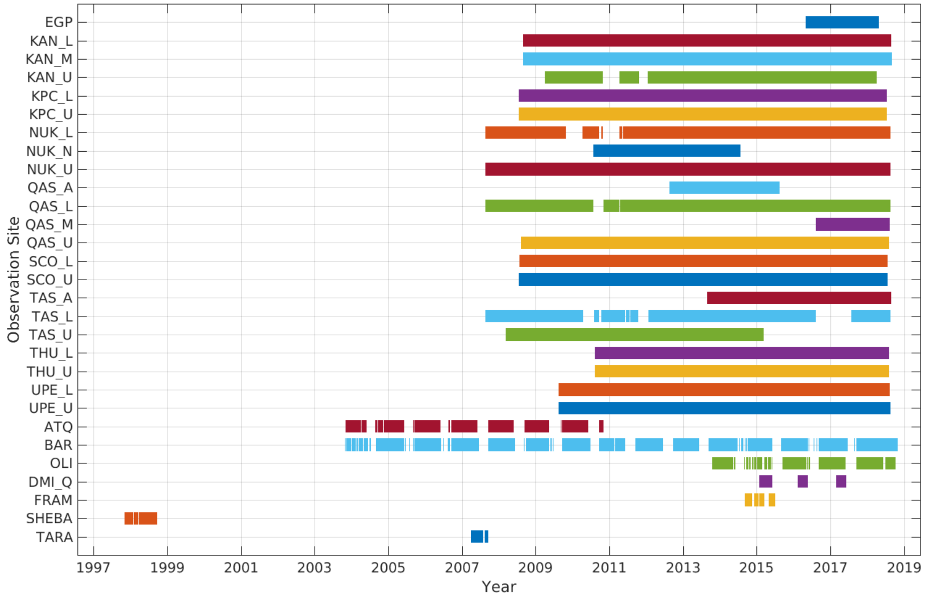

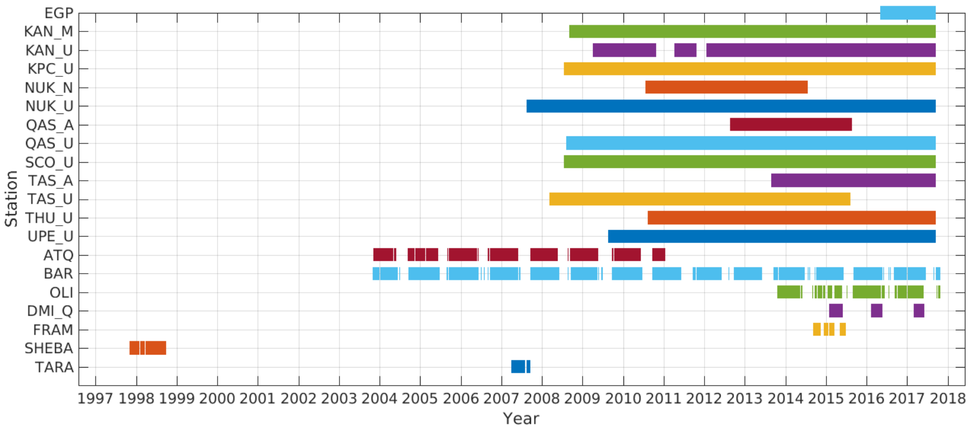

Figure 2~~1~~: Temporal coverage for each ~~data~~observation site included in this study.

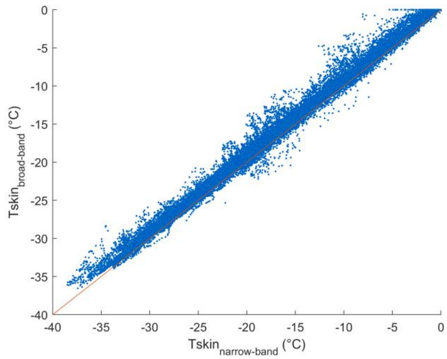

Figure 3: Scatterplot of Tskin estimated from narrow-band IR observations versus Tskin estimated from broad-band IR observations for DMI_Q.

Formateret: Normal

Formateret: Normal

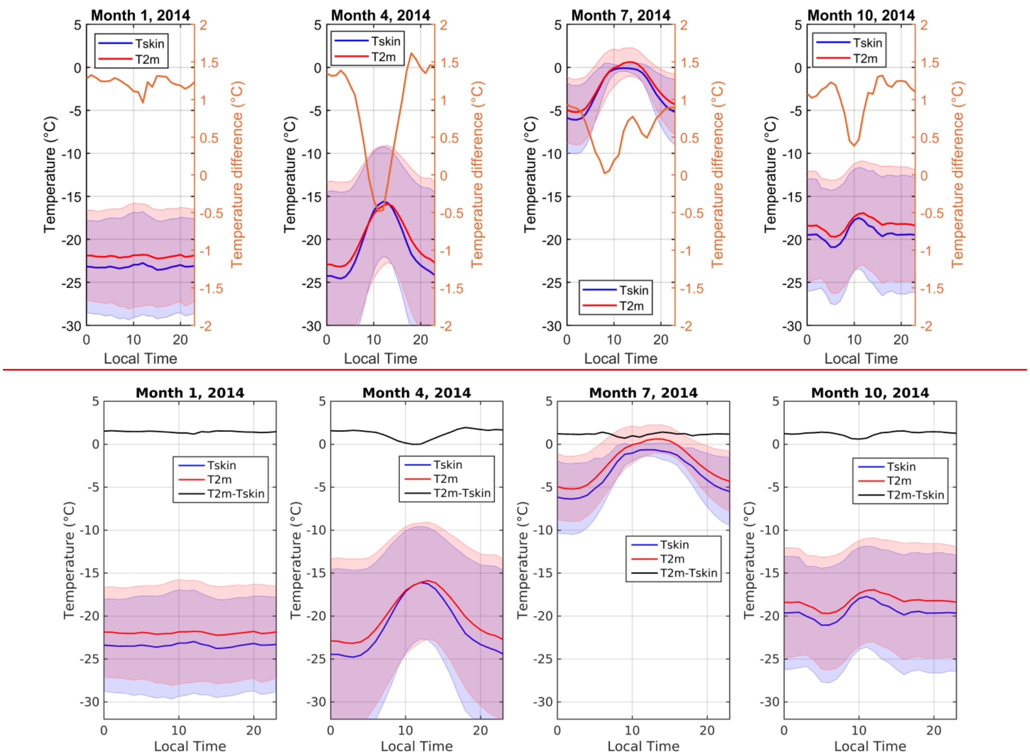

Figure 4~~3~~: Monthly diurnal variability of 2 m air temperature (red) and skin temperature (blue) at KAN_ U during the months: January, April, July and October. The ~~black~~ orange curves are the difference between the red and blue curves. The shadings indicate the standard deviations.

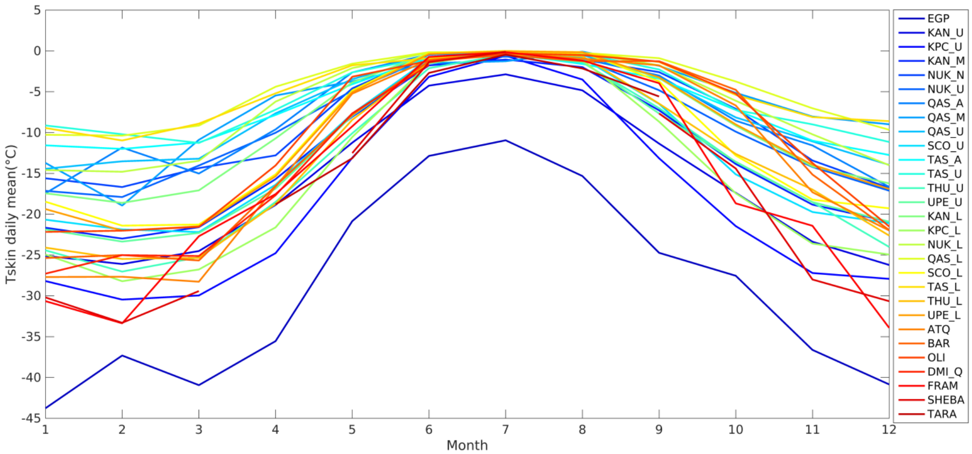

Tskin daily mean(°C)
Month
EGP
KAN_U
KPC_U
KAN_M
NUK_N
NUK_U
QAS_A
QAS_M
QAS_U
SCO_U
TAS_A
TAS_U
THU_U
UPE_U
KAN_L
KPC_L
NUK_L
QAS_L
SCO_L
TAS_L
THU_L
UPE_L
ATQ
BAR
OLI
DMI_Q
FRAM
SHEBA
TARA

(a)

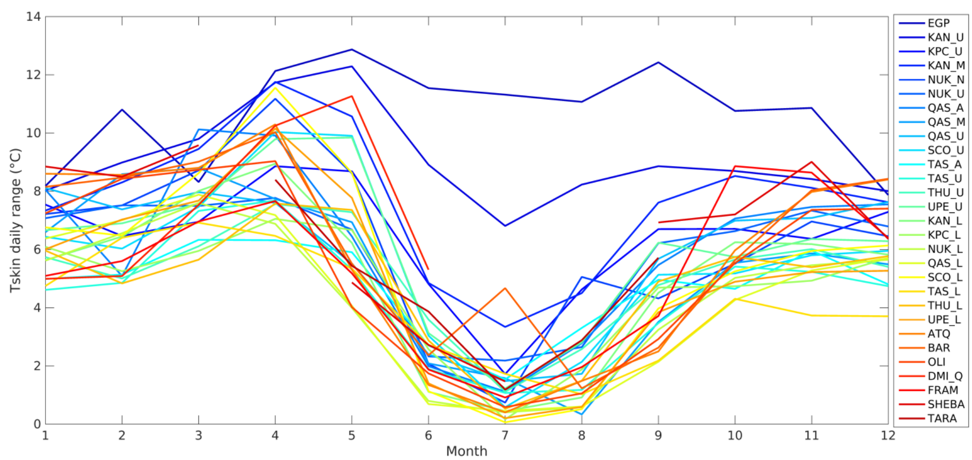

Tskin daily range (°C)
Month
EGP
KAN_U
KPC_U
KAN_M
NUK_N
NUK_U
QAS_A
QAS_M
QAS_U
SCO_U
TAS_A
TAS_U
THU_U
UPE_U
KAN_L
KPC_L
NUK_L
QAS_L
SCO_L
TAS_L
THU_L
UPE_L
ATQ
BAR
OLI
DMI_Q
FRAM
SHEBA
TARA

(b)

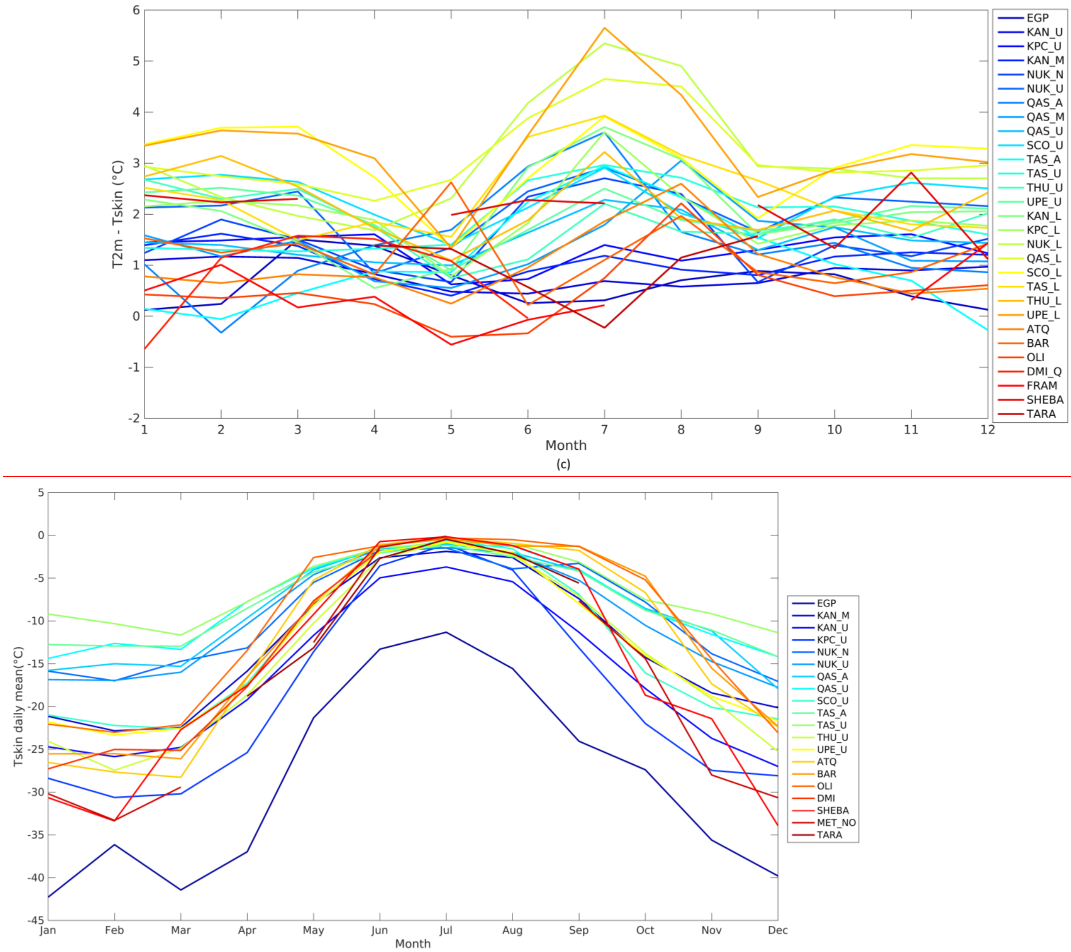

Figure 54: Monthly mean of -Tskin (a)~~skin temperature~~ daily range in Tskin (b) and T2m-Tskin difference (c), for all sites. See Table 1 for station locations and types.

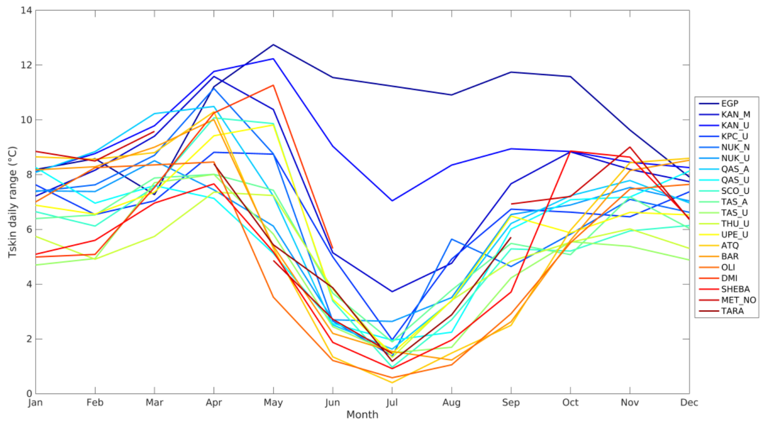

~~Figure 5: Daily range of skin temperature as a function of month for all sites. See Table 1 for station location and type.~~

Formateret: Normal

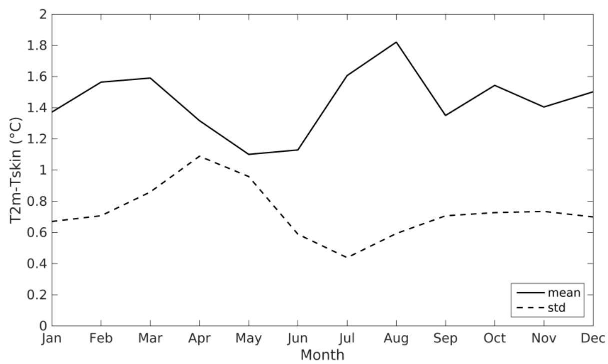

~~**Figure 6: Monthly mean difference in 2 m air temperature and skin temperature (T2m-Tskin) for all data sites with time coverage as listed in Table 1 (solid line). The dashed line shows the mean of the standard deviations from the different observation sites.**~~

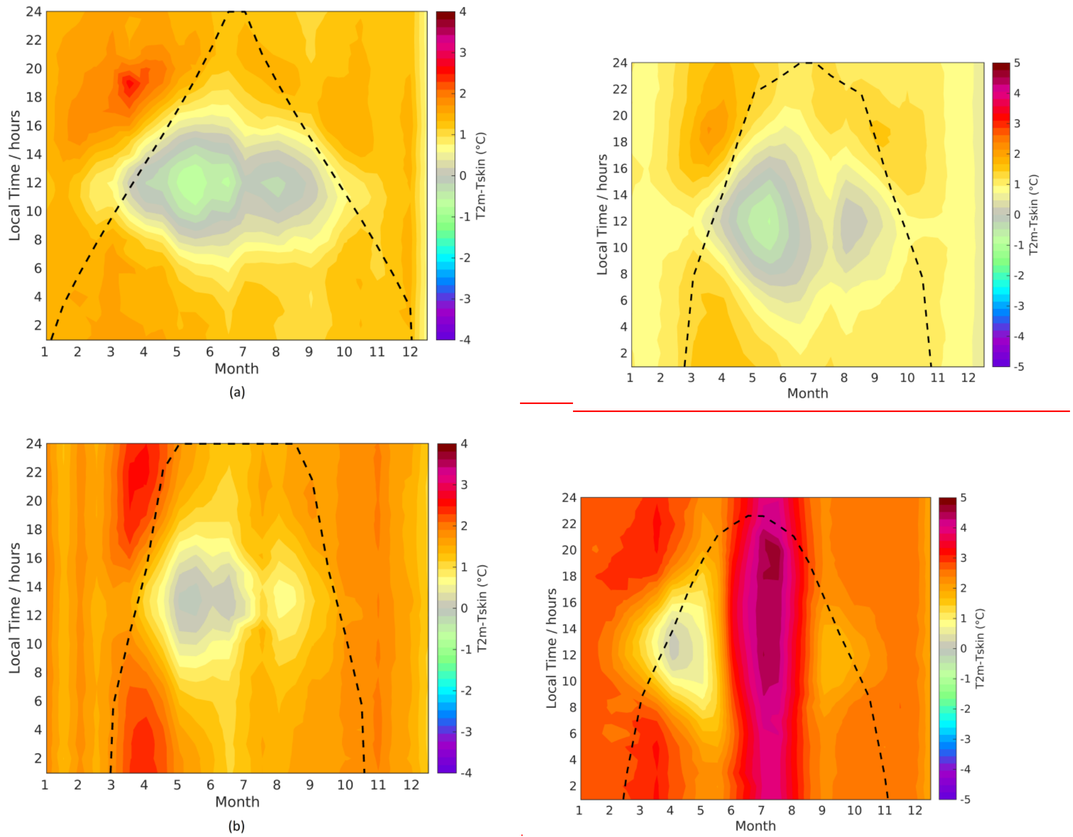

Figure 6~~7~~: Mean 2 m air temperature and skin temperature differences for ACC~~at KAN_U~~ (a) and ~~KPC_U~~LAB (b) as a function of time of year (with a bin size of 15 days) and local time of the day. The dotted black lines indicate the total hours of sunlight.

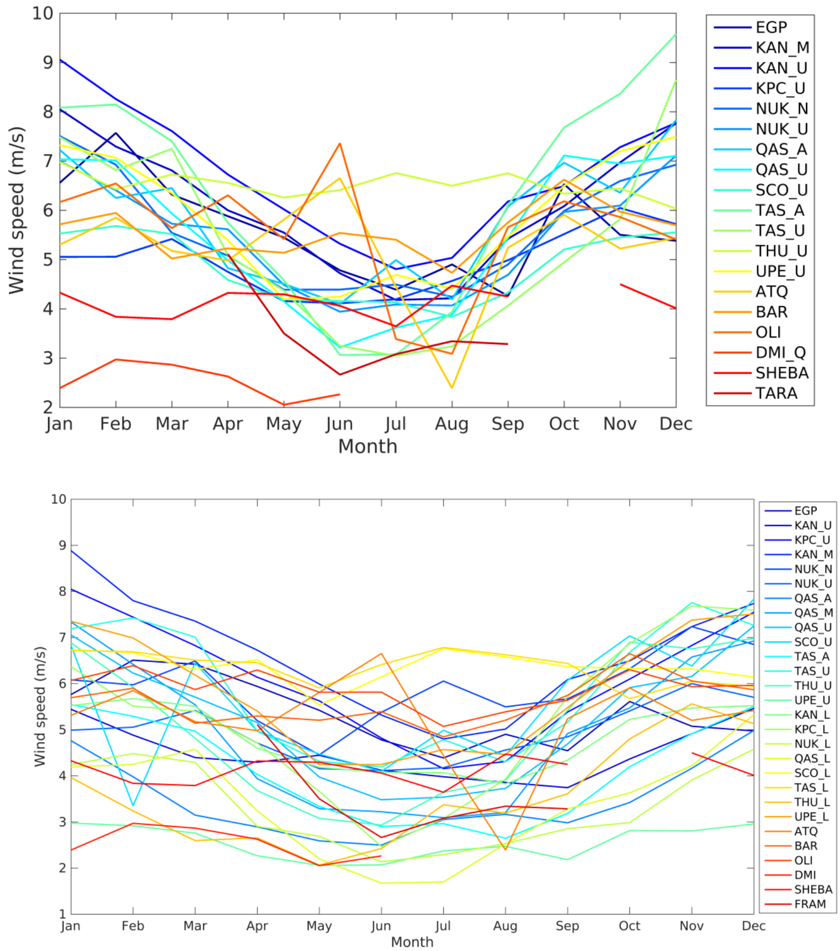

Figure 7~~8~~: The average annual cycle in wind speed for all sites.

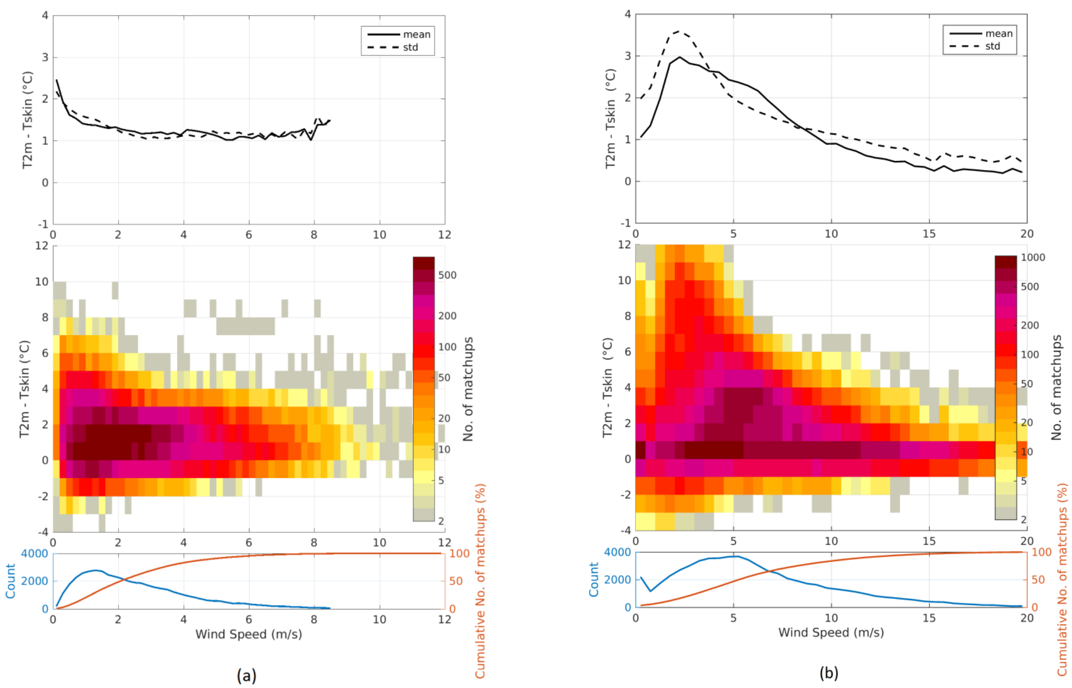
mean
std
T2m - Tskin (°C)
No. of matchups
Count
Cumulative No. of matchups (%)
Wind Speed (m/s)
(a)
(b)

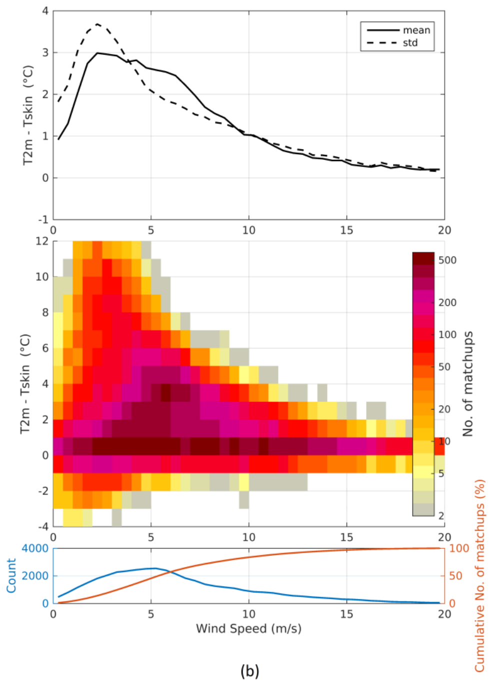

Figure 8~~9~~: 2 m air temperature and skin temperature difference as a function of binned wind speed for (a) DMI_Q and (b) THU_U. The wind speed bin size is 0.5 m s^{-1}, the T2m-Tskin bin size is 1°C, and only bins with more than 50 members are included. The upper plots show the standard deviation (dashed lines) and mean difference (solid lines). The middle plots show the number of ~~matchups~~ members in each bin, while the bottom plots show the number of ~~matchups~~ members (blue lines) and the cumulative percentage of ~~matchups~~ members (red lines) in each wind speed bin.

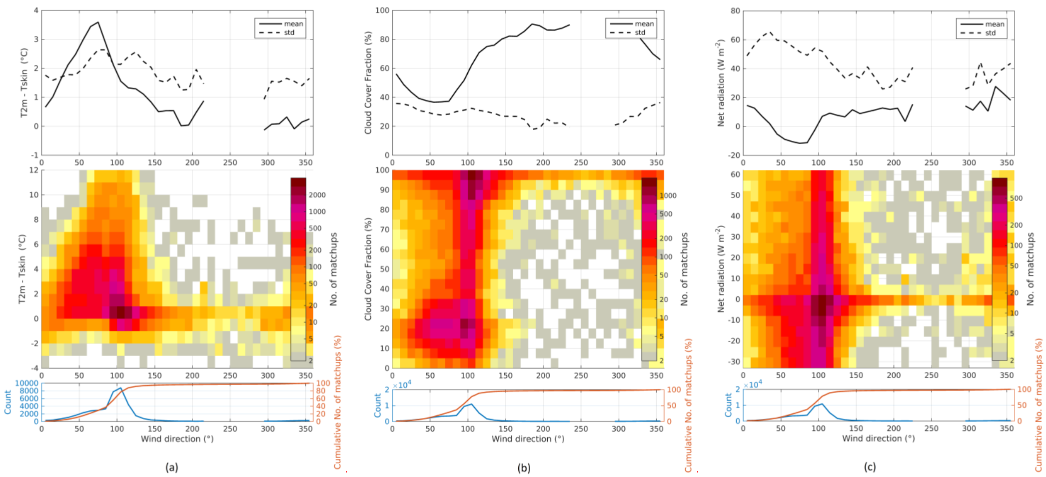

~~Figure 10: 2 m air temperature and Tskin difference (a), the cloud cover fraction (b), and the net radiation (c) as a function of binned wind direction for THU_U. The upper figures show the standard deviation (dashed lines) and mean difference (solid lines). The surface plots in the middle show the number of matchups in each bin, while the bottom plots show the number of matchups (blue lines) and the cumulative percentage of matchups (red lines) in each wind direction bin.~~

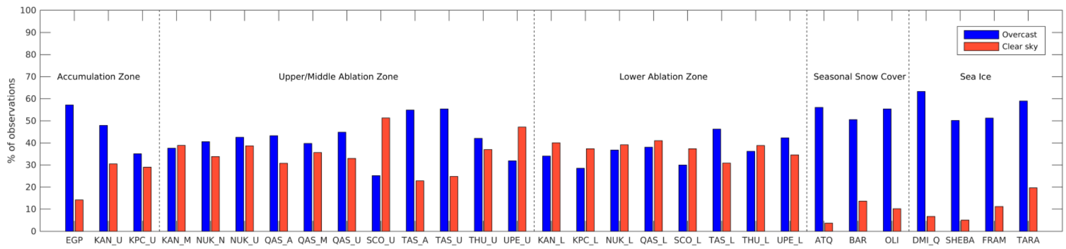

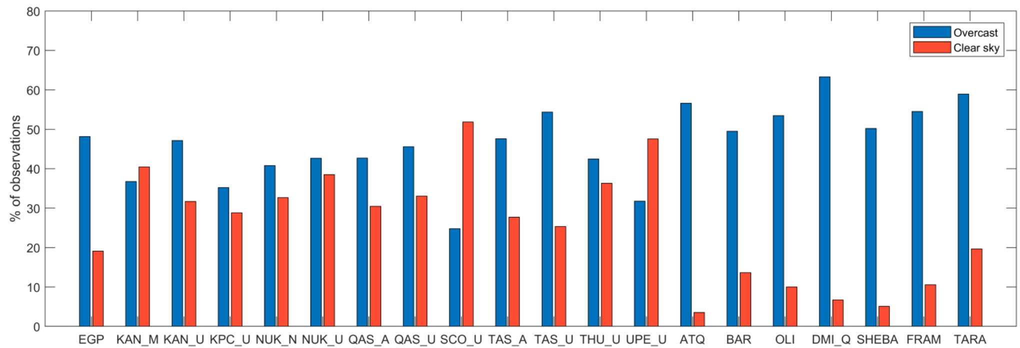

Figure 9~~11~~: Frequency of clear-sky and overcast observations in percent of all observations for each site.

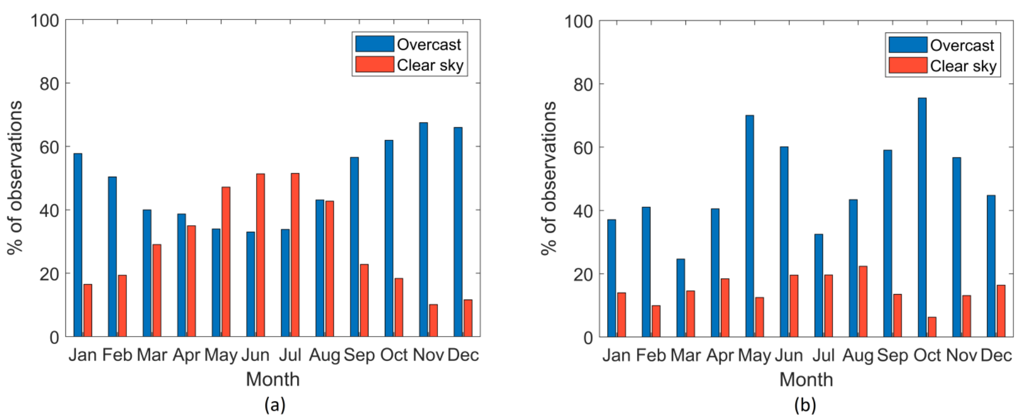

~~Figure 12: Frequency of clear-sky and overcast conditions for each month at KAN_U (a) and BAR (b).~~

Formateret: Normal

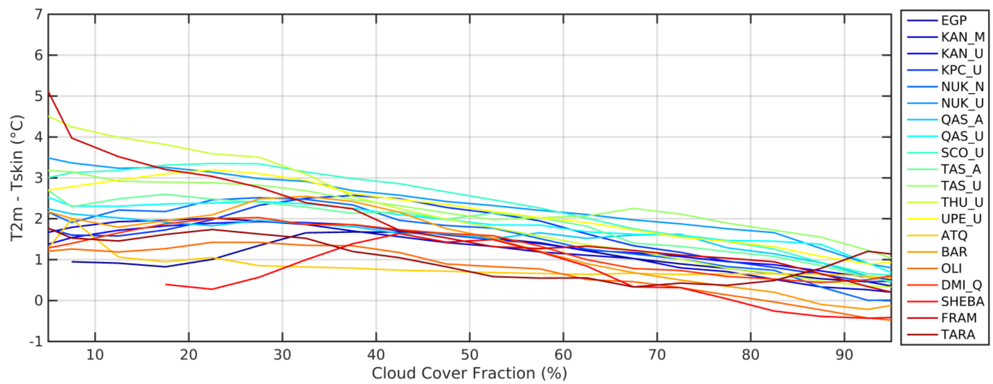

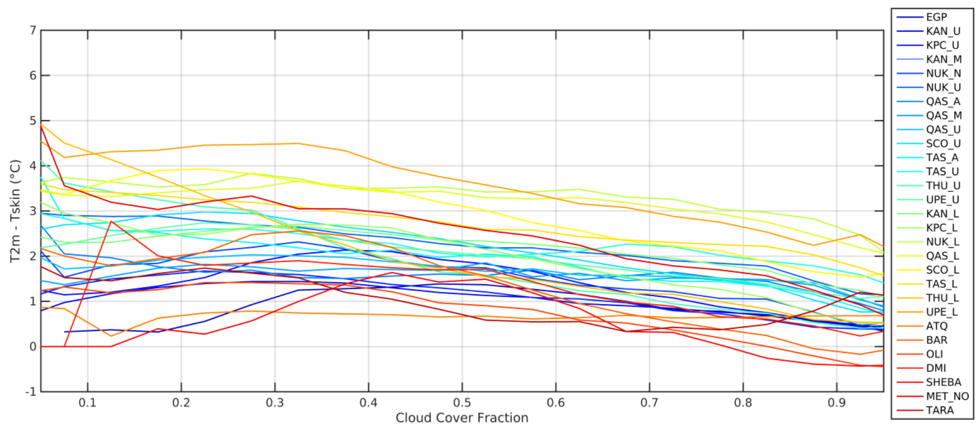

Figure 10~~3~~: 2 m air temperature and skin temperature differences for all sites as a function of binned cloud cover fraction (CCF). The CCF bin size is 0.05, the T2m-Tskin bin size is 1°C, and only bins with more than 50 members are considered.

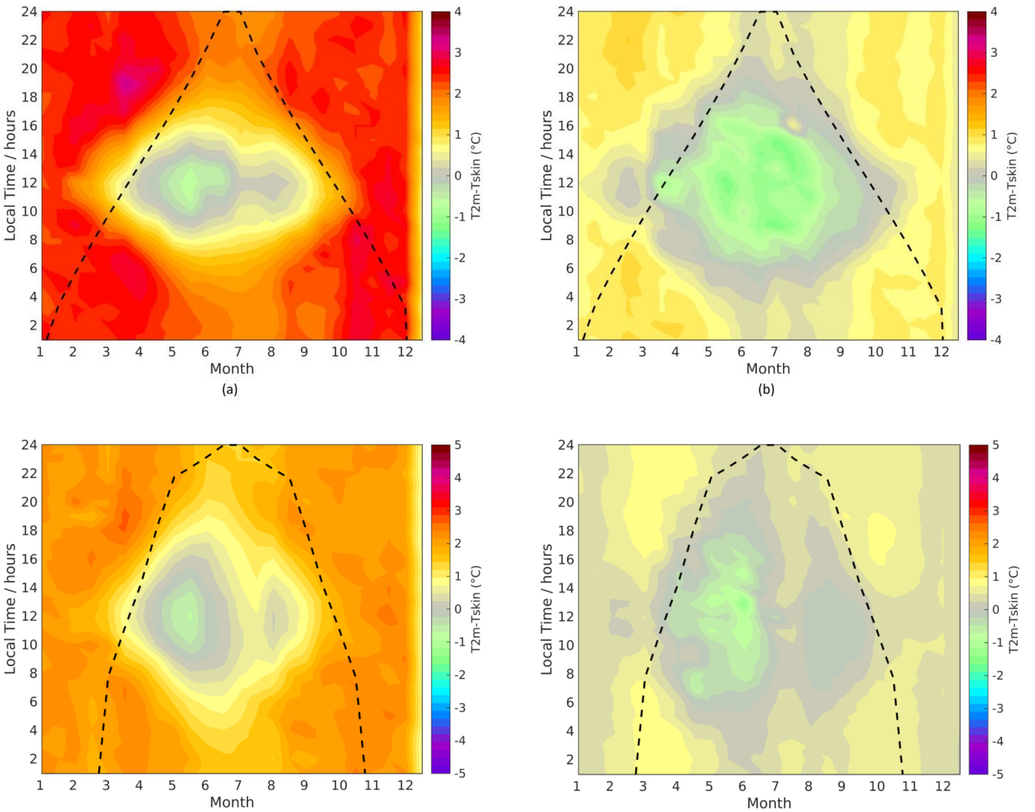

Figure 141: Similar to Fig. 7a but with 2 m air temperature and skin temperature differences for ACC sites~~at KAN_U~~ in cases of clear-sky (a), and overcast conditions (b). The dotted black lines indicate the total hours of sunlight each month.

Table 2 Overall 2 m air temperature and skin temperature differences (T2m-Tskin, °C) for ~~all sites (ALL), SEAICE+ (including the sea ice sites and ARM), and PROMICE~~each surface type under different circumstances in terms of season and sky conditions. The square brackets are the ranges of the T2m-Tskin differences for the stations included in each surface type category.

		Jun-Aug	Dec-Feb	All months
	Cloud	0.21 [0.13 – 0.34]	0.47 [0.16 – 0.66]	0.43 [0.35 – 0.49]
ACC	Clear	0.79 [0.26 – 1.29]	1.99 [1.55 – 2.46]	1.05 [0.58 – 1.50]
	All	0.69 [0.43 – 1.07]	0.88 [0.16 – 1.41]	0.91 [0.65 – 1.29]
	Cloud	1.77 [0.68 – 2.62]	0.67 [-0.79 – 1.52]	0.90 [0.16 – 1.45]
UAB	Clear	2.49 [1.12 – 3.16]	2.71 [1.35 – 4.76]	2.36 [1.45 – 3.38]
	All	2.20 [0.98 – 2.77]	1.60 [0.07 – 2.65]	1.65 [1.05 – 2.26]

LAB	Cloud	2.81 [1.15 – 4.23]	1.38 [0.49 – 2.10]	1.63 [0.66 – 2.41]
	Clear	3.94 [3.01 – 5.22]	3.90 [2.82 – 4.81]	3.44 [2.46 – 4.42]
	All	3.51 [2.28 – 4.74]	2.73 [2.06 – 3.45]	2.65 [1.99 – 3.34]
SSC	Cloud	-0.08 [-0.59 – 0.26]	-0.05 [-0.17 – 0.04]	-0.08 [-0.27 – 0.06]
	Clear	1.57 [1.01 – 2.25]	2.32 [1.75 – 2.93]	1.80 [1.34 – 2.19]
	All	0.40 [-0.22 – 0.96]	0.84 [0.47 – 1.41]	0.65 [0.35 – 0.97]
SICE ÷ DMI_Q	Cloud	0.71 [-0.00 – 1.34]	0.35 [-0.33 – 1.04]	0.64 [-0.38 – 1.29]
	Clear	1.95 [0.40 – 3.73]	2.33 [1.09 – 3.56]	2.10 [0.43 – 3.86]
	All	1.09 [0.08 – 2.30]	1.51 [0.99 – 2.03]	1.25 [0.42 – 2.08]

	~~Jun-Aug~~			~~Dec-Feb~~			~~All~~		
	~~ALL~~	~~SEAICE+~~	~~PROMICE~~	~~ALL~~	~~SEAICE+~~	~~PROMICE~~	~~ALL~~	~~SEAICE+~~	~~PROMICE~~
~~Cloud~~	~~0.58~~	~~0.30~~	~~0.73~~	~~0.57~~	~~0.09~~	~~0.79~~	~~0.53~~	~~0.31~~	~~0.65~~
~~Clear~~	~~1.94~~	~~1.86~~	~~1.97~~	~~2.90~~	~~2.09~~	~~3.24~~	~~2.31~~	~~1.98~~	~~2.46~~
~~All~~	~~1.29~~	~~0.73~~	~~1.58~~	~~1.50~~	~~0.89~~	~~1.78~~	~~1.37~~	~~0.88~~	~~1.64~~

Formateret tabel

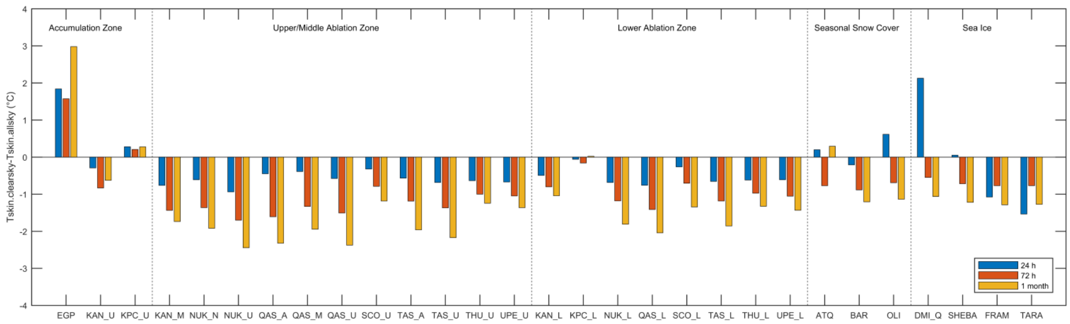

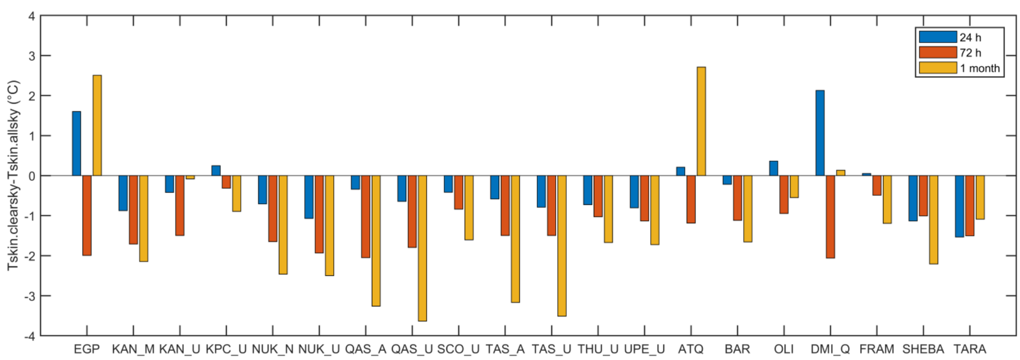

Figure 1~~5~~2: Observed clear-sky biases (Tskin_clearsky-Tskin_allsky) averaged for different time intervals, for all sites (°C).

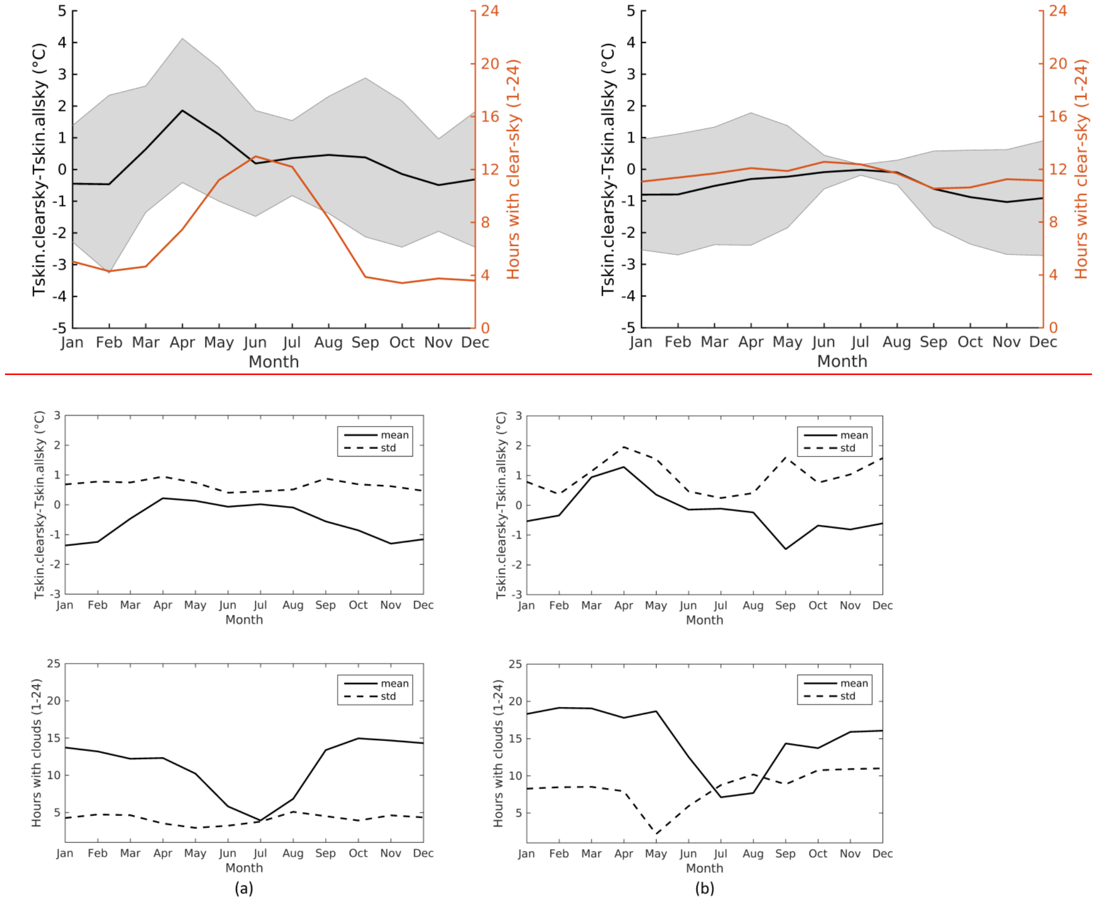

Figure 13~~6~~: D~~The top panels show the d~~ifferences between 24 h averaged clear-sky and all-sky skin temperatures for ~~PROMICE~~ ACC stations (a) and ~~SEAICE+~~LAB stations (b) for each month. ~~The solid lines are the mean clear-sky bias while the dashed lines are standard deviations.~~The red lines ~~The bottom panels~~ show the 24 h average~~d~~ number of hours with CCF>0.7~~70%~~ per day for each month.

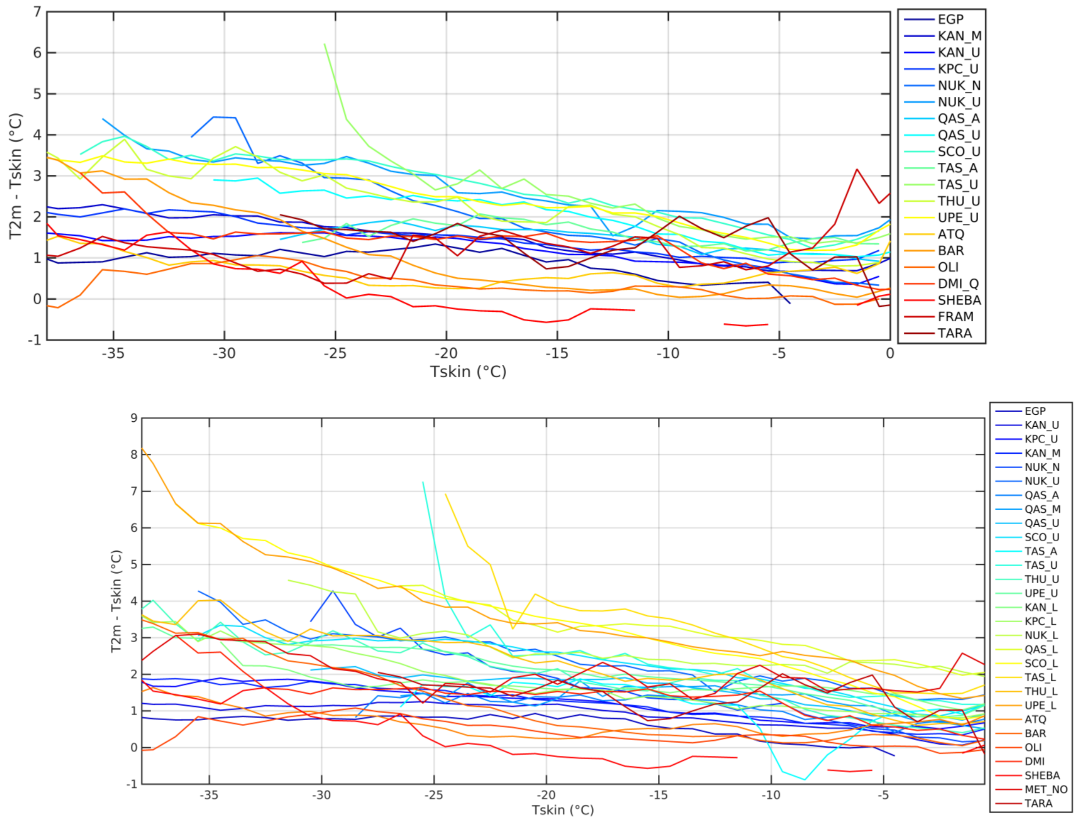

Figure 14~~7~~: Mean 2 m air temperature and skin temperature differences for all sites as a function of binned skin temperature. The Tskin bin size is 1°C, the T2m-Tskin bin size is 1°C, and only bins with more than 50 members are considered.

In situ observed relationships between snow and ice surface skin temperatures and 2 m air temperatures in the Arctic

Pia Nielsen-Englyst[1], Jacob L. Høyer[1], Kristine S. Madsen[1], Rasmus Tonboe[1], Gorm Dybkjær[1], Emy Alerskans[1]

[1]Danish Meteorological Institute, DK-2100 Copenhagen Ø, Denmark

Correspondence to: Pia Nielsen-Englyst (pne@dmi.dk)

Abstract.

To facilitate the construction of a satellite derived 2 m air temperature (T2m) product for the snow and ice covered regions in the Arctic, observations from weather stations are used to quantify the relationship between the T2m and skin temperature (Tskin). Multiyear data records of simultaneous Tskin and T2m from 29 different in situ sites have been analysed for 5 regions, covering the lower and upper ablation zone and the accumulation zone of the Greenland Ice Sheet (GrIS), sea ice in the Arctic Ocean, and seasonal snow covered land in northern Alaska. The diurnal and seasonal temperature variabilities and the impacts from clouds and wind on the T2m-Tskin differences are quantified. Considering all regions, T2m is on average 0.65-2.65°C higher than Tskin, with the largest differences for the lower ablation area and smallest differences for the sea ice sites. A negative surface radiation balance generally makes the surface colder than the atmosphere, resulting in a surface-driven surface air temperature inversion. Tskin and T2m are often highly correlated, and the two temperatures are almost identical (<0.5°C) at particularly times of the day and year, and during certain conditions. The data analysed here show the best agreement between Tskin and T2m around noon and early afternoon during spring and fall. However, Tskin is often lower than T2m by more than 2°C, with the largest differences occurring, when it is cold or when the surface is melting. In general, the inversion strength increases with decreasing wind speeds, except for the sites on the GrIS where the maximum inversion occurs at wind speeds of about 5 m s^{-1} due to the katabatic winds. Clouds tend to reduce the vertical temperature gradient, by warming the surface, resulting in a mean T2m-Tskin difference ranging from -0.08°C to 1.63°C, with the largest differences for the low ablation zone sites and the smallest differences for the seasonal snow covered sites. To assess the effect of using cloud limited Infrared satellite observations, the influence of clouds on temporally averaged Tskin has been assessed by comparing averaged clear-sky Tskin with averaged all-sky Tskin. The clear-sky effect has been assessed for temporal averaging windows of: 24 h, 72 h and 1 month. The largest clear-sky biases are generally found when 1 month averages are used and smallest for 24 h. In most cases all-sky averages are warmer than clear-sky averages, with the smallest bias during summer.

1 Introduction

The Arctic region is warming about twice as much as the global average because of Arctic amplification (Graversen et al., 2008). Greenland meteorological data show that the last decade (2000s) is the warmest since meteorological measurements of surface air temperatures started in the 1780s (Cappelen, 2016; Masson-Delmotte et al., 2012) and the period 1996-2014 yields an above average warming trend compared to the past six decades (Abermann et al., 2017). The reason for the Arctic amplification is a number of positive feedback mechanisms, e.g. the ice-albedo feedback which is driven by the retreat of Arctic sea ice, glaciers, and terrestrial snow cover. The atmospheric warming leads to a declining mass balance of the Greenland Ice Sheet (GrIS), contributing to global sea level rise. The increased mass loss of the GrIS partly comes from increased surface melt (Rignot, 2006), which is driven by changes in the surface energy balance. Several studies have focussed on the assessment of current albedo trends and their possible further enhancement of the impact of atmospheric warming on the GrIS (e.g. Box et al., 2012; Stroeve et al., 2013; Tedesco et al., 2011). However, recent studies have shown that uncorrected sensor degradation in MODIS Collection 5 data was contributing falsely to the albedo decline in the dry snow areas, while the decline in wet and ice areas remain but at lower magnitude than initially thought (Casey et al., 2017). Future projections of the GrIS mass balance show that the surface melt is exponentially increasing as a function of the surface air temperature (Franco et al., 2013). Further, the Arctic warming may contribute to mid latitude weather events (Cohen et al., 2014; Overland et al., 2015; Vihma, 2014; Walsh, 2014). It is therefore important to monitor the temperature of the Arctic to understand and predict the local as well as global effects of climate change. Current global surface temperature products are fundamental for the assessment of the climate change (Stocker et al., 2014) but in the Arctic these data traditionally include only near surface air temperatures from buoys and automatic weather stations (AWSs; Hansen et al., 2010; Jones et al., 2012; Rayner, 2003). However, in situ observations are not available everywhere and the time series have gaps and/or limited duration. In particular, the Arctic ice regions are sparsely covered with in situ measurements, due to the extreme weather conditions and low population density (Reeves Eyre and Zeng, 2017). The global surface temperature products are thus based on a limited number of observations in this very sensitive region. This means that crucial climatic signals and trends could be missed in the assessment of the Arctic climate changes due to poor coverage of the observational system.

Satellite observations in the thermal infrared have a large potential for improving upon the surface temperature products in the Arctic due to the good spatial and temporal coverage. However, the variable retrieved from infrared satellite observations is the surface skin temperature (Tskin), whereas current global surface temperature products estimate the 2 m air temperature (T2m; Hansen et al., 2010; Jones et al., 2012). An important step towards integrating the satellite observations in the near surface air products is thus to assess the relationships between Tskin and T2m as we do here.

A surface-based air temperature inversion is a common feature of the Arctic winter (Serreze et al., 1992; Zhang et al., 2011). The inversion exists because of an imbalance between the radiative fluxes, leading to a cooling of the surface, especially when the absorbed incoming solar radiation is small (during winter and night). An analysis based on observations from the

Antarctic Plateau showed that the inversion continues all the way to the surface with the largest gradient between the surface and 20 cm above it (Hudson and Brandt, 2005). The surface-driven temperature inversion causes a difference between the T2m and the actual skin temperature at the snow/air interface. Previously, work has been done to characterize the relationship between the T2m and land surface temperatures observed from satellites and identified land cover, vegetation fraction and elevation as the dominating factors (Good et al., 2017). A few studies have investigated the temperature inversion in the ice regions for the lowest 2 m of the atmosphere focusing on limited time periods and single locations e.g. Summit, Greenland (Adolph et al., 2018; Hall et al., 2008), the South Pole (Hudson and Brandt, 2005) and the Arctic sea ice (Vihma and Pirazzini, 2005). Until now, no systematic studies have yet been made for the high latitude ice sheets and over sea ice.

The difference between the T2m and Tskin is very important in validation studies of remotely sensed temperatures. Several studies have used T2m observations for validating satellite Tskin products on the GrIS (Dybkjær et al., 2012; Hall et al., 2008; Koenig and Hall, 2010; Shuman et al., 2014) and over the Arctic sea ice (Dybkjær et al., 2012) and found that a significant part of the differences could be attributed to the difference between the Tskin and T2m. Conversely, Rasmussen et al. (2018) used satellite Tskin observations in a simple way to correct the T2m in a coupled ocean and sea ice model and obtained an improved snow cover.

In order to facilitate the integrated use of Tskin and T2m from in situ observations, satellite observations and models, there is a need for a better understanding and characterization of the observed relationship. The aim of this paper is to bring further insight into this relationship, using in situ observations. This study extends the previous analyses to include multiyear observational records from 29 different sites located at the GrIS, Arctic sea ice, and the coastal region of northern Alaska. The aim is to identify the key parameters influencing the temperature difference between the surface and 2 m height and to assess under which conditions Tskin is, or is not, a good proxy for the T2m and to quantify the differences, using Tskin as a proxy for T2m. The findings are intended to aid the users of satellite data and to support the derivation of T2m using satellite Tskin observations. In the response to the latter, an effort has also been made to estimate a clear-sky bias of Tskin based on in situ observations. The paper is structured such that Sect. 2 describes the in situ data. Section 3 gives an introduction to the near surface boundary conditions. The results are presented in Sect. 4 and discussed in Sect. 5. Conclusions are given in Sect. 6.

2 Data

In situ observations have been collected from various sources and campaigns covering ice and snow surfaces in the Arctic. The focus has been on collecting in situ data with simultaneous observations of Tskin, derived from infrared radiometers and T2m measured with a shielded and ventilated thermometer about 2 m above the surface. Table 1 gives an overview of the data and the abbreviations used in this paper. The data has been divided into five different categories based on surface characteristics and location: accumulation area (ACC), upper/middle ablation zone (UAB), lower ablation zone (LAB) of the

GrIS, seasonal snow covered (SSC) sites in northern Alaska, and sea ice sites (SICE). All time series which cover multiple full years have been cut to cover an integer number of years (within 5 days), in order to avoid seasonal biases. The geographical distribution and elevations of all sites are shown in Fig. 1, while Fig. 2 shows the temporal data coverage. Observations from the sites in Table 1 include T2m, Tskin, wind speed, shortwave- and longwave radiation. Measurement heights vary depending on the site and snow depth, but for this paper near-surface air temperatures are referred to as 2 m air temperature despite these variations. The impact of these height variations are discussed in Sect. 5. Further details are provided for each data source in Sect. 2.1-2.6.

2.1 PROMICE

Data have been obtained from the Programme for Monitoring of the Greenland Ice Sheet (PROMICE) provided by the Geological Survey of Denmark and Greenland (GEUS). PROMICE was initiated in 2007 by the Danish Ministry of Climate and Energy, and operated by GEUS in collaboration with the National Space Institute at the Technical University of Denmark and Asiaq (Greenland Survey; e.g. Ahlstrøm et al., 2008). PROMICE collects in situ observations from a number of AWSs mostly located along the margin of the GrIS (Fig. 1). Each observational site has one or more stations; typically one located in the lower ablation zone close to the ice sheet margin, and one or two located in the middle/upper ablation zone near the equilibrium line altitude. Exceptions are KAN_U and KPC_U located in the lower accumulation area and EGP, which is located in the upper accumulation area. All 22 PROMICE AWSs located on the GrIS have been used in this study. PROMICE Tskin has been calculated from up-welling longwave radiation, measured by Kipp & Zonen CNR1 or CNR4 radiometer, assuming a surface longwave emissivity of 0.97 (van As, 2011). The air temperature is measured by a thermometer at a height of 2.7 m, while the wind speed is measured at about 3.1 m height, if no snow is present. Snow accumulation during winter reduces the measurement height. In this study, we use hourly averages of the data, provided by PROMICE.

2.2 ARM

The Atmospheric Radiation Measurement (ARM) Program (Ackerman and Stokes, 2003; Stamnes et al., 1999) was established in 1989 and it provides data on the cloud and radiative processes at high latitudes. Three ARM sites from the North Slope of Alaska (NSA) are used in this study: Atqasuk (ATQ), Barrows (BAR), and Oliktok Point (OLI). The stations provide surface snow infrared (IR) temperature measured using a Heitronics KT19.85 IR Radiation Pyrometer (Moris, 2006) and air temperature measured at 2 m height. Wind speed is measured at 10 m height. The ARM stations have seasonal snow coverage, i.e. the snow melts away in summer. Data where the surface albedo is less than 0.30 indicate that the snow has disappeared and these have been excluded to ensure that we only consider snow/ice covered surfaces.

2.3 ICEARC

We use the ICEARC sea ice temperature and radiation data set from the Danish Meteorological Institute (DMI) field campaign in Qaanaaq. The DMI AWS is deployed on first-year sea ice in Qaanaaq and is funded by the European climate research project, ICE-ARC. The AWS was deployed for the first time in late January 2015 at the north side of the fjord Inglefield Bredning and recovered in early June before break-up of the fjord ice. The campaign has been repeated every year since then and the data used in this study is procured by fieldwork done in the periods Jan.-Jun., 2015-2017. The AWS is equipped to measure snow surface IR temperature and air temperature at 1 and 2 m heights. In this study, the 1 m air temperature is used instead of the 2 m air temperature, as careful analysis of the 2 m air observations revealed anomalies that could arise from a systematic temperature dependent error. Using the 1 m instead of 2 m air temperatures observations will have an impact on the strength of the relationship with the Tskin observations, but the observations are included here as the dependency with other parameters, such as cloud cover and wind, is still important to assess. The data used here are 10 minute snapshots (Høyer et al., 2017) and are referenced as: DMI_Q in this paper.

2.4 SHEBA

The Surface Heat Budget of the Arctic (SHEBA) experiment was a multiagency program led by the National Science Foundation and the Office of Naval Research. The data used in this study originates from deployment of a Canadian icebreaker, DesGroseilliers, in the Arctic ice pack 570 km northeast of Prudhoe Bay, Alaska in 1997 (Uttal et al., 2002). During its year-long deployment, SHEBA provided atmospheric and sea ice measurements from the icebreaker and the surrounding frozen ice floe. The data used here contain hourly averaged data collected by the SHEBA Atmospheric Surface Flux Group (ASFG) and Dr. J. Liljegren from the ARM project. The SHEBA ASFG installed a 20 m tall tower, which was used to obtain measurements of the surface energy budget, focusing on the turbulent heat fluxes and the near surface boundary layer structure (Bretherton et al., 2000; Persson, 2002). Five different levels, varying in height from 2.2-18.2 m, had mounted a temperature/humidity probe and a sonic anemometer. We use air temperature and wind data from the lowest mounted instruments (2.2 m), which vary in height from 1.9 to 3 m depending on snow accumulation and snow melt. Three surface temperature measurements were measured from a General Eastern thermometer, an Eppley radiometer and a Barnes radiometer, available from April to September 2007. The Eppley is the most reliable, though there are periods when the other two are also reasonable, and one period (May), when the Eppley data may be slightly off (Persson, 2002). We use the best estimate of Tskin, which is based on slight corrections to the Eppley temperatures and the Barnes temperatures when Eppley was known to be wrong (Persson, 2002).

2.5 FRAM2014/15

The scientific program of the FRAM2014/15 expedition is carried out by the Nansen Center (NERSC) in co-operation with Alfred Wegener Institute, Helmholtz Centre for Polar and Marine Research, Germany, University of Bergen, Bjerknes

Center for Climate Research and Norwegian Meteorological Institute. FRAM2014/15 is a Norwegian ice drift station deployed near the North Pole in August 2014 using a medium-sized hovercraft as logistic and scientific platform (Kristoffersen and Hall, 2014). This type of mission allows exploration of the Arctic Ocean not accessible to icebreakers, and enables scientific field experiments, which require physical presence. The hovercraft was operated by two people and by the end of March 2015 they had drifted 1.450 km. During the drift with sea ice they obtained Tskin measurements by Campbell Scientific IR120 (later corrected for sky temperature and surface emissivity) and near surface air temperature from a temperature sensor.

2.6 TARA

TARA is a French polar schooner that was built to withstand the forces from the Arctic sea ice. In late August 2006 TARA sailed to the Arctic Ocean, where she drifted for fifteen months frozen into the sea ice. The TARA multidisciplinary experiment was a part of the international polar year DAMOCLES (Developing Arctic Modelling and Observing Capabilities for Long-term Environmental Studies) program (Gascard et al., 2008; Vihma et al., 2008). Air temperature and wind speed were measured from a 10 m tall Aanderaa weather mast at the heights of 1, 2, 5, and 10 m and wind direction was measured at 10 m height. We use the air temperatures and wind speed measured at 2 m height. They also had an Eppley broadband radiation mast with two sensors for longwave fluxes and two sensors for shortwave fluxes (upward and downward looking). The downward looking IR sensor also provided Tskin from April to September 2007. The data used in this study are 10 minute averages.

2.7 Radiometric observations of Tskin

The Tskin observations used in this study are all derived from radiometric observations, but with spectral characteristics that range from the Heitronics KT19.85 with a spectral response function from 9.5-11.5 μm over Campbell Scientific IR120 with a 8-14 μm spectral window to broadband longwave observations from ~4-40 μm. The emissivity of the ice surface varies for the different spectral windows and this leads to a difference in actual observed Tskin as the sky temperature, which is reflected, tends to be much colder than the ice surface in the infrared, in particular during cloud free conditions. The contribution from the reflected sky is thus included in the radiometric observations but the ice and snow surfaces have generally very high emissivities, which reduce the effects from the reflected sky radiation. In Høyer et al. (2017), the difference in emissivity between the KT15.85 and the IR120 was modelled using an IR snow emissivity model with the spectral response functions for the two types of instruments (e.g. Dozier and Warren, 1982). This resulted in averaged emissivities of 0.998 for the KT15.85 and 0.996 for the IR120 spectral windows for a typical snow surface and an incidence angle of 25 degrees. Using the same type of model for a broadband 4-40 μm spectrum resulted in an emissivity of 0.997. The high emissivities for all three instruments mean that the contributions from the sky are small. For realistic conditions in the

Arctic, this e.g. introduces an average difference of 0.06°C between the IR120 and the KT15.85 radiometer (which has a similar spectral response function as the KT19.85), with the IR120 being colder than the KT15.85 (Høyer et al., 2017).

Several of the stations (ATQ, BAR, OLI, DMI_Q, SHEBA and FRAM) used here observed both narrow band and wide band IR observations of the ice surface. The two types of Tskin have been calculated and compared for each of the stations. Figure 3 shows an example with a comparison of the two Tskin estimates from DMI_Q. There is close to a 1:1 relation between the two observations, meaning that there are no systematic temperature dependencies in the comparison. Considering all sites, a good agreement if found with a mean difference between the two Tskin types of 0.06°C and a mean root mean squared value of 0.96°C. In the following we use the narrow band Tskin observations when available and the broadband at the other stations and assume that all the Tskin derived observations have the same characteristics.

2.8 Longwave-equivalent cloud cover fraction

For each site, the cloud cover fraction (CCF) has been estimated based on the relationship between T2m and down-welling longwave radiation (LW_d), following the cloud cover estimation already included in the PROMICE data sets (van As, 2011; van As et al., 2005). It is based on Swinbank (1963), who presented a very simple approach for estimation of clear-sky (CCF=0) atmospheric longwave radiation as a function of T2m:

$$LW_{d\_clear} = 9.365 \cdot 10^{-6} \cdot \mathrm{T2m}^2 \cdot \sigma \cdot \mathrm{T2m}^4, \qquad (1)$$

where σ is Stefan-Boltzmann's constant. Overcast conditions (CCF=1) are assumed to occur when the observed LW_d exceeds the blackbody radiation emitted from the surface, which is calculated using T2m. The CCF for any observed T2m and LW_d pair from all individual observation sites is then calculated by linear interpolation of the observed LW_d, between the theoretical clear-sky (from Equation 1) and the overcast estimates. See van As (2011) for more details on the CCF calculation.

3. Introduction to the near surface boundary conditions

To perform an analysis of the Tskin and T2m relationship and interpret the results it is important to consider the surface energy balance and the specific characteristics that apply in the Arctic. The surface temperature and surface melt are driven by the surface energy balance. The net surface energy balance is defined by the fluxes of energy between the atmosphere, the snow/ice surface and the underlying land, snow/ice, or ocean. The surface energy balance can be written

$$SW_d - SW_u + LW_d - LW_u + SH + LH + G = M,$$

where M is the net energy flux at the surface and SW_d, SW_u, LW_d, LW_u, SH, LH, and G represent the down- and upwelling shortwave radiation, down- and upwelling longwave radiation, sensible and latent heat flux, and subsurface conductive heat flux, respectively. The energy fluxes have the unit W m^{-2}. All fluxes are positive when energy is added to the surface. A positive net surface energy balance results in warming of the surface, if the temperature is lower than the freezing point of water, or in melting of snow and ice (latent heat) if the temperature is at the freezing point. When the surface energy balance is negative the snow/ice will cool thus driving the conductive heat flux from warmer layers below. If the surface is melting, a negative energy balance results in freezing of liquid water.

The radiative budget of the polar regions is dominated by longwave radiation during much of the year and even during summer the shortwave radiation input is in the same order of magnitude as the incoming longwave radiation flux because of extensive cloud cover especially during late summer, and the high surface albedo of the snow (Maykut, 1986). SW_d is the dominating source for ice melt in Greenland (van den Broeke et al., 2008; Box et al., 2012; van As et al., 2012), even though non-radiative energy fluxes can dominate during shorter periods (Fausto et al., 2016). On average, the non-radiative fluxes are an order of magnitude smaller than the radiation fluxes. However, because the net radiation balance is small compared to the individual radiation fluxes the variations in SH and LH fluxes are important for the total surface energy balance and thus the surface temperature. Surface winds interact strongly with the surface energy fluxes as the turbulent mixing increases as a function of wind speed (van As et al., 2005).

During winter and clear-skies when *SWd* is negligible, *LWu* is higher than the *LWd*. This drives a positive sensible heat flux and it results in a stable stratification of the lower atmospheric boundary layer (Maykut, 1986). When the heat conduction flux from below is limited on thick sea ice and on continental ice sheets the negative radiation budget at the surface makes the surface temperature colder than the surface air temperature, resulting in a surface-based temperature inversion. At low to moderate wind-speeds, when turbulent mixing is limited, this creates a very stable stratification of the lower atmosphere. On a sloping surface, the surface air starts to flow downslope, driven by the existence of a horizontal temperature gradient and gravity. The generated winds are called inversion or katabatic winds, and are characterised by stronger winds at more negative surface net radiation and a strong correlation between slope and wind direction (Lettau and Schwerdtfeger, 1967). In the case of PROMICE sites on GrIS, we will refer to these winds as katabatic winds and in the case of interior Antarctic studies these winds are referred to as inversion winds for consistency with referenced studies.

Clouds play a complex role in the Arctic surface energy budget e.g. they both reflect SW_d, leading to a cloud shortwave cooling effect, and absorb LW_u and emit LW_d, which tend to have a warming effect. In the Arctic clouds have a predominantly warming effect on the surface (Intrieri, 2002; Walsh and Chapman, 1998) as the dry atmosphere, with lower emissivity and with that absorptivity to *LW* radiation, enhances the cloud longwave warming effect, while the high surface albedo and the high solar zenith angles thus the impact of the cloud shortwave cooling effect (Curry et al., 1996; Curry and Herman, 1985; Zygmuntowska et al., 2012).

4 Results

4.1 Diurnal and seasonal temperature variability

The local air and surface temperature conditions in the Arctic are to a large extent influenced by the length of the day or night in the Arctic, with extreme variations depending on latitude and time of the year. The temperature variability has several important temporal scales. In this study we will focus on the diurnal and seasonal temperature variations, which are key temporal scales of variability, considering the aim of deriving T2m from satellite observations. As an example of the large seasonal variations, Fig. 4 shows the 2014 monthly mean diurnal temperature variation of Tskin and T2m at the upper PROMICE site in Kangerlussuaq, KAN_U, during January, April, July and October. The seasonal variability in the diurnal temperature at KAN_U is representative of the conditions at the other stations, except for the general temperature level at each station, which changes with latitude and altitude. Considering all months individually, there is high correlation between Tskin and T2m ranging from an average value of 0.92 in January to an average of 0.99 in July considering the entire time series of KAN_U. The high correlations arise from hourly variability and daily cycles in temperatures that are seen in both temperature records. The correlation decreases for stations which have occasional surface melt, where Tskin is constrained to the freezing point of water. Both Tskin and T2m reach a maximum in July, while the coldest month is December (not shown). During winter and polar night, there is no clear diurnal cycle in either T2m or Tskin, and T2m is higher than Tskin. However, during spring there is a strong diurnal cycle, with Tskin lower than T2m at night and small T2m-Tskin differences during daytime. The shadings indicate the standard deviations in T2m and Tskin, respectively. The largest variability is found in spring and winter as a result of more frequent and rapid passages of cold and warm air masses in contrast to the summer months (Steffen, 1995). The summer temperature variability is moreover limited by the upper limit of 0°C on Tskin when the surface melting begins.

The large seasonal variations in Fig. 4 and the relationship between T2m and Tskin are typical for all sites. Figure 5a shows the monthly mean Tskin for all sites and all years. EGP is by far the coldest site due to its high elevation, with a monthly mean Tskin of -42°C in January and a maximum of -11°C in July. All sites reach a maximum in Tskin in July, regardless of latitude. July is also the month with least variation in temperature among sites, where melt at most stations (exception is ACC sites) constrains Tskin, while the winter months show a larger variance in Tskin among sites since local conditions are dominating Tskin. The AWS data from the GrIS show the effect of altitude and latitude on Tskin, with the high altitude sites being the coldest (EGP, KAN_U and KAN_M) together with the most northern sites (THU_U and KPC_U). The southern (e.g. QAS_A and QAS_U) and low altitude sites (most LAB sites, TAS_U, TAS_A) occur to be the warmest. The SICE sites are comparable in temperature with the coldest sites on the GrIS (except from EGP), but are slightly warmer in summer and fall.

Figure 5b shows the mean daily range (daily max – daily min difference) of Tskin as a function of month for all sites and all years. Again, the observations show a similar pattern across the diverse geographical locations. During summer, the high elevation sites tend to have the largest daily range in Tskin, while the observations from LAB and SICE sites show the smallest daily range. This is very likely an effect of the warmer temperatures and the Tskin upper temperature limit at 0°C, the melting point for ice. This constraint is seen during summer at almost all data records included in this study (exceptions are the ACC sites). Figure 5c shows the mean difference between T2m and Tskin for all observation sites as a function of time of year. In general, the SICE sites show the weakest inversion, while the LAB sites show the strongest inversion. For the ACC sites the weakest inversion is found during summer, while the LAB sites tend to have the strongest inversion during summer. This is explained by differences in surface conditions during summer, where the LAB sites have surface melt in contrast to the high elevation ACC sites, where the surface warms but not reaches the ceiling of variability (the melting point).

Figure 5 indicates both yearly and daily variations in the observed Tskin and T2m relationship. A detailed analysis of these variations can be seen in Figures 6a-b, which illustrate the mean diurnal and seasonal T2m-Tskin differences for the ACC and LAB sites, respectively. The SSC and SICE sites have not been included as none of the individual sites have a continuous data record throughout the year without gaps. As also noticed in Fig. 4, the winter months have very little diurnal variability in the T2m-Tskin difference, with an approximately constant difference of about 1.5-2.5°C for the LAB sites and 0.5-1.5 °C for the ACC sites. During spring and summer the differences decrease at the ACC sites and the weakest vertical stratification is found around noon or early afternoon, where Tskin may even exceed T2m slightly resulting in an unstable stratification of the surface air column. For the LAB sites, the weakest stratification is found in spring and fall, around noon and early afternoon. The summer months show large differences due to the constrain of Tskin for melting surfaces, which is common to all LAB sites. At night the net radiation is negative, thus cooling the surface resulting in a surface-based inversion for both surface types. The T2m-Tskin differences are higher (especially in summer) at the LAB sites compared to the ACC sites, and the UAB sites have temperature differences in between. The reason for the higher temperature difference at the lower altitude sites is the longer time periods with surface melt.

4.2 Impact from wind

The surface wind speed is an important component in the near surface thermal stratification since the turbulent mixing increases as a function of wind speed (Monin and Obukhov, 1954). Figure 7 shows how the wind regimes differ among the observation sites used in this study. In general, winds on the GrIS are strongest in winter and reach a minimum around July (see also Steffen and Box, 2001). The surface radiative cooling and the terrain play the primary role in the generation of the surface winds. The direction and strength of the prevailing surface winds are closely related to the direction and steepness of the slope and the strength of the inversion. Surface winds at the PROMICE sites generally have a high directional persistence (see Fig. 4 in van As et al., 2014), commonly blowing from inland, which is an indication that local winds are often katabatic winds. High elevation sites experience stronger winds due to the larger radiative cooling of the surface (provided a comparable surface slope is present; Fig. 8; van As et al., 2014). The SSC and SICE sites show less variability in wind speed on annual basis. At these sites the wind is determined by large scale synoptic conditions combined with local topography.

The expectation is that stronger inversions can develop in low wind speed conditions because of reduced turbulent mixing. Figure 8a-b shows the T2m-Tskin difference as a function of binned wind speed. The middle plots show the binned distribution of the T2m-Tskin difference (with bin size of 1 K) as a function of binned wind speed, where the colour bar is the number of members in each bin. The top plots show the mean (solid lines) and standard deviation (dashed lines) of the T2m-Tskin difference as a function of the binned wind speeds. Figure 8a shows data from the DMI_Q AWS on sea ice. As expected, the strongest temperature inversion occurs at low wind speeds and larger wind speeds have larger turbulent mixing and thus smaller vertical temperature differences between Tskin and T2m. However, THU_U (Fig. 8b) shows that this relationship is more complex. The maximum inversion is reached at wind speeds from 3-5 m s^{-1}, whereas the mean and standard deviation decrease for calm winds (<2.5 m s^{-1})

The wind dependencies shown in Fig. 8 are representative for all the stations in this paper, where the SICE and the SSC sites resemble Fig 8a and all the PROMICE stations have a wind dependency similar to Fig. 8b. The pattern is explained by the inversion combined with a surface slope that results in a flow, which actually destroys its own forcing and as a result there is an optimum in inversion strength and wind speed. The PROMICE behaviour is also found by Adolph et al. (2018) at the Summit station on the GrIS. Miller et al. (2013) also found that the surface based inversion intensity peaks at wind speeds ranging from 3 to 10 m s^{-1} at Summit based on microwave radiometer retrieved profiles. Furthermore, Hudson and Brandt (2005) show that at the South Pole the maximum inversion strength occurs at wind speeds of 3-5 m s^{-1}. They suggest that it is not the weak wind of 3-5 m s^{-1} that promotes the strong inversion, but the inversion which forces the air flow resulting in an inversion wind. They investigated this using the model by Mahrt and Schwerdtfeger (1970), which relates the slope of the terrain and the strength of the inversion to the inversion wind. Their results supported the idea that the inversion wind can explain the "unexpected" location of the maximum in inversion strength. It seems that the nature of the surface winds and the directional constancy are highly comparable between the sloping surfaces of Antarctica and Greenland (van den Broeke et al., 1994; King and Turner, 1997) and in both cases the maximum inversion occurs at non-zero wind speeds.

4.3 Impact from clouds

The difference in LW_d radiation between clear-sky and overcast conditions can result in large differences in both T2m and Tskin due to the cloud effects on the surface radiation budget. As satellite Tskin can only be retrieved during clear-sky conditions, the assessment of the cloud effects on the average conditions is essential to facilitate the combination of satellite and in situ observations. In this section, we therefore assess the inversion strength as a function of the cloud cover and in Sect. 4.3.1 the clear-sky bias is estimated for all sites.

Clear-sky conditions are defined to be cases where CCF<0.3, while overcast conditions are defined to have CCF>0.7. The frequency of clear-sky (overcast) observations is defined as the number of clear-sky (overcast) observations compared to the total number of observations. Figure 9 shows the frequency of clear-sky and overcast observations for each of the observation sites used in this study. The SSC, SICE sites, and EGP all show a much larger frequency of overcast conditions compared to the frequency of clear-sky conditions. The ACC sites show a strong seasonal dependence with more clear-sky observations during summer and more overcast conditions during winter. A similar but much weaker seasonal cycle is seen for UAB. The LAB and SSC sites show limited seasonal variability, while the SICE sites have almost only clear-sky observations from April to July.

The relation between the inversion strength and CCF is shown in Fig 10 for all sites. As expected, the inversion strength decreases with increasing LW_d radiation due to a more extensive cloud cover. The average slope is calculated for each category: ACC=-0.011±0.0037 °C/%, UAB = -0.019±0.0012 °C/%, LAB = -0.021±0.0016 °C/%, SSC = -0.016±0.0026 °C/%, SICE = -0.017±0.0048 °C/% where the uncertainties are given as 95% confidence intervals.

Figure 11a-b show how the temperature differences at the ACC sites vary as a function of season and local time for clear-sky and overcast conditions, respectively. Clear-sky conditions show the largest stratification with temperature differences up to 2-3°C during winter and night time. Overcast conditions reduce the temperature gradient at all times, with the maximum temperature differences of about 1°C. During summer around noon, overcast conditions usually lead to an unstable stratification of the order of -1°C. An unstable stratification may also occur during clear-sky conditions and large solar insolation. This behaviour is common for all sites included in this study, but the strength of the inversion varies among the different sites

The impact of season and sky conditions on the T2m-Tskin differences is quantified in Table 2. The table summarizes the findings of the dependencies of cloud/clear and summer/winter on the T2m-Tskin difference for all 5 categories. Note that DMI_Q is withheld from the averaging for the SICE sites to avoid systematic impacts from the 1 m height observations. The categories which experience summer surface melt (UAB + ACC) tend to have larger T2m-Tskin differences during summer than winter. The SSC sites also experience melt, but the snow melts away in summer, which limits the time where Tskin is constrained to the melting point. It is difficult to interpret the results for the SICE sites, as none of the individual sites cover an entire year. For all surface types and for all times of the year, cloud cover tends to decrease the inversion strength.

4.3.1 Clear-sky bias

The most accurate surface temperature satellite observations are thermal IR observations that can only be observed during clear-sky conditions. As the satellite IR observations thus have gaps in cloudy conditions, the satellite Tskin products are often averages of the available satellite observations within 1-3 days (see e.g. Rasmussen et al., 2018). However, these satellite averages can be colder than the all-sky average temperature due to a clear-sky bias arising from the fact that Tskin is typically colder in clear-sky conditions compared to the cloudy conditions where the satellite cannot observe. When using the averaged Tskin observations for monitoring or in combination with ocean, sea ice or atmospheric models, it is therefore important to assess the impact on the clear-sky bias, by using different temporal averaging windows. Hall et al. (2012) show monthly temperature maps from MODIS and discuss the fact that the monthly average temperatures (from satellites) are likely lower that the all-sky monthly average temperatures. Here, we use the in situ observations to estimate the clear-sky effects that satellite observations would introduce. We use the cloud mask derived from the longwave-equivalent cloud cover fraction and assume that it is equivalent to the cloud masks used for IR satellite processing. The clear-sky bias has been assessed by comparing clear-sky Tskin observations with all-sky Tskin (where clear-sky has been defined as a CCF < 0.3) observations, averaged for different time windows: 24 h, 72 h and 1 month, for all sites. The results are shown in Fig. 12. For most stations all-sky observations are warmer than clear-sky observations for all time windows. However, there is large variability among the stations and at a few stations e.g. EGP, KPC_U, ATQ, OLI and DMI_Q the all-sky observations are colder than clear-sky observations using one or more of the time windows.

The larger clear sky biases for longer temporal averaging windows arise from persistent cloud cover lasting for days. For e.g. the 72 hours temporal averaging intervals, observations from periods with >1 day persistent cloud cover (and higher Tskin) are included, which are otherwise missing in the 24 hour clear-sky averages, resulting in a warmer all-sky averaged Tskin, compared to the average clear-sky Tskin.

Figure 13 shows the monthly mean difference in 24 h averaged clear-sky and all-sky Tskin for the ACC stations (a) and the LAB stations (b). For both groups of stations it is found that the 24 h averaged clear-sky bias is closest to zero during summer, which can partly be explained by the smaller daily Tskin range in summer (Fig. 5b). The UAB sites look very similar to the LAB sites, but with a slightly more pronounced seasonal cycle in the clear-sky bias. The figures have not been produced for the SSC and SICE sites as none of the individual sites included in these categories cover an entire season. The orange graphs show the mean number of hours with clear-sky per day, which illustrate more hours with clear-skies for LAB stations compared to ACC stations except for May-July. The positive clears-sky biases observed in Fig. 12 are very likely an effect of seasonal differences in cloud cover e.g. it is found that EGP has no clear-sky observations in Dec.-Feb. and at DMI_Q there is no clear-sky observations available Jan-Mar., which means that the results in Fig. 12 is biased towards the months where a zero or positive clear-sky bias is observed. The 72 h and 1 month averaged clear-sky biases show the same seasonal variation as in Fig. 13, with the smallest biases in summer and largest biases in winter.

4.4 Relationship with skin surface temperature

Section 4.3 showed how clouds impact the T2m and Tskin relationship, and Sect. 4.3.1 revealed a close relationship between Tskin and the CCF. With the aim of deriving T2m based upon satellite Tskin observations, it is important to examine how the T2m-Tskin difference is related to the skin temperature itself. The relationship with Tskin is corroborated in Fig. 14 where the strength of the surface-based inversion is shown as a function of Tskin. All PROMICE sites show an almost linear trend towards weaker inversion strength for higher skin temperatures with the steepest slope of the curve for low elevation sites. The average slopes for all categories are found to: ACC=-0.030±0.003, UAB =-0.066±0.004, LAB=-0.101±0.004, SSC = -0.044±0.005, SICE = -0.043±0.007, where the uncertainty estimates are given as 95 % confidence intervals. The results of this section are very encouraging in a situation where we would like to relate Tskin to T2m, but the cloud cover and longwave radiation are not available, such as the case with satellite observations.

5 Discussion

The T2m and Tskin variability shows that the coldest month ranges from December to March, whereas the warmest month is July for all sites considering both Tskin and T2m. This is in agreement with mean air temperatures found in Steffen and Box (2001) for Greenland GC-Net AWSs, Persson (2002) for Arctic sea ice and Rigor et al. (2000) for North Pole stations and land stations in Alaska. The monthly mean daily temperature range is largest in April-May and reaches a minimum in July, related to the upper temperature limit when the ice or snow is melting. Surface temperature inversions are very common for the Arctic region. Considering all categories the mean temperature difference between T2m and Tskin is on average 0.65-2.65°C with the strongest inversion for the sites located in the lower part of the ablation zone and the weakest inversion for the sea ice sites. Inversions are predominantly found during winter (low-sun and polar night periods), which allows for a strong radiative cooling at the surface. Smaller temperature differences are dominating in spring and summer, around noon and early afternoon, where the sun is warming the surface. This is in agreement with Adolph et al. (2018) who found large T2m-Tskin differences during night time and small differences during the peak solar irradiance (see Fig. 5 in Adolph et al., 2018). During summer and local noon Tskin has the closest coupling to T2m and the satellite observed Tskin observations will therefore have the best agreement with the T2m at these times.

Increasing wind speeds are expected to decrease the inversion strength through increased turbulence, and mixing warmer air downwards. This is also seen at the ARM sites and Arctic sea ice sites, where the strongest inversion occurs at calm winds and weaker inversions occur with increasing wind speed. The relationship is more complicated over a sloping terrain with the maximum inversion strength at winds of about 5 m s^{-1} and not at calm winds. This feature has previously been identified by others for Antarctica (Hudson and Brandt, 2005) and at Summit, GrIS (Adolph et al., 2018; Miller et al., 2013) and can be explained by the presence of a katabatic wind driven by the surface temperature inversion over a sloping terrain. The katabatic wind destroys part of its own forcing and as a result there exist an optimum in inversion strength and wind speed. This is in agreement with what Hudson and Brandt (2005) found for the Antarctic ice sheet.

The analysis of the impact of clouds showed an almost linear relationship between cloud cover and the T2m-Tskin difference, with a trend towards zero with increasing CCF (Fig. 10). Considering all categories the T2m-Tskin difference decreases from an all-sky mean value ranging from 0.65-2.65°C to a difference ranging from -0.08-1.63°C considering observations with a CCF above 0.7. On the other hand, the difference increases to the range of 1.05-3.44°C by only considering observations with CCFs below 0.3. The smaller inversion strength under cloudy conditions is explained by the fact that clouds have a predominantly warming effect on the surface in the Arctic (Intrieri, 2002; Walsh and Chapman, 1998). In cases where the cloud cover and longwave radiation are not available, the relationship can be quantified by using the Tskin. We have found an almost linear relationship between the inversion strength and the skin temperatures, with weaker inversions for higher Tskin. This is in agreement with Adolph et al. (2018) who found larger T2m-Tskin differences at lower temperatures at the Summit station, during summer.

As mentioned earlier, the measurement height changes with snowfall and snow melt at with that the strength of the inversion measured. The PROMICE data includes a height of the sensor boom, which can be used to determine the impact of using different measurement height on our results. We reproduced the numbers in Table 2, based upon observations measured at a height of 1.9-2.1 m only and found overall all-sky, all-months differences less than 0.22°C for all the different PROMICE regions. In addition, the screening did not change the conclusions regarding the impact of clouds and the seasonal behaviour of the T2m-Tskin differences. Data from the other sites do not all include such information on the measurement height. For consistency, we therefore chose not to screen the PROMICE data. In addition, we chose not to perform an adjustment of the observations, as we estimate the uncertainty of such an adjustment to be equal to or larger than the actual uncertainty on the results obtained here and again, it would not be possible to make such a correction for all sites.

To assess if there is any impact of clear-sky observations on the radiometer observations due to the different spectral characteristics (broad band versus narrow band, as discussed in Sect. 2.7), the T2m-Tskin differences as a function of CCF were calculated for narrow band Tskin and broad band Tskin for the stations containing both instruments (ATQ, BAR, OLI, DMI_Q, SHEBA, and FRAM). This resulted in a small change in the slope from -0.017 to 0.020°C/% for narrow band and broad band Tskin estimates, respectively. Similarly, the T2m-Tskin differences were calculated for both types of radiometers as a function of Tskin. Again, the change in trend was small from -0.046 to -0.055.

The influence of clouds on Tskin has been assessed by comparing clear-sky Tskin observations with all-sky Tskin observations averaged for different time intervals: 24 h, 72 h and 1 month, for all sites. In general, the clear-sky average is colder than the all-sky average with increasing bias with the length of the averaging time interval and the clear-sky bias is smaller during summer than winter for all averaging windows. This is also reported by Comiso (2000), who finds a monthly mean clear-sky bias of about -0.3°C during summer (Jan.) and -0.5°C during winter (Jul.) at Antarctic stations. The range in temperature over the averaging window as well as the frequency and timing of clear-sky observations are factors partly explaining the clear-sky bias variations observed among the stations.

The observed clear-sky bias explains part of the cold bias observed in IR satellite retrievals of skin surface temperature compared to in situ surface temperatures (Høyer et al., 2017; Rasmussen et al., 2018; Shuman et al., 2014). Another part of the explanation is related to the fact that the satellite skin observations are compared to in situ measured at typically 2 m height, where the temperature gradients in the lowest 2 m of the atmosphere will result in the satellite retrievals of surface temperature being colder than the in situ measurements at 2 m height.

6 Conclusions

Coincident in situ skin temperature (Tskin) and 2 m air temperatures (T2m) from 29 deployments in the Arctic region have been analysed to assess the variability and the factors controlling the Tskin and T2m variations in order to facilitate the combined use of satellite observed Tskin and traditional observations of T2m. The extensive data set used in this study represents a wide range of conditions including all-year observations from Arctic sea ice, land ice in northern Alaska as well as low and high altitude land ice covering the lower, middle and upper ablation zones and the accumulation region of the Greenland Ice Sheet. It has been found that there is a good correspondence between the Tskin and T2m and that the main factors influencing the relationship are seasonal variations, wind speed, cloud cover and the Tskin of the surface. The assessment of the tight relationship and the identification of the main variables that controls the variability are important findings when developing a statistical model that can convert satellite Tskin observations to T2m. All the identified parameters can be derived from either the satellite retrievals themselves or from NWP analysis and the generation of a daily satellite derived T2m product for the Polar Regions is thus made possible with these results. Such a satellite derived product will be independent of other existing surface temperature products and NWP reanalysis and can therefore contribute significantly to improvements in the Arctic climate change assessment since the satellite era started in the early 1980'ies.

7 Author contribution

Pia Nielsen-Englyst, Kristine S. Madsen, Rasmus Tonboe, Gorm Dybkjær and Emy Alerskans compiled the in situ data. Pia Nielsen-Englyst, Jacob L. Høyer and Kristine S. Madsen designed the experiments and Pia Nielsen-Englyst carried them out. Pia Nielsen-Englyst prepared the manuscript with contributions from all authors.

8 Competing interests

The authors declare that they have no conflict of interest.

9 Acknowledgements

This study was carried out as a part of the European Union Surface Temperatures for All Corners of Earth (EUSTACE), which is financed by the European Union's Horizon 2020 Programme for Research and Innovation, under Grant Agreement no 640171. The aim of EUSTACE is to provide a spatially complete daily field of air temperatures since 1850 by combining satellite and in situ observations. The author would like to thank the data providers. Data was provided by PROMICE, which is funded by the Danish Ministry of Climate, Energy and Building, operated by the Geological Survey of Denmark and Greenland and conducted in collaboration with the National Space Institute (DTU Space) and Asiaq (Greenland Survey) at http://www.promice.dk. Data were also obtained from the Atmospheric Radiation Measurement (ARM) Climate Research Facility, a U.S. Department of Energy Office of Science user facility sponsored by the Office of Biological and Environmental Research. We thank our colleagues in the SHEBA Atmospheric Surface Flux Group, Ed Andreas, Chris Fairall, Peter Guest, and Ola Persson for help collecting and processing the data. The National Science Foundation supported this research with grants to the U.S. Army Cold Regions Research and Engineering Laboratory, NOAA's Environmental Technology Laboratory, and the Naval Postgraduate School. Data was also provided by Timo Palo from the Tara expedition, supported by the European Commission 6th Framework Integrated Project DAMOCLES and in part by the Academy of Finland through the CACSI project. We thank Steinar Eastwood from the Norwegian Meteorological Institute for providing us with data from the FRAM2014/15 expedition. Finally, we would like to thank the anonymous reviewers for their carefully reading and their insightful suggestions and comments, which substantially improved this manuscript.

References

Abermann, J., Hansen, B., Lund, M., Wacker, S., Karami, M. and Cappelen, J.: Hotspots and key periods of Greenland climate change during the past six decades, Ambio, 46(S1), 3–11, doi:10.1007/s13280-016-0861-y, 2017.

Ackerman, T. P. and Stokes, G. M.: The Atmospheric Radiation Measurement Program, Phys. Today, 56(1), 38–44, doi:10.1063/1.1554135, 2003.

Adolph, A. C., Albert, M. R. and Hall, D. K.: Near-surface temperature inversion during summer at Summit, Greenland, and its relation to MODIS-derived surface temperatures, The Cryosphere, 12(3), 907–920, doi:10.5194/tc-12-907-2018, 2018.

Ahlstrøm, A., van As, D., Citterio, M., Andersen, S., Fausto, R., Andersen, M., Forsberg, R., Stenseng, L., Lintz Christensen, E. and Kristensen, S. S.: A new Programme for Monitoring the Mass Loss of the Greenland Ice Sheet, Geol. Surv. Den. Greenl. Bull., 15, 61–64, 2008.

Box, J. E., Fettweis, X., Stroeve, J. C., Tedesco, M., Hall, D. K. and Steffen, K.: Greenland ice sheet albedo feedback: thermodynamics and atmospheric drivers, The Cryosphere, 6(4), 821–839, doi:10.5194/tc-6-821-2012, 2012.

Bretherton, C. S., Roode, S. R. de, Jakob, C., Andreas, E. L., Intrieri, J., Moritz, R. E. and Persson, O. G.: A comparison of the ECMWF forecast model with observations over the annual cycle at SHEBA. Unpublished manuscript, 2000.

Cappelen, J.: Greenland—DMI Historical Climate Data Collection 1784–2015. Danish Meteorological Institute., 2016.

Casey, K. A., Polashenski, C. M., Chen, J. and Tedesco, M.: Impact of MODIS sensor calibration updates on Greenland Ice Sheet surface reflectance and albedo trends, The Cryosphere, 11(4), 1781–1795, doi:10.5194/tc-11-1781-2017, 2017.

Cohen, J., Screen, J. A., Furtado, J. C., Barlow, M., Whittleston, D., Coumou, D., Francis, J., Dethloff, K., Entekhabi, D., Overland, J. and Jones, J.: Recent Arctic amplification and extreme mid-latitude weather, Nat. Geosci., 7(9), 627–637, doi:10.1038/ngeo2234, 2014.

Comiso, J. C.: Variability and Trends in Antarctic Surface Temperatures from In Situ and Satellite Infrared Measurements, J. Clim., 13(10), 1674–1696, doi:10.1175/1520-0442(2000)013<1674:VATIAS>2.0.CO;2, 2000.

Curry, J. A. and Herman, G. F.: Infrared Radiative Properties of Summertime Arctic Stratus Clouds, J. Clim. Appl. Meteorol., 24(6), 525–538, doi:10.1175/1520-0450(1985)024<0525:IRPOSA>2.0.CO;2, 1985.

Curry, J. A., Schramm, J. L., Rossow, W. B. and Randall, D.: Overview of Arctic Cloud and Radiation Characteristics, J. Clim., 9(8), 1731–1764, doi:10.1175/1520-0442(1996)009<1731:OOACAR>2.0.CO;2, 1996.

Dozier, J. and Warren, S. G.: Effect of viewing angle on the infrared brightness temperature of snow, Water Resour. Res., 18(5), 1424–1434, doi:10.1029/WR018i005p01424, 1982.

Dybkjær, G., Tonboe, R. and Høyer, J. L.: Arctic surface temperatures from MetOp AVHRR compared to in situ ocean and land data, Ocean Sci., 8(6), 959–970, doi:10.5194/os-8-959-2012, 2012.

Franco, B., Fettweis, X. and Erpicum, M.: Future projections of the Greenland ice sheet energy balance driving the surface melt, The Cryosphere, 7(1), 1–18, doi:10.5194/tc-7-1-2013, 2013.

Gascard, J.-C., Festy, J., le Goff, H., Weber, M., Bruemmer, B., Offermann, M., Doble, M., Wadhams, P., Forsberg, R., Hanson, S., Skourup, H., Gerland, S., Nicolaus, M., Metaxian, J.-P., Grangeon, J., Haapala, J., Rinne, E., Haas, C., Wegener, A., Heygster, G., Jakobson, E., Palo, T., Wilkinson, J., Kaleschke, L., Claffey, K., Elder, B. and Bottenheim, J.: Exploring Arctic Transpolar Drift During Dramatic Sea Ice Retreat, Eos Trans. Am. Geophys. Union, 89(3), 21, doi:10.1029/2008EO030001, 2008.

Good, E. J., Ghent, D. J., Bulgin, C. E. and Remedios, J. J.: A spatiotemporal analysis of the relationship between near-surface air temperature and satellite land surface temperatures using 17 years of data from the ATSR series, J. Geophys. Res. Atmospheres, 122(17), 9185–9210, doi:10.1002/2017JD026880, 2017.

Graversen, R. G., Mauritsen, T., Tjernström, M., Källén, E. and Svensson, G.: Vertical structure of recent Arctic warming, Nature, 451(7174), 53–56, doi:10.1038/nature06502, 2008.

Hall, D., Box, J., Casey, K., Hook, S., Shuman, C. and Steffen, K.: Comparison of satellite-derived and in-situ observations of ice and snow surface temperatures over Greenland, Remote Sens. Environ., 112(10), 3739–3749, doi:10.1016/j.rse.2008.05.007, 2008.

Hall, D. K., Comiso, J. C., DiGirolamo, N. E., Shuman, C. A., Key, J. R. and Koenig, L. S.: A Satellite-Derived Climate-Quality Data Record of the Clear-Sky Surface Temperature of the Greenland Ice Sheet, J. Clim., 25(14), 4785–4798, doi:10.1175/JCLI-D-11-00365.1, 2012.

Hansen, J., Ruedy, R., Sato, M. and Lo, K.: Global surface temperature change, Rev. Geophys., 48(4), doi:10.1029/2010RG000345, 2010.

Høyer, J. L., Lang, A. M., Tonboe, R., Eastwood, S., Wimmer, W. and Dybkjær, G.: Towards field inter-comparison experiment (FICE) for ice surface temperature (ESA Tech. Rep. FRM4STS OP-40)., [online] Available from: http://www.frm4sts.org/wp-content/uploads/sites/3/2017/12/OFE-OP-40-TR-5-V1-Iss-1-Ver-1-Signed.pdf, 2017.

Hudson, S. R. and Brandt, R. E.: A Look at the Surface-Based Temperature Inversion on the Antarctic Plateau, J. Clim., 18(11), 1673–1696, doi:10.1175/JCLI3360.1, 2005.

Intrieri, J. M.: An annual cycle of Arctic surface cloud forcing at SHEBA, J. Geophys. Res., 107(C10), doi:10.1029/2000JC000439, 2002.

Jones, P. D., Lister, D. H., Osborn, T. J., Harpham, C., Salmon, M. and Morice, C. P.: Hemispheric and large-scale land-surface air temperature variations: An extensive revision and an update to 2010:, J. Geophys. Res. Atmospheres, 117(D5), n/a-n/a, doi:10.1029/2011JD017139, 2012.

King, J. C. and Turner, J.: Antarctic Meteorology and Climatology, Cambridge University Press, Cambridge., 1997.

Koenig, L. S. and Hall, D. K.: Comparison of satellite, thermochron and air temperatures at Summit, Greenland, during the winter of 2008/09, J. Glaciol., 56(198), 735–741, doi:10.3189/002214310793146269, 2010.

Kristoffersen, Y. and Hall, J.: Hovercraft as a Mobile Science Platform Over Sea Ice in the Arctic Ocean, Oceanography, 27(2), doi:10.5670/oceanog.2014.33, 2014.

Lettau, H. H. and Schwerdtfeger, W.: Dynamics of the surface-wind regime over the interior of Antarctica, Antarct. J. U. S., 2(5), 155–158, 1967.

Mahrt, L. J. and Schwerdtfeger, W.: Ekman spirals for exponential thermal wind, Bound.-Layer Meteorol., 1(2), 137–145, doi:10.1007/BF00185735, 1970.

Masson-Delmotte, V., Swingedouw, D., Landais, A., Seidenkrantz, M.-S., Gauthier, E., Bichet, V., Massa, C., Perren, B., Jomelli, V., Adalgeirsdottir, G., Hesselbjerg Christensen, J., Arneborg, J., Bhatt, U., Walker, D. A., Elberling, B., Gillet-Chaulet, F., Ritz, C., Gallée, H., van den Broeke, M., Fettweis, X., de Vernal, A. and Vinther, B.: Greenland climate change: from the past to the future: Greenland climate change, Wiley Interdiscip. Rev. Clim. Change, 3(5), 427–449, doi:10.1002/wcc.186, 2012.

Maykut, G. A.: The Surface Heat and Mass Balance, in The Geophysics of Sea Ice, edited by N. Untersteiner, pp. 395–463, Springer US, Boston, MA., 1986.

Miller, N. B., Turner, D. D., Bennartz, R., Shupe, M. D., Kulie, M. S., Cadeddu, M. P. and Walden, V. P.: Surface-based inversions above central Greenland, J. Geophys. Res. Atmospheres, 118(2), 495–506, doi:10.1029/2012JD018867, 2013.

Monin, A. S. and Obukhov, A. M.: Basic Laws of Turbulent Mixing in the Surface Layer of the Atmosphere, Contrib. Geophys. Inst. Slovak Acad. Sci., USSR 151.163, 1954.

Moris, V. R.: Infrared Thermometer (IRT) Handbook Atmospheric Radiation Measurement publication ARM TR-015 available from https://www.arm.gov/instruments/irt, 2006.

Overland, J., Francis, J. A., Hall, R., Hanna, E., Kim, S.-J. and Vihma, T.: The Melting Arctic and Midlatitude Weather Patterns: Are They Connected?*, J. Clim., 28(20), 7917–7932, doi:10.1175/JCLI-D-14-00822.1, 2015.

Persson, P. O. G.: Measurements near the Atmospheric Surface Flux Group tower at SHEBA: Near-surface conditions and surface energy budget, J. Geophys. Res., 107(C10), doi:10.1029/2000JC000705, 2002.

Rasmussen, T. A. S., Høyer, J. L., Ghent, D., Bulgin, C. E., Dybkjaer, G., Ribergaard, M. H., Nielsen-Englyst, P. and Madsen, K. S.: Impact of Assimilation of Sea-Ice Surface Temperatures on a Coupled Ocean and Sea-Ice Model, J. Geophys. Res. Oceans, 123(4), 2440–2460, doi:10.1002/2017JC013481, 2018.

Rayner, N. A.: Global analyses of sea surface temperature, sea ice, and night marine air temperature since the late nineteenth century, J. Geophys. Res., 108(D14), doi:10.1029/2002JD002670, 2003.

Reeves Eyre, J. E. J. and Zeng, X.: Evaluation of Greenland near surface air temperature datasets, The Cryosphere, 11(4), 1591–1605, doi:10.5194/tc-11-1591-2017, 2017.

Rignot, E.: Changes in the Velocity Structure of the Greenland Ice Sheet, Science, 311(5763), 986–990, doi:10.1126/science.1121381, 2006.

Rigor, I. G., Colony, R. L. and Martin, S.: Variations in Surface Air Temperature Observations in the Arctic, 1979–97, J. Clim., 13(5), 896–914, doi:10.1175/1520-0442(2000)013<0896:VISATO>2.0.CO;2, 2000.

Serreze, M. C., Schnell, R. C. and Kahl, J. D.: Low-Level Temperature Inversions of the Eurasian Arctic and Comparisons with Soviet Drifting Station Data, J. Clim., 5(6), 615–629, doi:10.1175/1520-0442(1992)005<0615:LLTIOT>2.0.CO;2, 1992.

Shuman, C. A., Hall, D. K., DiGirolamo, N. E., Mefford, T. K. and Schnaubelt, M. J.: Comparison of Near-Surface Air Temperatures and MODIS Ice-Surface Temperatures at Summit, Greenland (2008–13), J. Appl. Meteorol. Climatol., 53(9), 2171–2180, doi:10.1175/JAMC-D-14-0023.1, 2014.

Stamnes, K., Ellingson, R. G., Curry, J. A., Walsh, J. E. and Zak, B. D.: Review of Science Issues, Deployment Strategy, and Status for the ARM North Slope of Alaska–Adjacent Arctic Ocean Climate Research Site, J. Clim., 12(1), 46–63, doi:10.1175/1520-0442-12.1.46, 1999.

Steffen, K.: Surface energy exchange at the equilibrium line on the Greenland ice sheet during onset of melt, Ann. Glaciol., 21, 13–18, doi:10.3189/S0260305500015536, 1995.

Steffen, K. and Box, J.: Surface climatology of the Greenland Ice Sheet: Greenland Climate Network 1995-1999, J. Geophys. Res. Atmospheres, 106(D24), 33951–33964, doi:10.1029/2001JD900161, 2001.

Stocker, T. F., Qin, D., Plattner, G.-K., Tignor, M., Allen, S. K., Boschung, J., Nauels, A., Xia, Y., Bex, V., Midgley, P. M. and (eds.): Climate Change 2013 - The Physical Science Basis: Working Group I Contribution to the Fifth Assessment Report of the Intergovernmental Panel on Climate Change, Cambridge University Press, Cambridge., 2014.

Stroeve, J., Box, J. E., Wang, Z., Schaaf, C. and Barrett, A.: Re-evaluation of MODIS MCD43 Greenland albedo accuracy and trends, Remote Sens. Environ., 138, 199–214, doi:10.1016/j.rse.2013.07.023, 2013.

Swinbank, W. C.: Long-wave radiation from clear skies, Q. J. R. Meteorol. Soc., 89(381), 339–348, doi:10.1002/qj.49708938105, 1963.

Tedesco, M., Fettweis, X., van den Broeke, M. R., van de Wal, R. S. W., Smeets, C. J. P. P., van de Berg, W. J., Serreze, M. C. and Box, J. E.: The role of albedo and accumulation in the 2010 melting record in Greenland, Environ. Res. Lett., 6(1), 014005, doi:10.1088/1748-9326/6/1/014005, 2011.

Uttal, T., Curry, J. A., Mcphee, M. G., Perovich, D. K., Moritz, R. E., Maslanik, J. A., Guest, P. S., Stern, H. L., Moore, J. A., Turenne, R., Heiberg, A., Serreze, M. C., Wylie, D. P., Persson, O. G., Paulson, C. A., Halle, C., Morison, J. H., Wheeler, P. A., Makshtas, A., Welch, H., Shupe, M. D., Intrieri, J. M., Stamnes, K., Lindsey, R. W., Pinkel, R., Pegau, W. S., Stanton, T. P. and Grenfeld, T. C.: Surface Heat Budget of the Arctic Ocean, Bull. Am. Meteorol. Soc., 83(2), 255–275, doi:10.1175/1520-0477(2002)083<0255:SHBOTA>2.3.CO;2, 2002.

van As, D.: Warming, glacier melt and surface energy budget from weather station observations in the Melville Bay region of northwest Greenland, J. Glaciol., 57(202), 208–220, doi:10.3189/002214311796405898, 2011.

van As, D., Broeke, M. van den, Reijmer, C. and Wal, R. van de: The Summer Surface Energy Balance of the High Antarctic Plateau, Bound.-Layer Meteorol., 115(2), 289–317, doi:10.1007/s10546-004-4631-1, 2005.

van As, D., Fausto, R., Steffen, K., Ahlstrøm, A., Andersen, S. B., Andersen, M. L., Box, J., Charalampidis, C., Citterio, M., Colgan, W. T., Edelvang, K., Larsen, S. H., Nielsen, S., Martin, V. and Weidick, A.: Katabatic winds and piteraq storms: Observations from the Greenland ice sheet, Geol. Surv. Den. Greenl. Bull., (31), 83–86, 2014.

van den Broeke, M., Duynkerke, P. and Oerlemans, J.: The observed katabatic flow at the edge of the Greenland ice sheet during GIMEX-91, Glob. Planet. Change, 9(1–2), 3–15, doi:10.1016/0921-8181(94)90003-5, 1994.

Vihma, T.: Effects of Arctic Sea Ice Decline on Weather and Climate: A Review, Surv. Geophys., 35(5), 1175–1214, doi:10.1007/s10712-014-9284-0, 2014.

Vihma, T. and Pirazzini, R.: On the Factors Controlling the Snow Surface and 2-m Air Temperatures Over the Arctic Sea Ice in Winter, Bound.-Layer Meteorol., 117(1), 73–90, doi:10.1007/s10546-004-5938-7, 2005.

Vihma, T., Jaagus, J., Jakobson, E. and Palo, T.: Meteorological conditions in the Arctic Ocean in spring and summer 2007 as recorded on the drifting ice station Tara, Geophys. Res. Lett., 35(18), doi:10.1029/2008GL034681, 2008.

Walsh, J. E.: Intensified warming of the Arctic: Causes and impacts on middle latitudes, Glob. Planet. Change, 117, 52–63, doi:10.1016/j.gloplacha.2014.03.003, 2014.

Walsh, J. E. and Chapman, W. L.: Arctic Cloud–Radiation–Temperature Associations in Observational Data and Atmospheric Reanalyses, J. Clim., 11(11), 3030–3045, doi:10.1175/1520-0442(1998)011<3030:ACRTAI>2.0.CO;2, 1998.

Zhang, Y., Seidel, D. J., Golaz, J.-C., Deser, C. and Tomas, R. A.: Climatological Characteristics of Arctic and Antarctic Surface-Based Inversions, J. Clim., 24(19), 5167–5186, doi:10.1175/2011JCLI4004.1, 2011.

Zygmuntowska, M., Mauritsen, T., Quaas, J. and Kaleschke, L.: Arctic Clouds and Surface Radiation – a critical comparison of satellite retrievals and the ERA-Interim reanalysis, Atmospheric Chem. Phys., 12(14), 6667–6677, doi:10.5194/acp-12-6667-2012, 2012.

Table 1 Observation sites used in this study covering the following surface types: Accumulation zone (ACC), upper/middle ablation zone (UAB), lower ablation zone (LAB), seasonal snow cover (SSC), sea ice (SICE).

Project	Site	Station	Surface Type	Latitude (°N)	Longitude (°W)	Elevation (m)	Start date	End date
PROMICE	East Grip	EGP	ACC	75.62	35.97	2660	01/05/2016	30/04/2018
PROMICE	Kangerlussuaq	KAN_U	ACC	67.00	47.03	1840	04/04/2009	03/04/2018
PROMICE	Crown Prince Christian Land	KPC_U	ACC	79.83	25.17	870	17/07/2008	16/07/2018
PROMICE	Kangerlussuaq	KAN_M	UAB	67.07	48.84	1270	02/09/2008	01/09/2018
PROMICE	Nuuk	NUK_N	UAB	64.95	49.89	920	25/07/2010	24/07/2014
PROMICE	Nuuk	NUK_U	UAB	64.51	49.27	1120	20/08/2007	19/08/2018
PROMICE	Qassimiut	QAS_A	UAB	61.24	46.73	1000	20/08/2012	19/08/2015
PROMICE	Qassimiut	QAS_M	UAB	61.10	46.83	630	11/08/2016	10/08/2018
PROMICE	Qassimiut	QAS_U	UAB	61.18	46.82	900	07/08/2008	06/08/2018
PROMICE	Scoresbysund	SCO_U	UAB	72.39	27.23	970	21/07/2008	20/07/2018
PROMICE	Tasiilaq	TAS_A	UAB	65.78	38.90	890	28/08/2013	27/08/2018
PROMICE	Tasiilaq	TAS_U	UAB	65.67	38.87	570	11/03/2008	10/03/2015
PROMICE	Thule	THU_U	UAB	76.42	68.15	760	09/08/2010	08/08/2018
PROMICE	Upernavik	UPE_U	UAB	72.89	53.58	940	18/08/2009	17/08/2018
PROMICE	Kangerlussuaq	KAN_L	LAB	67.10	49.95	670	01/09/2008	31/08/2018
PROMICE	Crown Prince Christian Land	KPC_L	LAB	79.91	24.08	370	17/07/2008	16/07/2018
PROMICE	Nuuk	NUK_L	LAB	64.48	49.54	530	20/08/2007	19/08/2018
PROMICE	Qassimiut	QAS_L	LAB	61.03	46.85	280	24/08/2007	23/08/2018
PROMICE	Scoresbysund	SCO_L	LAB	72.22	26.82	460	22/07/2008	21/07/2018
PROMICE	Tasiilaq	TAS_L	LAB	65.64	38.90	250	23/08/2007	22/08/2018
PROMICE	Thule	THU_L	LAB	76.40	68.27	570	09/08/2010	08/08/2018
PROMICE	Upernavik	UPE_L	LAB	72.90	54.30	220	17/08/2009	16/08/2018
ARM	Atqasuk	ATQ	SSC	70.47	149.89	2	07/11/2003	06/11/2010

ARM	Barrow	BAR	SSC	71.32	156.62	8	31/10/2003	28/10/2018
ARM	Oliktok Point	OLI	SSC	70.50	157.41	20	18/10/2013	13/10/2018
ICEARC	Qaanaaq	DMI_Q	SICE	77.43	69.14	Sea level	31/01/2015	08/06/2017
FRAM2014/15	Arctic Ocean	FRAM	SICE	82.22-89.35	-180.00-180.00	Sea level	05/09/2014	3/07/2015
SHEBA	Arctic Ocean	SHEBA	SICE	74.62-80.37	143.92-168.15	Sea level	01/11/1997	26/09/1998
TARA	Arctic Ocean	TARA	SICE	71.41-88.54	0.01-148.28	Sea level	01/04/2007	20/09/2007

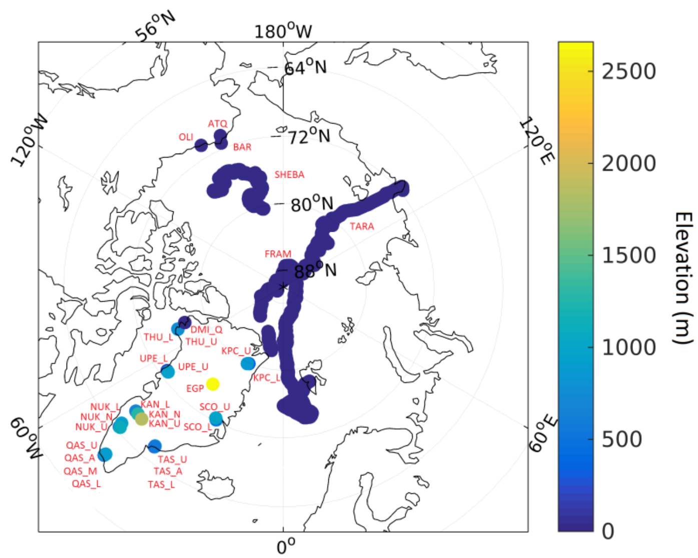

Figure 1: Spatial coverage and elevation for each site included in this study. The colour bar is elevation in meters.

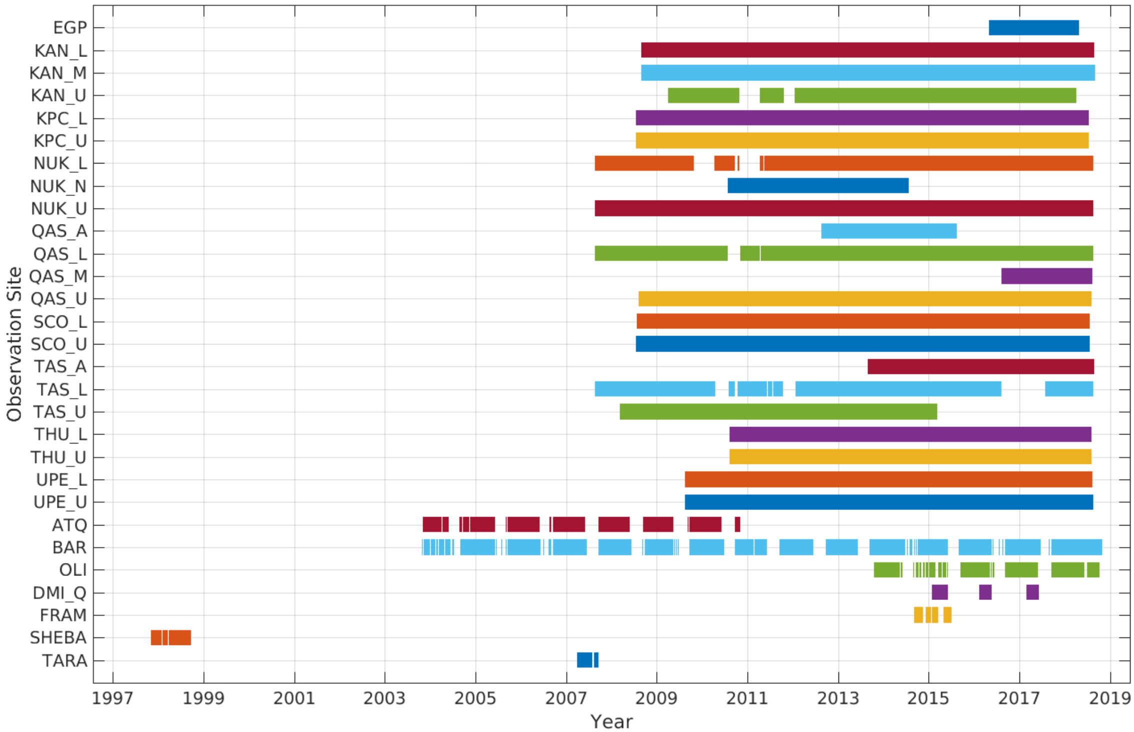

Figure 2: Temporal coverage for each observation site included in this study.

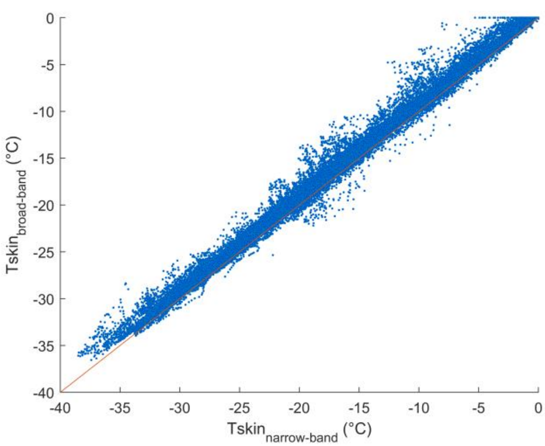

Figure 3: Scatterplot of Tskin estimated from narrow-band IR observations versus Tskin estimated from broad-band IR observations for DMI_Q.

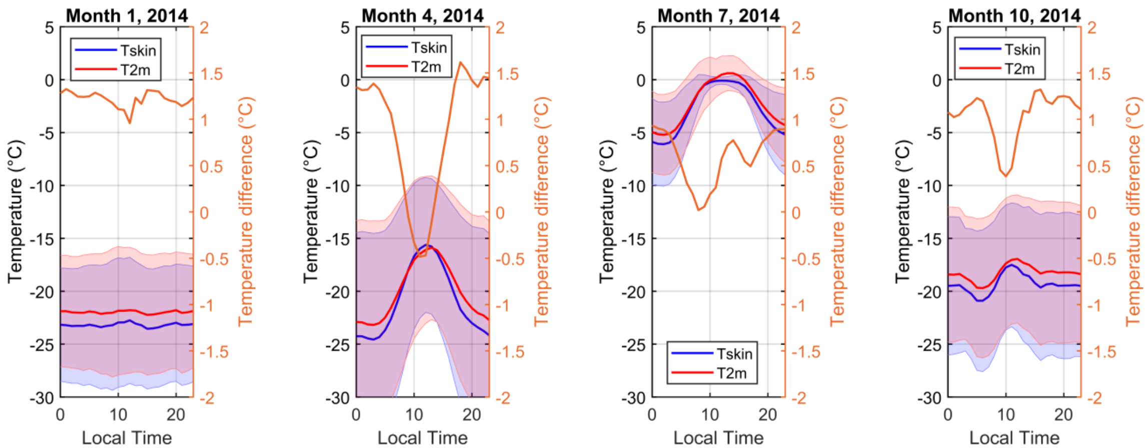

Figure 4: Monthly diurnal variability of 2 m air temperature (red) and skin temperature (blue) at KAN_ U during the months: January, April, July and October. The orange curves are the difference between the red and blue curves. The shadings indicate the standard deviations.

5

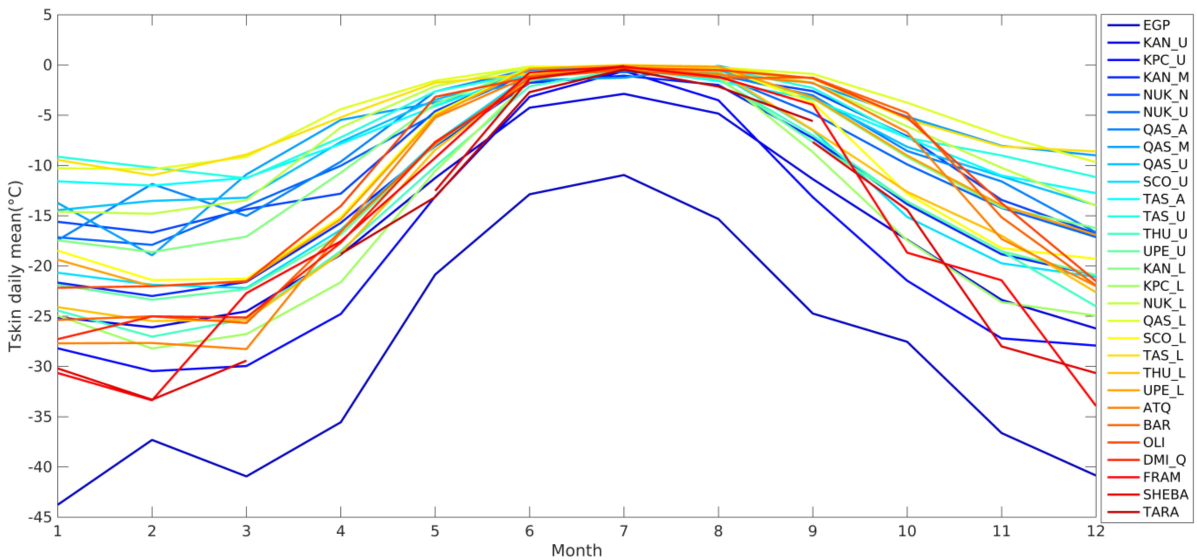

(a)

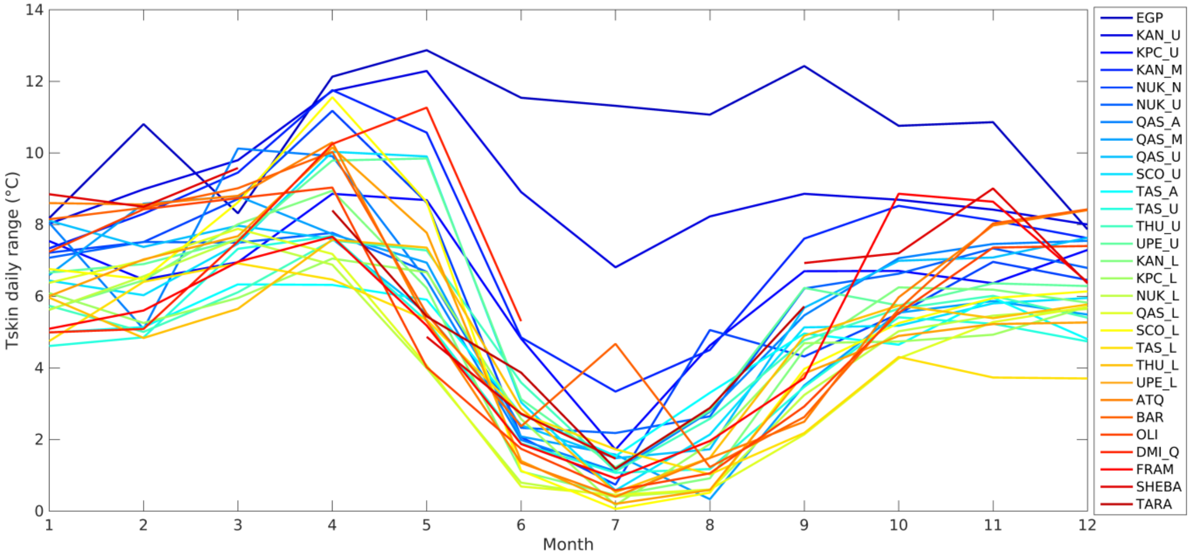

(b)

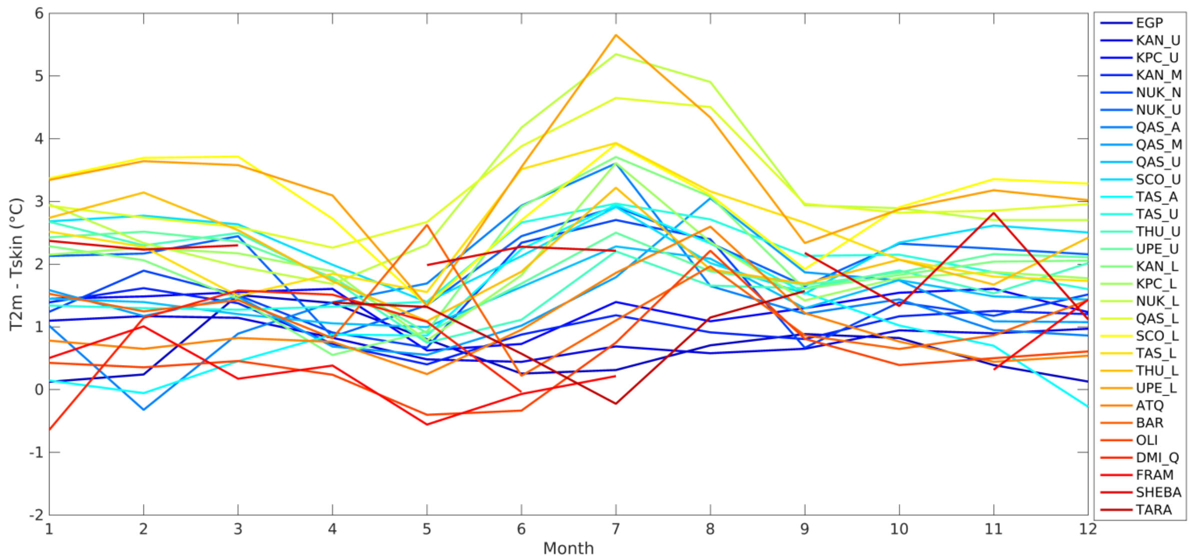

(c)

Figure 5: Monthly mean of Tskin (a) daily range in Tskin (b) and T2m-Tskin difference (c), for all sites. See Table 1 for station locations and types.

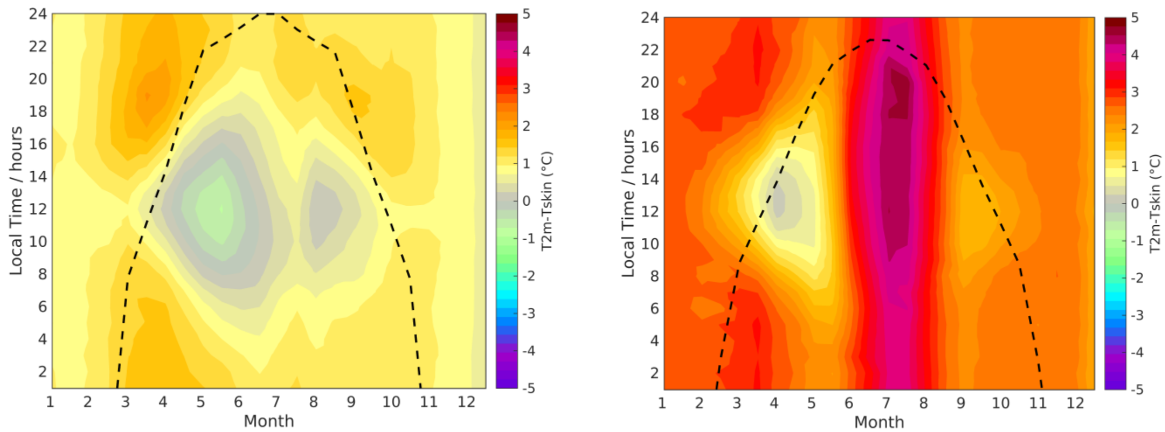

Figure 6: Mean 2 m air temperature and skin temperature differences for ACC (a) and LAB (b) as a function of time of year (with a bin size of 15 days) and local time of the day. The dotted black lines indicate the total hours of sunlight.

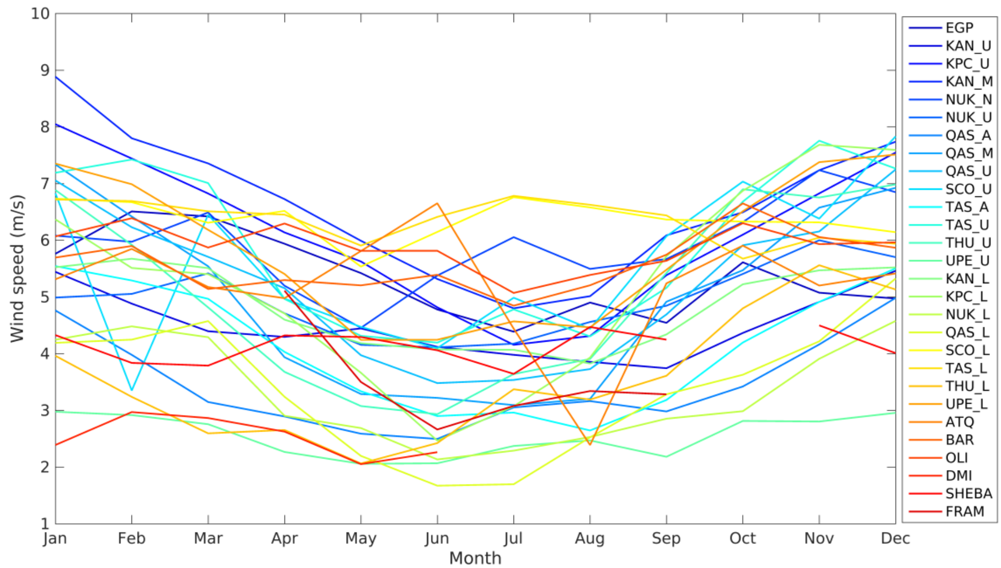

5 **Figure 7: The average annual cycle in wind speed for all sites.**

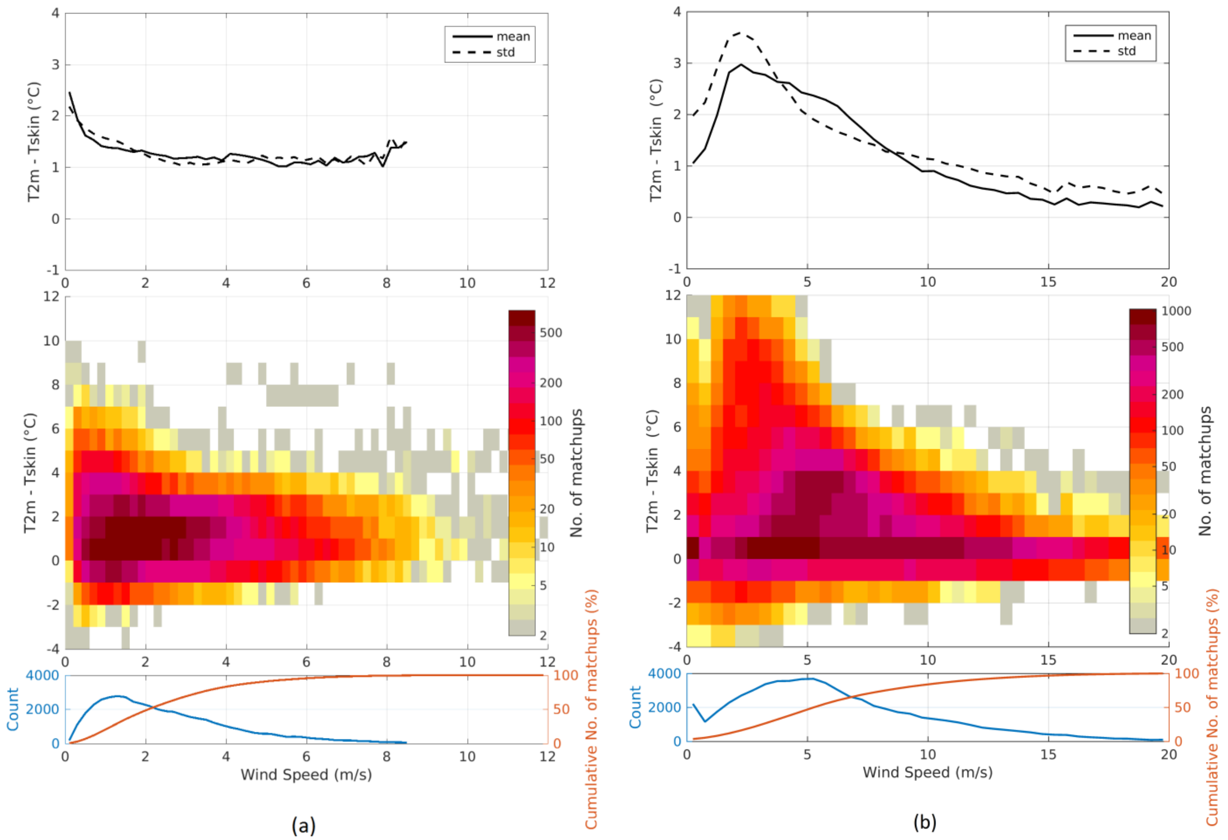

Figure 8: 2 m air temperature and skin temperature difference as a function of binned wind speed for (a) DMI_Q and (b) THU_U. The wind speed bin size is 0.5 m s^{-1}, the T2m-Tskin bin size is 1°C, and only bins with more than 50 members are included. The upper plots show the standard deviation (dashed lines) and mean difference (solid lines). The middle plots show the number of members in each bin, while the bottom plots show the number of members (blue lines) and the cumulative percentage of members (red lines) in each wind speed bin.

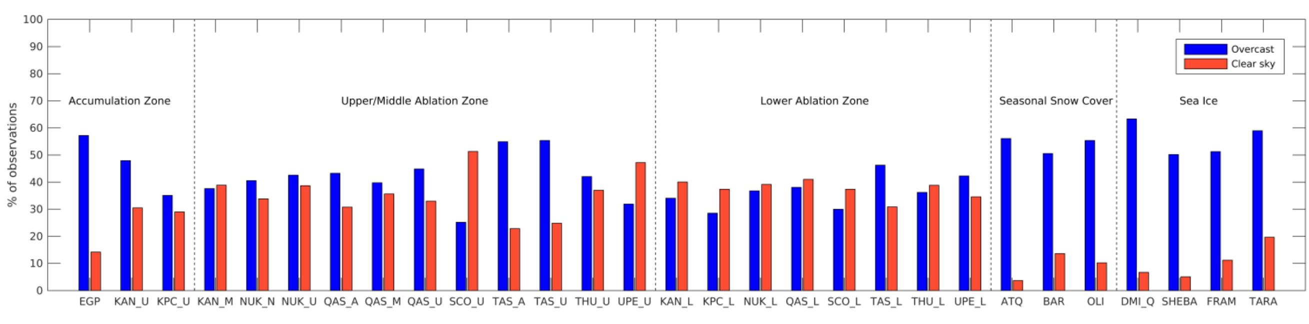

Figure 9: Frequency of clear-sky and overcast observations in percent of all observations for each site.

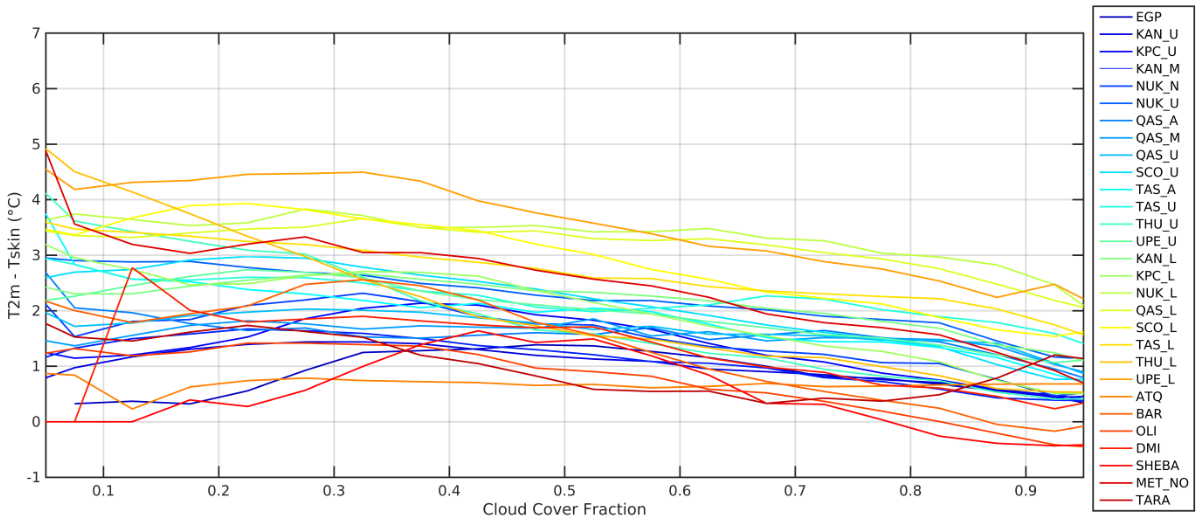

Figure 10: 2 m air temperature and skin temperature differences for all sites as a function of binned cloud cover fraction (CCF). The CCF bin size is 0.05, the T2m-Tskin bin size is 1°C, and only bins with more than 50 members are considered.

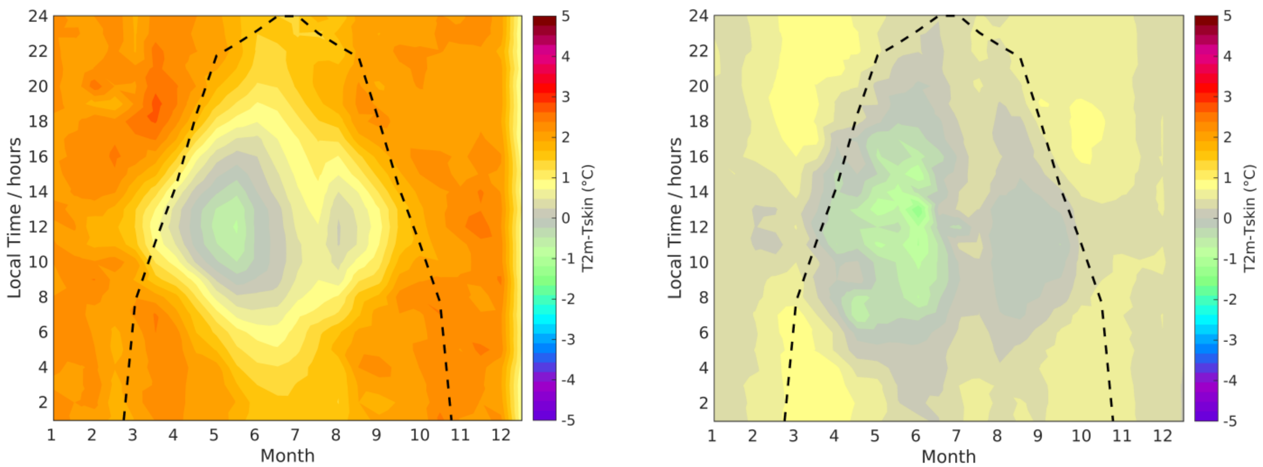

Figure 11: Similar to Fig. 7a but with 2 m air temperature and skin temperature differences for ACC sites in cases of clear-sky (a), and overcast conditions (b). The dotted black lines indicate the total hours of sunlight each month.

Table 2 Overall 2 m air temperature and skin temperature differences (T2m-Tskin, °C) for each surface type under different circumstances in terms of season and sky conditions. The square brackets are the ranges of the T2m-Tskin differences for the stations included in each surface type category.

	Jun-Aug	Dec-Feb	All months

ACC	Cloud	0.21 [0.13 – 0.34]	0.47 [0.16 – 0.66]	0.43 [0.35 – 0.49]
	Clear	0.79 [0.26 – 1.29]	1.99 [1.55 – 2.46]	1.05 [0.58 – 1.50]
	All	0.69 [0.43 – 1.07]	0.88 [0.16 – 1.41]	0.91 [0.65 – 1.29]
UAB	Cloud	1.77 [0.68 – 2.62]	0.67 [-0.79 – 1.52]	0.90 [0.16 – 1.45]
	Clear	2.49 [1.12 – 3.16]	2.71 [1.35 – 4.76]	2.36 [1.45 – 3.38]
	All	2.20 [0.98 – 2.77]	1.60 [0.07 – 2.65]	1.65 [1.05 – 2.26]
LAB	Cloud	2.81 [1.15 – 4.23]	1.38 [0.49 – 2.10]	1.63 [0.66 – 2.41]
	Clear	3.94 [3.01 – 5.22]	3.90 [2.82 – 4.81]	3.44 [2.46 – 4.42]
	All	3.51 [2.28 – 4.74]	2.73 [2.06 – 3.45]	2.65 [1.99 – 3.34]
SSC	Cloud	-0.08 [-0.59 – 0.26]	-0.05 [-0.17 – 0.04]	-0.08 [-0.27 – 0.06]
	Clear	1.57 [1.01 – 2.25]	2.32 [1.75 – 2.93]	1.80 [1.34 – 2.19]
	All	0.40 [-0.22 – 0.96]	0.84 [0.47 – 1.41]	0.65 [0.35 – 0.97]
SICE ÷ DMI_Q	Cloud	0.71 [-0.00 – 1.34]	0.35 [-0.33 – 1.04]	0.64 [-0.38 – 1.29]
	Clear	1.95 [0.40 – 3.73]	2.33 [1.09 – 3.56]	2.10 [0.43 – 3.86]
	All	1.09 [0.08 – 2.30]	1.51 [0.99 – 2.03]	1.25 [0.42 – 2.08]

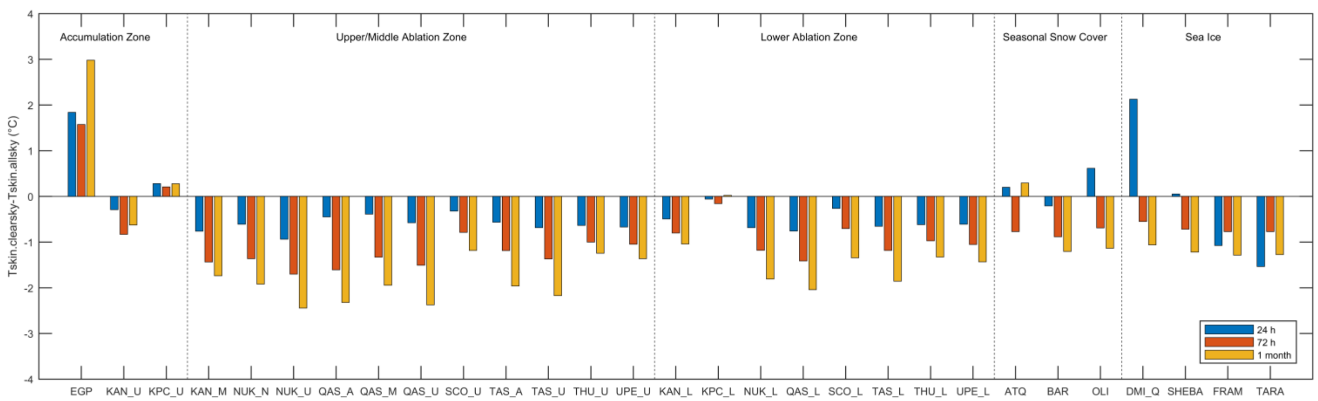

Figure 12: Observed clear-sky biases (Tskin_clearsky-Tskin_allsky) averaged for different time intervals, for all sites (°C).

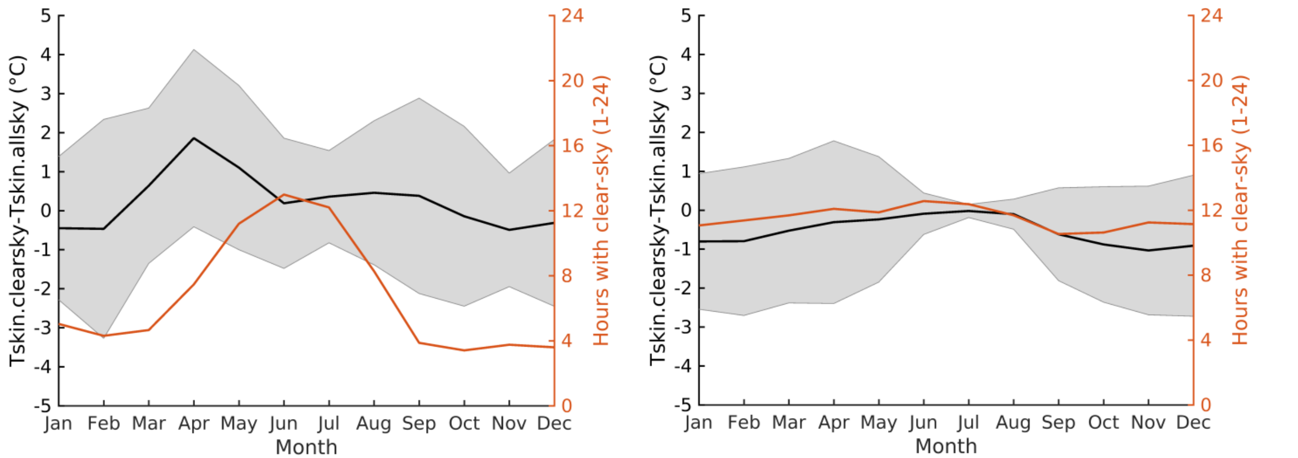

Figure 13: Differences between 24 h averaged clear-sky and all-sky skin temperatures for ACC stations (a) and LAB stations (b) for each month. The red lines show the 24 h average number of hours with CCF>0.7 per day for each month.

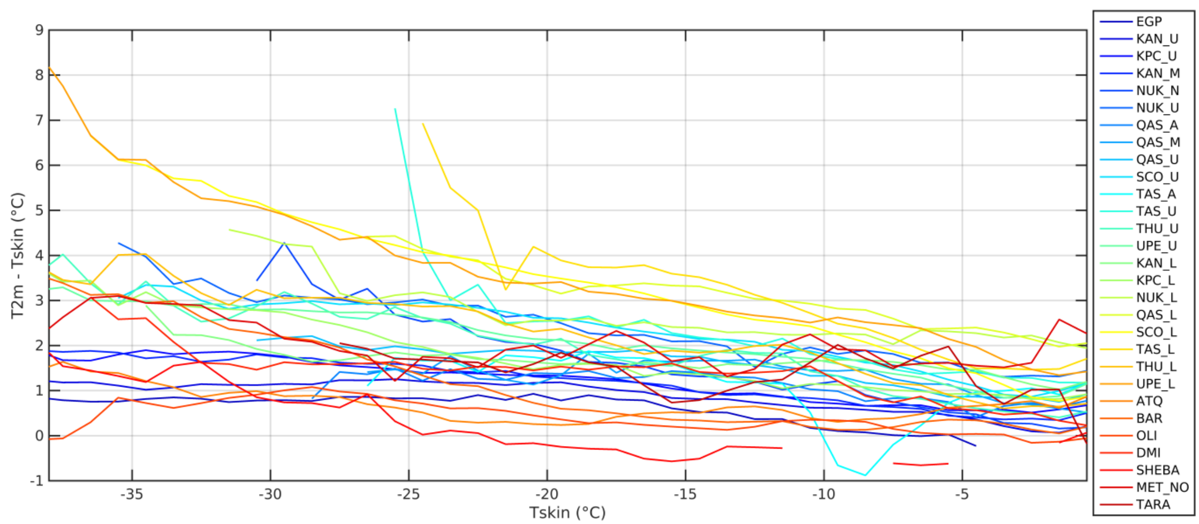

Figure 14: Mean 2 m air temperature and skin temperature differences for all sites as a function of binned skin temperature. The Tskin bin size is 1°C, the T2m-Tskin bin size is 1°C, and only bins with more than 50 members are considered.